REPUBLIQUE DU CAMEROUN
****
UNIVERSITE DE YAOUNDE I
****
FACULTE DES SCIENCES
****
CENTRE DE RECHERCHE ET DE FORMATION DOCTORALE EN SCIENCES TECHNOLOGIE ET GEOSCIENCES
****
UNITE DE RECHERCHE ET DE FORMATION DOCTORALE EN PHYSIQUES ET APPLICATIONS
****
B.P 812 Yaoundé
Email : crfd_stg@uy1.uninet.cm

REPUBLIC OF CAMEROON
****
THE UNIVERSITY OF YAOUNDE I
****
FACULTY OF SCIENCES
****
POST GRADUATE SCHOOL OF SCIENCES, TECHNOLOGY GEOSCIENCES
****
DOCTORAL RESEARCH UNIT AND TRAINING IN PHYSICS AND APPLICATIONS
****
B.P 812 Yaoundé
Email : crfd_stg@uy1.uninet.cm

LABORATOIRE DE MECANIQUE, MATERIAUX ET STRUCTURES
LABORATORY OF MECHANICS, MATERIALS AND STRUCTURES

EFFECTS OF QUINTESSENCE, PERFECT FLUID DARK MATTER AND ROTATION ON THE THERMODYNAMICS OF THE NON-LINEAR MAGNETIC-CHARGED BLACK HOLE

Thesis submitted and defended publically in partial fulfillment of the requirements for the award of the degree of Doctor of Philosophy (PhD) in Physics.

Speciality: **Fundamental Mechanics and Complex Systems**

By

NDONGMO TSAFACK Ragil Brand

Registration number: **12W0316**

Holder of a Master Degree in Physics

Co-Director

MAHAMAT Saleh
Associate Professor
University of Maroua

Co-Director

BOUETOU BOUETOU Thomas
Professor
University of Yaoundé I

Year 2024

UNIVERSITE DE YAOUNDE I
FACULTE DES SCIENCES

UNIVERSITY OF YAOUNDE I
FACULTY OF SCIENCE

DEPARTEMENT DE PHYSIQUE

DEPARTMENT OF PHYSICS

ATTESTATION DE CORRECTION DE LA THESE DE DOCTORAT/PhD

Nous, Professeurs **DJUIDJE KENMOE Germaine, KUETCHE KAMGANG Victor, HONA Jacques** et Professeur **OWONO OWONO Luc Calvin**, respectivement Examinateurs et Président du jury de la thèse de Doctorat/PhD de Monsieur **NDONGMO TSAFACK Ragil Brand** Matricule **12W0316**, préparée sous la direction des Professeurs **MAHAMAT Saleh et BOUETOU BOUETOU Thomas,** intitulée : **«EFFECTS OF QUINTESSENCE, PERFECT FLUID DARK MATTER AND ROTATION ON THE THERMODYNAMICS OF THE NON-LINEAR MAGNETIC-CHARGED BLACK HOLE** », soutenue le **Mardi, 16 Janvier 2024**, en vue de l'obtention du grade de Docteur/PhD en Physique, Spécialité **Mécanique, Matériaux et Structures**, attestons que toutes les corrections demandées par le Jury de soutenance ont été effectuées.

En foi de quoi, la présente attestation lui est délivrée pour servir et valoir ce que de droit.

Fait à Yaoundé le 12 Février 2024

Examinateur

Pr. HONA J.

Pr. Kuetche K.V

DJUIDJE

Le Président du Jury

Luc C. Owono Owono
Professeur

Le Chef de Département de Physique

UNIVERSITE DE YAOUNDE I
FACULTE DES SCIENCES
Le Chef de Département
DEPARTEMENT DE PHYSIQUE

Professeur

Dedication

I dedicate this thesis to :

my parents ***NDONGMO Raymond Etienne***
and
TSAFACK NGUEPI Geneviève

Acknowledgements

First of all, I would like to give thanks to God who guided me on the right path and gave me the wisdom and the mind necessary to better approach this work.

This work being the representation of my first research work, I would like through these few lines, to address my thanks to people who participated directly or indirectly in the realization of this thesis.

So, my thanks go to :

- *Pr* ***BOUETOU BOUETOU Thomas****, Head of Department of computer engineering at the National Advanced School of Engineering of the University of Yaoundé I, for having accepted to co-supervise this research work in the area of cosmology.*

- *Pr* ***MAHAMAT Saleh****, at the Higher Teacher Training College of the University of Maroua, the co-supervisor of my thesis, who guided and supported me during my work despite his multiple occupations.*

- *Pr* ***KOFANE Timoléon Crépin****, from the Botswana international University, for his support, his advices and valuable lessons during my bachelor's and master's programmes on special relativity and tensor calculus which were of great help during my work.*

- *Pr* ***TABI conrad Bertrand*** *from the Botswana international University, for his friendliness and his multiple advices to improve the quality of my research.*

- *Pr* ***NDJAKA Jean Marie****, Head of the Department of Physics, at the University of Yaoundé I, for his administrative support and his availability.*

- *Pr* ***BEN-BOLIE Germain Hubert****, Head of the laboratory of Nuclear Physics and Radioprotection at the University of Yaoundé I, for his support and multiple advices.*

- *Pr* ***Sunny Vagnozzi****, physicist at the Cambridge University in United Kingdom, for his support and advices, despite his multiple occupations.*

- *Pr* ***ABOSSOLO Monique****, vice-dean in charge of the Research and Cooperation at the Faculty of Science of the University of Yaoundé I,for her moral support and the multiple exchanges we had for my initiatives of promoting scientific research in Cameroon.*

- *Mr* ***ABÉ NGOMO****, for the multiple discussions which allowed me to talk about astrophysics in a digestible and simple way.*

- *the members of my family* ***TSAKEM Marie Madeleine, MOUAFO Madeleine, DONGMO Josée, NDONGMO Pierre-Marie, DONGMO Célestin and Tchoumi Jean Claude, ZANGUE Suzanne, NGUEPI Fidèle, MANFO Auguste and DONFACK Innocent,*** *for their moral and financial support and multiple advices they gave to me.*

- *All the members of jury, for the honour they give me by accepting to be part of the examination jury of my thesis.*

- *In general, to all the teachers of the Department of Physics of the University of Yaoundé I, in particular those from the laboratory of Mechanics, Materials and Structures, for all the theoretical and practical training received.*

- *To all my friends and classmates, such as:* ***ZANGA Dieudonné, NAHA Fernand, DEJO Arlette, MEKONTCHOU Foudjo Michael and***

MAPOUOKAM Astride*, for their moral and material support.*

- *To all my family who have always supported me and who, without necessarily realizing it, contributed to my career. May this thesis strengthen and perpetuate the fraternity and the spirit of love in our great family.*

Contents

List of Figures

List of Tables

ABSTRACT

In this thesis, we analyse the effects of quintessence dark energy, perfect fluid dark matter and rotation onto the thermodynamic behaviour of the nonlinear magnetic-charged black hole. To do that, we study the thermodynamics of various models of black holes with nonlinear distribution of magnetic charge. Accordingly, for each study, we compute various thermodynamic quantities of the black hole, such as mass(energy), temperature, potential provided from the magnetic charge, thermodynamic pressure and heat capacity. This allows to have a good appreciation of the behaviour of the nonlinear magnetic-charged black hole, and the effects of quintessence and perfect fluid dark matter on its thermodynamics. Through the thermodynamic analysis, we find various effects, such as the loss of the rotating black hole mass, the decrease of the black holes temperatures, and the occurrence of phase transitions. For instance, the black hole we study undergo a second-order phase transition due to rotation, dark matter or dark energy. This is remarked by the presence of a discontinuity on the plot of the heat capacity. Furthermore, taking into account the AdS spacetime, we find that the black hole behaves like a van der Waals fluid, which indicates the occurrence of the small/large black hole first order-phase transition.
Keywords: Quintessence, perfect fluid dark matter, rotating black hole, phase transitions, thermodynamics.

RÉSUMÉ

Dans cette thèse, nous analysons les effets de la quintessence, de la matière noire de type fluide parfait et de la rotation sur le comportement thermodynamique du trou noir chargé magnétiquement de manière non linéaire. Pour ce faire, nous étudions la thermodynamique de différents modèles de trous noirs avec distribution non linéaire de charge magnétique. Ainsi, pour chaque modèle, nous calculons différentes grandeurs thermodynamiques du trou noir, telles que la masse (énergie), la température, le potentiel fourni par la charge magnétique, la pression thermodynamique et la capacité calorifique. Cela nous permet d'avoir une bonne appréciation du comportement de notre système, et des effets de la quintessence et de la matière noire de type fluide parfait sur sa thermodynamique. Grâce à l'analyse thermodynamique, nous mettons en exergue divers effets, tels que la perte de masse du trou noir en rotation, la diminution des températures des trous noirs et l'apparition de transitions de phases. Par exemple, le trou noir que nous étudions subit une transition de phase du second ordre due à la rotation, de la matière noire ou de l'energie noire. Ceci est remarqué par la présence d'une discontinuité sur le tracé de la capacité calorifique. De plus, en tenant compte de l'espace-temps AdS, nous trouvons que le trou noir se comporte comme un gaz de van der Waals, d'où l'apparition d'une transition de phase du premier ordre de type petite/grande taille des trous noirs.
Mots clés: Quintessence, matière noire de type fluide parfait, trou noir rotatif, transitions de phase, thermodynamique.

INTRODUCTION

In the early 1970s, one of the very impressive discovery on the general relativity theory, is that black holes radiate as black bodies [1]. Such results offered some early hints about the nature of quantum gravity. As a result, black holes may behave like thermodynamic objects, with characteristic temperature and entropy, as it is presented in Hawking [2] and Bekenstein [3] works. Indeed, their works were the start of the thermodynamic study of black holes .

Accelerated expansion of the universe is the most recent fascinating result of observational cosmology [4–6]. To explain this extraordinary phenomenon, an exotic scalar field with a large negative pressure called "dark energy", is proposed as being one of the content of the Universe, which constituted about 73% of the total energy of the universe [7]. There are several candidates for dark energy. One of them is the cosmological constant [8–11], and another one, is "Quintessence" . Quintessence dark energy is characterized by a state parameter ϵ, which is the ratio of the pressure to the energy density of the dark energy, and the value of ϵ falls in the range $-1 \leq \epsilon \leq -\frac{1}{3}$ [7,12,13]. Kiselev [14] first derived the solutions of the black hole surrounded by the quintessence. Since then, many authors studied several kinds of black holes in the quintessence field [15–23], in order to appreciate the impact of quintessence on black holes. Recently, A. Abdujabbarov [24] studied the shadow of the rotating black hole with quintessential energy in the presence of plasma, and showed that the shadow of this black hole is significantly modified, when we take into account the quintessential field parameter.

Beside dark energy, another unsolved problem in cosmology and astrophysics is dark matter, which constitutes about 23% of the total mass-energy of the universe [25], according to the Standard Model of Cosmology. Beside Cold Dark Matter (CDM) [26], Warm Dark Matter [27, 28] and Scalar Field Dark Matter [29, 30], the Perfect fluid dark matter(PFDM) is one among them, and it has been shown that the PFDM can explain the asymptotically flat rotation curves concerning spiral galaxies [31]. Hence, the PFDM has been introduced in many works concerning black holes [32–35].

Recently, a new proof of existence of black holes has been shown by the Event Horizon Telescope collaboration [36–40]. They have presented the first image of a central supermassive black hole, named M87*(the supermassive object at the center of the galaxy M87). However, Bambi et *al.* [41] have derived constraints on the nature of M87*. They found that a superspinar might be mimicking this black hole, finding an excellent agreement for a large region of parameter space. On the other hand, the proof that these supermassive black holes are rotating has been shown by observations [42,43]. Then, it could be necessary to carry out a theoretical study of these stars and their interactions within the dark energy. Therefore, this kind of work could lead to better appreciate astrophysical black holes. Thereby, the rotational Kiselev black hole (RKBH) solution has been obtained [21, 44–47].

On the other hand, one of the properties of black holes is known as Singularity, at which densities and curvature become infinite [48]. Among the different alternatives to solve this strange behaviour concerning black holes, a kind of black hole with regular non-singular geometry and with an event horizon satisfying weak energy condition was constructed by Bardeen [49,50]. This has been obtained by introducing an energy-momentum tensor, interpreted as the gravitational field of some sort of a nonlinear magnetic monopole charge Q. Thereby, many authors studied the possible influence of the magnetic field on the black hole's dynamics [51–55]. In that way, Nam [56] obtained the metric of nonlinear magnetic-charged black hole surrounded by quintessence. Furthermore, Benavides et *al.* [57] found the metric of rotating and nonlinear magnetic-charged black hole in the quintessence field, which is the combination of both previous metrics. Their results give many informations about many physical properties of this black hole.

Since seminal works of Hawking and Page [58], it has been shown that black holes undergo a phase transition, in the AdS/CFT correspondence. Furthermore, the understanding of the phase transition could be extended to the one between small-large black hole, as in Refs. [59–61], for which they showed a complete analogy with the van der Waals liquid-gas system. Unlike the classical thermodynamics, there is no usual $P-V$ term in the first law of the black hole thermodynamics. Therefore, in order to restore it, it has been suggested that the Cosmological constant Λ plays the role of the pressure P and its conjugate quantity as a thermodynamic volume V in the extended phase space, and then the black hole mass can be considered as the enthalpy, as suggested in Refs. [62–64]. Thereby, this reasoning has enriched several studies on the thermodynamic study of black holes [65–73].

Another way to study phase transitions of black holes is through the behaviour of its heat capacity [7]. Especially, Husain and Mann [74] suggested that the specific heat of a black hole becomes positive after a phase transition near the Planck scale, and the presence of a discontinuity in the plot of the heat capacity shows the presence of a second-order phase transition. Afterwards, it has been studied in several works, in order to explore the black hole phase transition(see Refs [7,49,75–79]). Therefore, what could we have if we also take into account rotation, quintessence dark energy and perfect fluid dark matter, in the spacetime of a nonlinear magnetic charged black hole?

In this thesis, we aim at studying the impact of quintessence dark energy, perfect fluid dark matter and rotation onto the thermodynamic behaviour of a nonlinear magnetic-charged black hole. In order to achieve this goal, our work will be organized in three chapters. In chapter (1), we talk about black holes. Especially, we present how they are classified according to their mass, to their electrical charge and angular momentum, then we also present how black holes are detected. We highlight different kinds of dark energy and dark matter, and their role in the evolution of the Universe. After that, we present some tools on thermodynamics and the laws of black holes mechanics. In chapter (2), concerning materials and methods used for our study, we derive the metrics necessary for our study. Indeed, we work out the metric of a nonlinear magnetic charged black hole, in the presence of quintessence dark energy and perfect fluid dark matter, and afterwards, we take into account the rotating case of our black hole in the quintessence field to get another metric. Then, we present some tools on black hole thermodynamic analysis, such as thermodynamic quantities which are computed in the study, the Ehrenfest classification of phase transitions and the liquid-gaz phase transition observed in van der Waals fluid are also presented. In chapter (3), we show the effects of quintessence dark energy, perfect fluid dark matter and rotation on the thermodynamic of the nonlinear magnetic-charged black hole. We conduct four thermodynamic studies, and this is done by finding thermodynamic quantities, such as entropy, temperature, potential and heat capacity, which leads to analyse the thermodynamic stability of the black hole.

Chapter I

GENERALITIES ON BLACK HOLES, DARK ENERGY, DARK MATTER AND THERMODYNAMICS OF BLACK HOLES

1.1 Introduction

According to the NASA, a black hole is a place in space where gravity pulls so much that even light can not get out. The gravity is so strong because matter has been squeezed into a tiny space. Over the time, scientists came to realize that several types of black holes exist, depending on the size and the mass of the black hole. Hence the motivation to understand how such bodies are formed. Fortunately, one of the way to make a theoretical study of these objects is a theory, named Einstein's general theory of relativity, which allows the existence of black holes of any size, including very small ones [80].

However, one can notice that black holes have far more important potential consequences for the universe and life. And this is why scientists have devoted so much time and efforts in recent years to understand how they form, as well as their properties. The most common way to get them is after a tremendously violent process, where a gigantic quantity of matter is compressed into an extremely small space. Moreover, the energy produced would have to be millions of times larger than those people normally deem catastrophic, including earthquakes, volcanic eruptions, and the crash of asteroids onto planetary surfaces. In this chapter, we will present first some generalities about black holes, their formations and their different types. Secondly, we will discuss about dark energy and dark matter. Finally, we will present some generalities on the black hole thermodynamics.

1.2 Black holes

Black holes are some of the strangest and most fascinating objects found in outer space. They are objects of extreme density, with such strong gravitational attraction that even light cannot escape from their grasp if it comes near enough. Also, the theory which predicts that a sufficiently compact mass can deform spacetime to form a black hole is the Einstein theory of general relativity [81, 82].

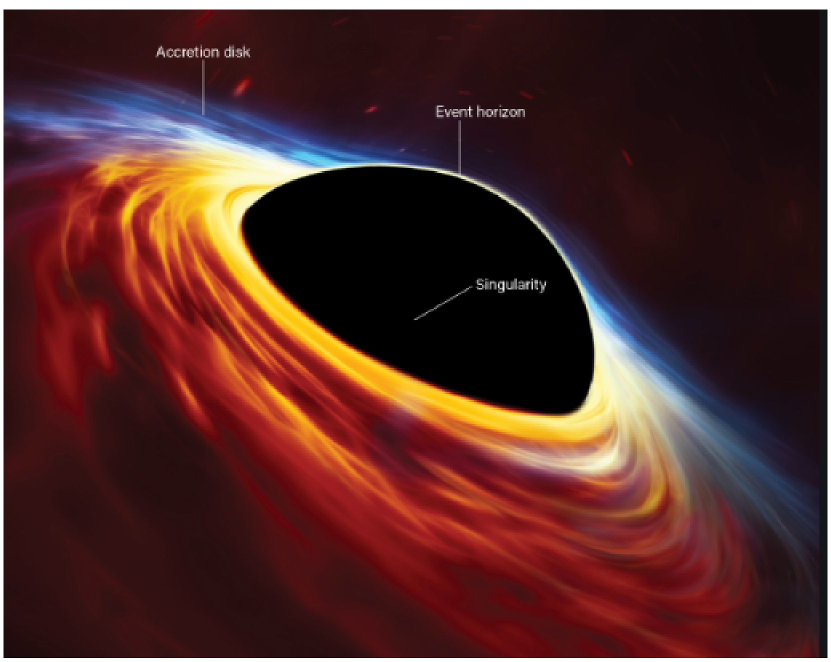

Figure 1.1: Anatomy of the black hole (Accretion disk, Event horizon, singularity)

The idea of a body so massive that even light could not escape was briefly proposed by astronomical pioneer John Michell in a letter published in 1784 [83]. Hence, he

Figure 1.2: Illustration of a black hole

is the first person known to have proposed the existence of black holes. Michell's simplistic calculations assumed that such a body might have the same density as the Sun, and concluded that such a body would form when a star's diameter exceeds the Sun's by a factor of 500, and the surface escape velocity exceeds the usual speed of light. Michell correctly noted that such supermassive but non-radiating bodies might be detectable through their gravitational effects on nearby visible bodies. Also, Pierre-Simon Laplace published a mathematical 'proof' of the existence of this mysterious object in 1799 [84].

Albert Einstein first predicted black holes in 1916 with his general theory of relativity [85]. Back holes are usually found through their interaction with other matter and with electromagnetic radiation, which can be visible. When matter falls inward into a black hole, it creates an accretion disk heated by friction, and this could create quasars, some of the brightest objects in the Universe. Before being swallowed, stars which are very close to massive black holes can be teared. Commonly, the presence and mass of black holes are determined through stars orbiting around them.

The term "black hole" was coined in 1967 by the American astronomer John Wheeler, and the first object considered to be a black hole is Cygnus X-1 [86]. The boundary of the region from which no escape is possible is called the event horizon(See figure (1.1) [87]). Another region, which is inside the black hole is called Singularity, which corresponds to the point that every physical quantity becomes infinite, and the radius is null [85].

Nowadays, around a dozen of black holes have been localized in our galaxy the Milky Way, but there are thought to be hundreds of millions. The problem is that it is very difficult to identify them when there is no light source like stars orbiting, hence they are evolving solitary [88].

1.2.1 Black holes classification

There exists a huge variety of black holes in the universe. However, they can be classified in two ways, first in term of their mass, and secondly according to their electric charge and momentum. Indeed, results of physical study of black holes are found depending on their parameters.

I- The no-hair theorem

The no-hair theorem states that, once it achieves a stable condition after formation, a black hole has only three independent physical properties: mass, charge, and angular momentum [89]. Physically meaning, the electric charge is the physical property of matter that causes it to experience a force when placed in an electromagnetic field, and it can also produce electric field [90], while the angular momentum is one of the properties of rotating objects. Two black holes that share the same values for these properties, or parameters, are indistinguishable according to classical (i.e. non-quantum) mechanics.

Furthermore, when matter falls into a black hole, it is permanently inaccessible to any external observer. This is also the case for the matter which participated to the formation of the black hole, such as the matter of the supermassive star arrived at its end of life [91]. Let notice that this theorem is established with zero cosmological constant, which has been established first by Einstein in his theory of general relativity. Hereby, scientists think that these three physical properties can be extended in the case of positive cosmological constant [92]. Also, if confirmed by experimentation, magnetic charges(magnetic monopoles) can be the fourth physical property.

II- Classification of black holes according to their mass

Astrophysical black holes can be classified depending on their mass. Here, we have four types, namely

a) Stellar black holes

Black holes do not exist since the dawn of time. Indeed, they can be created by physical processes, and the well known process is through the death of stars, which could lead to black holes. In the same way that people undergo a life cycle starting with birth and ending with death, stars undergo the same cycle, except that the durations are infinitely longer. The nursery of a typical star, including one like the Sun, is an extremely large cloud of gases and dust floating through space(See figure (1.3) [93]). Such clouds are formed when ”wind” created by exploding stars blow scattered molecules of gas and particles of dust around [80].

When such a cloud becomes concentrated enough, gravity causes it to contract still further over time. This contraction also produces heat, which makes the gases and dust grow steadily hotter. Soon, the center of the cloud becomes hot enough; then it reaches the temperature of a blast furnace; and finally, after a few million years, the temperature at the cloud’s core becomes hot enough to fuse hydrogen atoms and thereby ignite nuclear reactions(See figure (1.4) [94]). At that instant, the core emits a huge burst of blinding light and other energy that blows away the

Figure 1.3: A nursery of stars, Nebula of Orion

cooler outer layers of the cloud, leaving behind a giant ball of white-hot gases-a newborn star [80].

Figure 1.4: Protostar

The new star has enough hydrogen inside to keep its nuclear reactions self-sustaining for a very long time. And throughout this longest portion of its life cycle, which is about billions of years, it continues producing light and heat. Also, this period is favourable for many phenomena, such as the formation of a planet at the right distance from the star, the presence of water and the rise of life possible in that solar system. No significant danger is posed to such life as long as the star remains stable. what allows such a star to remain stable for so long is the presence of two enormous forces occurring in the object's body against each other, creating a stable equilibrium. Gravity is one of these forces, which makes the massive quantities of matter in the star's outer layers fall inward, creating great pressure, while the second force is created by nuclear reactions present in the star's core(See figure (1.5) [95]). Indeed, as everyone can easily see and feel, the Sun is not a cold body. Stars like the Sun produce enormous amounts of energy. The nuclear reactions taking place in a star's core release immense amounts of heat, light, and tiny particles that travel outward, toward the surface [80].

Finally, after using up its fuel, a disaster occurs in the star in which most of its matter is forced into an extremely dense state. Indeed, once the core of the star has completely burned to iron, energy production stops and the core rapidly collapses resulting in a supernova explosion. The core of the star can then take one of three different forms, depending on the star's initial mass; in each case, a superdense object is created(See figure (1.6) [95]). Two of these objects are white dwarfs and neutron stars while the third is the black hole. If the core is greater than about 2-3 solar masses (the maximum mass of a neutron star), the pressure of neutrons is unable to stop the collapse and a stellar black hole is formed. Packing all of that bulk many times the mass of our own sun into such a tiny point gives to black holes their powerful gravitational pull. Thousands of these stellar-mass black holes may lurk within our own Milky Way galaxy [96]. These black holes are generally modelled as Kerr black holes(rotating), as it is expected that the original rotation

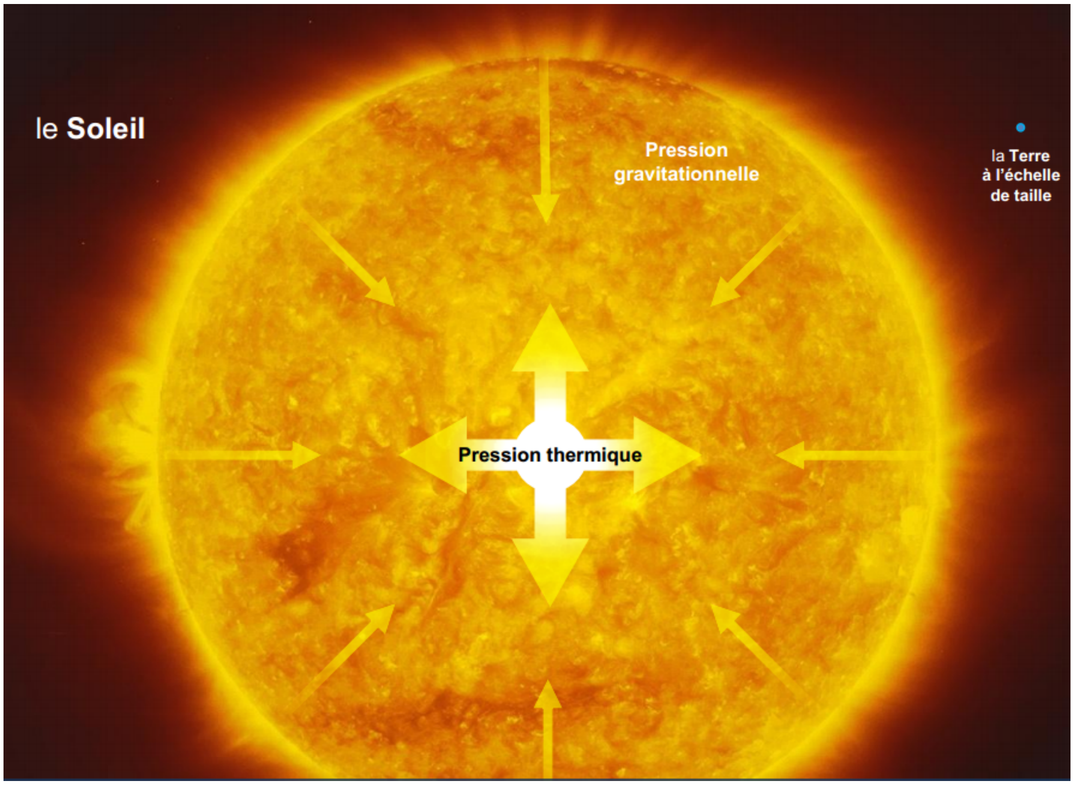

Figure 1.5: two forces present in stars

of the massive star would be conserved during the collapse, and that black holes contain little electric charge [97].

Examples of stellar black holes, are presented in table (1.1) [98].

b) Supermassive black holes

As the name suggests, supermassive black holes contain between a million and a billion times more mass than a typical stellar black hole [99]. Although there are

Name	Black hole(Solar masses)	Distance from Earth(light years)
LB-1	68 +11/-13	15,000
A0620-00/V616 Mon	11 ± 2	3,500
XTE J1118+480	6.8± 0.4	6,200
Cyg X-1	11 ± 2	6,000-8,000

Table 1.1: Some stellar black holes

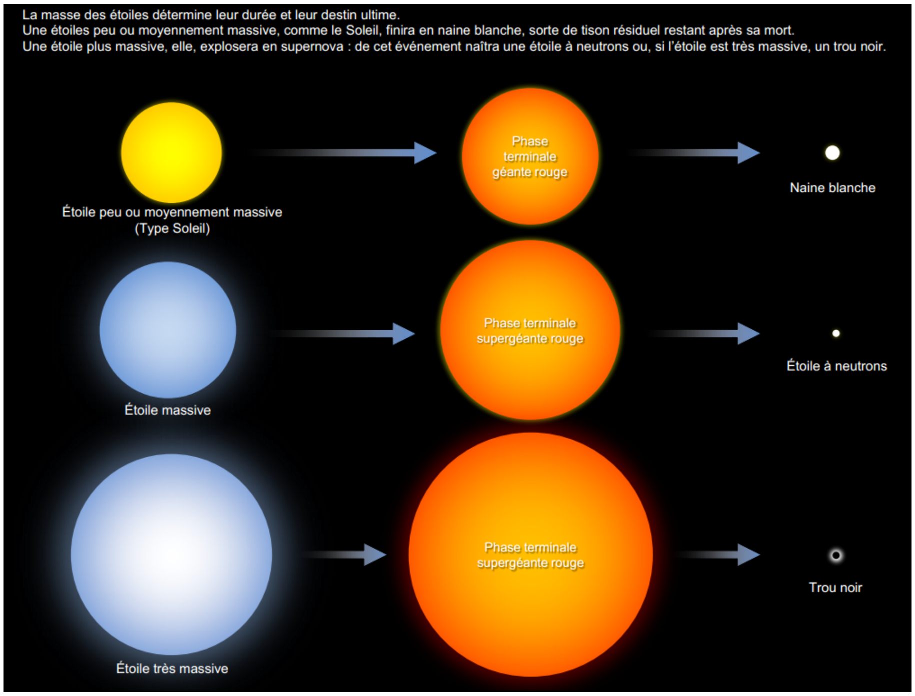

Figure 1.6: The three different object forms, depending on the star's initial mass

only a handful of confirmed supermassive black holes (most are too far away to be observed), they are thought to exist at the centre of most large galaxies, including the centre of our own galaxy, the Milky Way(See figure (1.7) [100]).

Historically, the first investigation was made by Maarten Schmidt [101], where he found a radio source (astronomical objects that emit relatively large amounts of radio waves, meaning that less than 300 GHz) in 1963. While it was considered to be a star, the spectrum seemed puzzling, and the rate of light variation of the source was similar to a quasi-star(quasars) object. One of the explanation to this behaviour proposed in 1963 by Fred Hoyle and W. A. Fowler is the existence of hydrogen burning supermassive stars. These would have a mass of about 10^5 to 10^9 solar masses [102]. Nevertheless, It has been found by Richard Feynman [103, 104], that such stars above a certain critical mass are dynamically unstable, and then would collapse onto a stellar black holes. Therefore, in 1970, Edwin E. Salpeter and Yakov Zeldovich [105] found that matter falling onto a massive compact object

Figure 1.7: our Solar system in the Milky Way

would explain the properties of quasars. Hence, quasars can be powered by a central supermassive black hole.

The formation of supermassive black holes are not actually well know, even though scientists agree that black holes can grow by accretion of matter around and also by merging with other black holes [106]. However the problem this theory faces is that supermassive black holes are found even in the early universe, then, stellar black holes and stars would not exist in this period to create supermassive black holes. This is why David Elbaz [107] proposed a model according to which supermassive black holes are formed rapidly in the early universe, through the chaos present on that period. And the proof is that quasars containing theses supermassive black holes emit a huge radiation jet which is able to create stars around it, and afterwards both quasars and interstellar matter merge to form a proper galaxy(See figure (1.8) [104]).

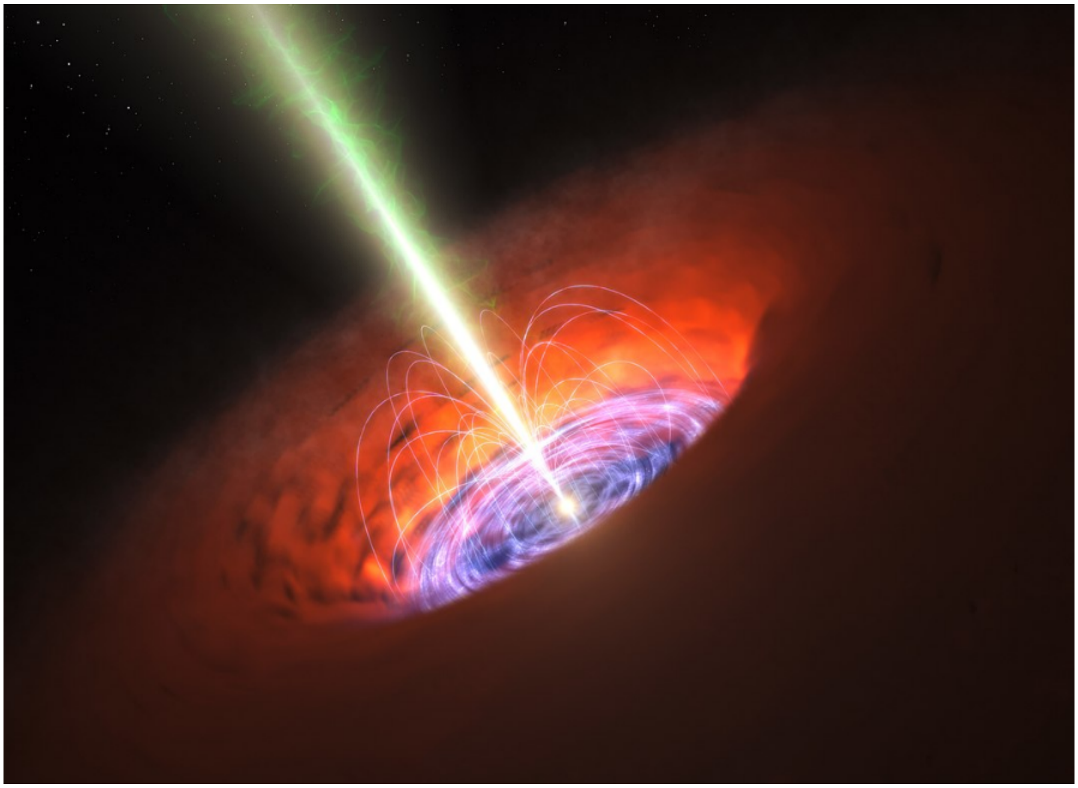

Figure 1.8: An artist's conception of a supermassive black hole surrounded by an accretion disk and emitting a relativistic jet

c) Intermediate-mass black holes

Scientists once thought black holes came in only small and large sizes, but research has revealed the possibility for the existence of mid size, or intermediate, black holes. They are in the range $10^2 - 10^5$ solar masses. Based on indirect gas cloud velocity and accretion disk spectra observations, many of them have been localized in our galaxy and nearby [108]. The first intermediate-mass black hole, named "GCIRS 13E" has been found in 2004, orbiting three light-years from Sagittarius A* [109], with mass of 1,300 solar masses and is within a cluster of seven stars. Out of our galaxy, astronomers found "HLX-1(Hyper-Luminous X-ray source 1)", present in the galaxy ESO 243-49, and is inside a small cluster(See figure (1.9) [108]). More recently, in 2020, astronomers would have found "3XMM J215022.4-055108" an intermediate-mass black hole present in the direction of Aquarius constellation [110].

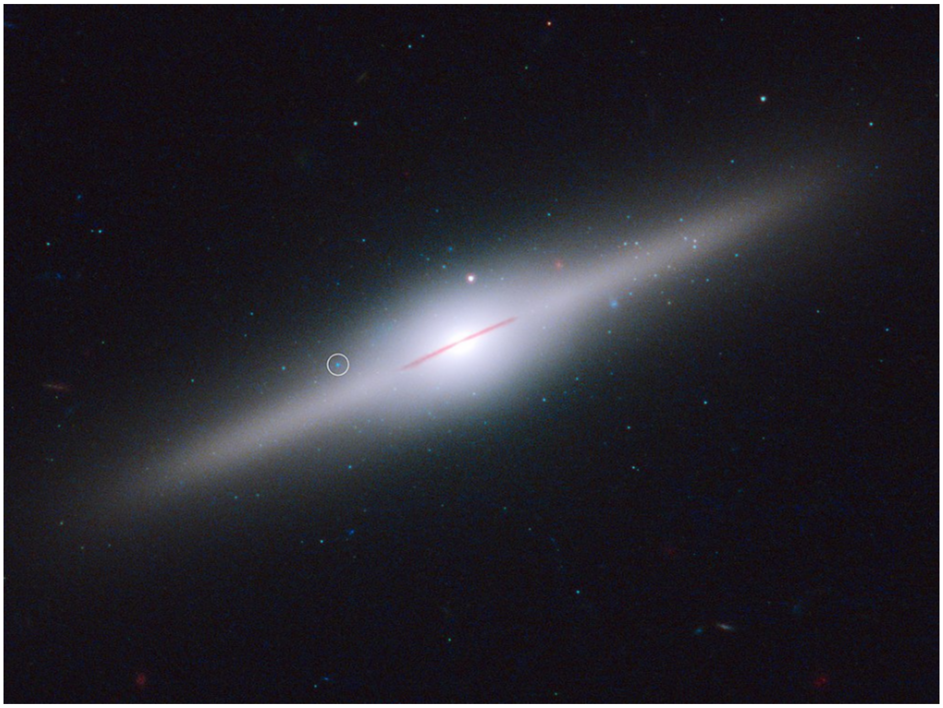

Figure 1.9: Localization of HLX-1(the encircled region) in his galaxy host ESO 243-49

Comparing to stellar black holes, it is evident that intermediate-mass black holes cannot be formed through the gravitational collapse. One of the possible scenario is the merging of many stellar black holes and the accretion of matter around [108], while the second scenario is the gravitational collapse of a dense stellar cluster for which stars collide in a chain reaction [108]. Also, another possibility is that they come from the growth of primordial black holes [108].

d) Primordial black holes in the Big Bang theory

Apart from the black holes mentioned above, there would be microscopic black holes whose quantum effects would cause a phenomenon called Hawking evaporation, these are the primordial black holes. [111]. As it is known, gravitational collapse requires great density. In the current epoch of the universe, a gravitational collapse of compact objects with mass more than about three Solar mass can create a black hole [112, 113]. However, in the early universe shortly after the Big Bang, densities were much greater, possibly allowing for the creation of black holes. In order for primordial black holes to be formed in such a dense medium, there must be initial density perturbations that can then grow under their own gravity. Different models for the early universe vary widely in their predictions of the size of these perturbations. Various models predict the creation of black holes, ranging from a Planck mass to hundreds of thousands of solar masses [111]. Furthermore, these primordial black holes could be formed by many different mechanisms, e.g., we have initial density inhomogeneities [114, 115], nonlinear metric perturbations [116–118], and blue spectra of density fluctuations [119–121]. Another classification of black holes is according to their electrical charge and angular momentum.

III- Classification of black holes according to their electrical charge and angular momentum

Since black holes can be distinguished by the presence or not of the electrical charge and angular momentum, we have the following classification

a) Schwarzschild black hole

Found by the German astrophysicist Karl Schwarzschild in 1916, it is the first, non-trivial and exact solution of the equations of general relativity [122]. It is characterised by the absence of the electric charge and angular momentum. This is a vacuum black hole. Its gravitational influence outside the event horizon is described by the Schwarzschild metric. In Schwarzschild coordinates, this metric has the signature(-,+,+,+), and is given by [123]

$$ds^2 = g_{\mu\nu}dx^\mu dx^\nu = -c^2 d\tau^2 = -\left(1 - \frac{r_s}{r}\right) c^2 dt^2 + \frac{1}{\left(1 - \frac{r_s}{r}\right)} dr^2 + r^2 d\Omega^2, \tag{1.1}$$

where

- $g_{\mu\nu}$ is the metric tensor,
- $d\Omega^2 = d\theta^2 + \sin^2\theta d\phi^2$ is the metric on the two sphere,
- r_s is the Schwarzschild radius of the massive body, a scale factor which is related to its mass M by $r_s = \frac{2GM}{c^2}$, where G is the gravitational constant,
- τ represents the proper time, which means the time measured by a clock moving along the same world line with a test particle,
- t is for $r > r_s$ the time coordinate, meaning that it can be measured by a stationary clock located infinitely far from the massive body,
- r is for $r > r_s$ the radial coordinate,
- θ is the colatitude of Ω (angle from north, in units of radians) defined after arbitrarily choosing a $z-$axis,
- ϕ is the longitude of Ω (also in units of radians) around the chosen z-axis,

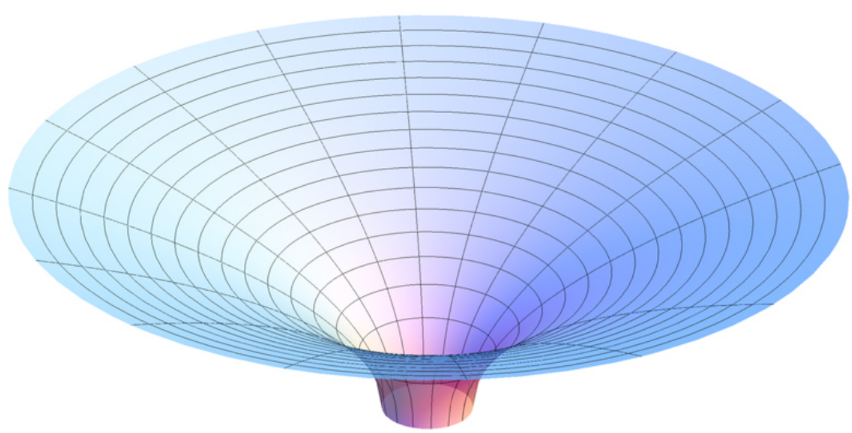

Figure 1.10: Representation of the 3-dimensional spatial geometry around a Schwarzschild black hole

b) Reissner-Nordström black hole

Its metric was discovered independently by Hans Reissner [124] in 1916 and by Gunnar Nordstöm [125] in 1918. The Reissner-Nordström geometry describes the geometry of empty space surrounding a charged black hole. If the charge of the black hole is less than its mass (measured in geometric units $G = c = 1$), then the geometry contains two horizons, an outer horizon and an inner horizon(See figure (1.11) [126]). Between the two horizons space is like a waterfall, falling faster than the speed of light, carrying everything with it. Upstream and downstream of the waterfall, space moves slower than the speed of light, and relative calm prevails [126].

In spherical coordinates (t, r, θ, ϕ), the Reissner-Nordström metric is expressed as [127]

$$ds^2 = g_{\mu\nu}dx^\mu dx^\nu = -c^2 d\tau^2 = -\left(1 - \frac{r_s}{r} + \frac{r_Q^2}{r^2}\right)c^2 dt^2 + \frac{1}{\left(1 - \frac{r_s}{r} + \frac{r_Q^2}{r^2}\right)}dr^2 + r^2 d\Omega^2, \tag{1.2}$$

where

- $g_{\mu\nu}$ is the metric tensor
- $d\Omega^2 = d\theta^2 + \sin^2\theta d\phi^2$ is the metric on the two sphere,
- r_s is the Schwarzschild radius of the massive body, a scale factor which is related to its mass M by $r_s = \frac{2GM}{c^2}$, where G is the gravitational constant,
- and r_Q is a characteristic length scale given by $r_Q^2 = \dfrac{Q^2 G}{4\pi\varepsilon_0 c^4}$,
- τ represents the proper time, which means the time measured by a clock moving along the same world line with a test particle,
- t is for $r > r_s$ the time coordinate, meaning that it can be measured by a stationary clock located infinitely far from the massive body,

- r is for $r > r_s$ the radial coordinate,
- θ is the colatitude of Ω ,
- ϕ is the longitude of Ω.

Here, the total mass of the central body and its irreducible mass can be found as [127, 128] $M_{\text{irr}} = \dfrac{c^2}{G}\sqrt{\dfrac{r_+^2}{2}} \;\rightarrow\; M = \dfrac{Q^2}{16\pi\varepsilon_0 G M_{\text{irr}}} + M_{\text{irr}}$.

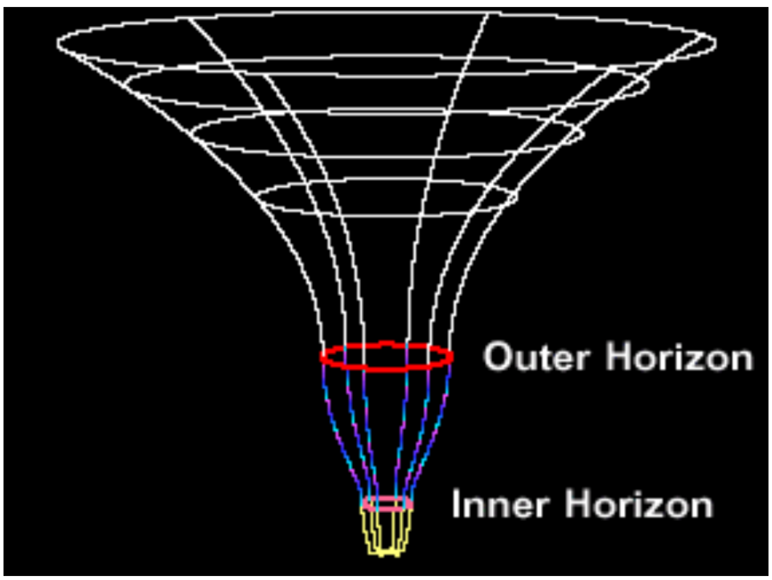

Figure 1.11: Representation of the 3-dimensional spatial geometry at an instant of Reissner-Nordström time

Fundamental charged particles like electrons and quarks are not black holes: their charge is much greater than their mass, and they do not contain horizons.

c) Kerr black hole and Kerr-Newman black hole

The Kerr black hole is a black hole that has no electric charge but does have angular momentum. In other words, a Kerr black hole is an uncharged black hole that rotates about a central axis. Like all bodies in the Universe, actual black holes must be in rotation. An exact solution of the Einstein equations corresponding to a black hole in rotation and without electric charge was discovered in 1963 by the New Zealand mathematician Roy Kerr [129]. This is also a vacuum black hole. Kerr black holes has inner horizon, outer horizon and an ergosphere, which is region where it is theoretically possible to extract energy and mass(See figure (1.12) [130]). outside the ergosphere a given particle can have a stable orbit. The corresponding metric is given by [130]

$$\begin{aligned} ds^2 &= g_{\mu\nu}dx^\mu dx^\nu = -c^2 d\tau^2 \\ &= -\left[1-\frac{\gamma}{\Sigma}\right]dt^2 + \frac{\Sigma}{\Delta}dr^2 - \frac{2a\gamma\sin^2\theta}{\Sigma}dtd\phi \\ &+ \Sigma d\theta^2 + \sin^2\theta\left[r^2+a^2+\frac{a^2\gamma\sin^2\theta}{\Sigma}\right]d\phi^2, \end{aligned} \tag{1.3}$$

where

$$\begin{aligned} \gamma &= r_s r, \\ \Delta &= r^2-\gamma+a^2, \\ \Sigma &= r^2+a^2\cos^2\theta. \end{aligned} \tag{1.4}$$

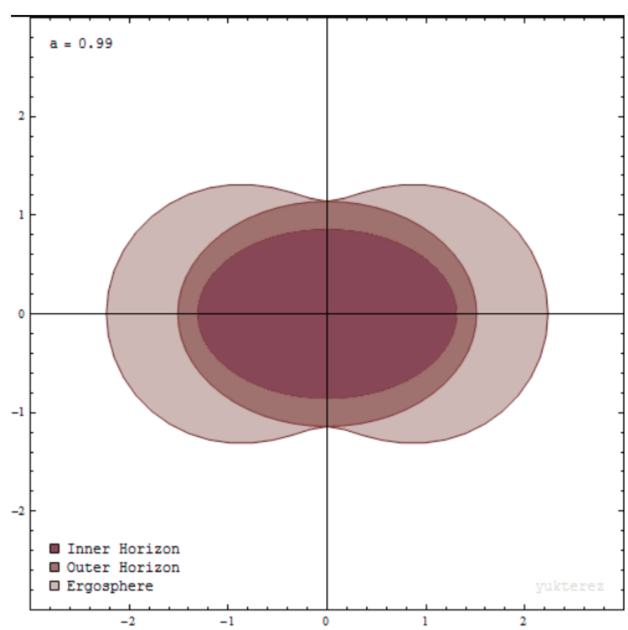

Figure 1.12: The boundaries of a Kerr black hole

On the other hand, the Kerr-Newman black hole is a black hole for which the metric is the most general asymptotically flat, stationary solution of the Einstein–Maxwell equations in general relativity that describes the spacetime geometry in the region surrounding an electrically charged and rotating mass. Its corresponding metric is similar to the Kerr metric, but the difference is located on

$$\begin{aligned} \gamma &= r_s r - r_Q^2, \\ \Delta &= r^2 - \gamma + a^2. \end{aligned} \tag{1.5}$$

Since at the singularity the predictive power of physical laws is completely broken down, then it is necessary to construct an alternative solution which avoids singularity. These solutions are called regular black holes.

e) Regular black holes

The existence of a singularity inside black holes causes a huge problem in physics, since it is characterised by the break of physical laws. Furthermore, quantum gravity could be a good frame work to apprehend this region, due to its size, but a complete theory has not been putted out. Nevertheless, an alternative approach has been constructed, and this led to regular black holes. They are black holes with no singularity, and their solution are found through the Einstein's field equations with modification to gravity, or coupled to Maxwell equations with the introduction of some exotic field, usually some form of nonlinear electrodynamic.

The first model constructed is the Bardeen black hole [131], for which there are horizons, but no singularity. Another model, Hayward black hole [132], is considered as a Bardeen-like black hole, and is surrounded by a vacuum region with a finite density and pressure, vanishing rapidly at a large distance while behaving as a cosmological constant at a small distance. another one is the modification of the Bardeen black hole by considering that the black hole comes from the gravitational collapse of some magnetic monopole in the nonlinear electrodynamics [50]. It can also be called the nonlinear magnetic-charged black hole.

Let notice that the magnetic charge is an hypothetical elementary particle which corresponds to an isolated magnet, with only one magnetic pole. Analogously to electrical charge which can be either positive or negative, the magnetic monopole can have either a net north or south magnetic charge(See figure (1.13) [133]). While they have not been detected, they have attracted a lot of interest in Grand Unified Theory(GUT) and quantum gravity.

However, it is important to notice that in the framework of astrophysics, only the mass and the kinetic momentum are really important, since the electric charge tends to be neutralized by the surrounding electrical charges [134]. Nevertheless, in cosmology, considering a distribution of charges around black holes leads to reveal several phenomenon such as thermal stability. Also it allows to get closer to quasi-real conditions at the event horizon, since telescopes are not yet able to directly identify these charges.

Mathematical study of black holes is not enough to prove their existence, this is why it is necessary to observe them. However, they are not visible, since even light cannot escape. This is why scientists have found may indirect ways to detect them.

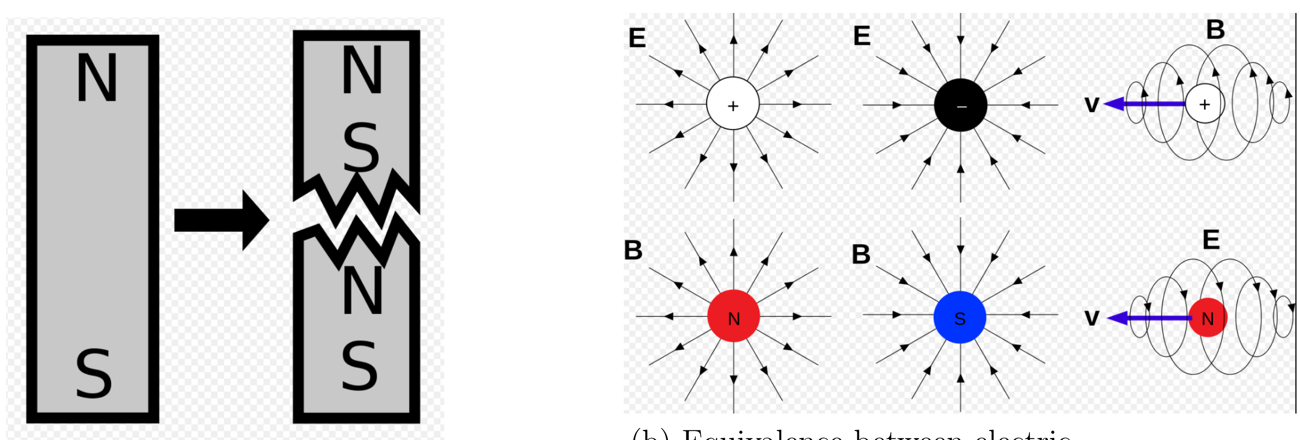

(a) A bar of magnet cut in half

(b) Equivalence between electric and magnetic charge

Figure 1.13: Magnetic monopole

1.2.2 Black holes detection

Over the past twenty years, astronomers and physicists around the world have sought to prove the existence of black holes. In this context, several methods have been developed among which we can mention:

- **Light deflection:** The black hole has a gravitational field so strong that it can bend the light that passes at a certain distance from it. It is this curvature that would prove its presence [135, 136].

- **Observation of x-rays:** Despite the fact that black holes do not emit light, their effects are detectable. As matter is pulled into the black hole, it accelerates and heats up, which leads the atoms of matter to be ionized, as the temperature increases. Once the atoms reach temperatures of a few million Kelvin, x-rays are emitted and can be detected [137]. While there are other possible x-ray sources in the universe other than black holes, black holes have fluctuating x-ray emission intensity since matter is not pulled into the black hole at a uniform, constant rate [137]

- **The determination of the mass of the two components of a binary star, from the orbital parameters**: The observation of stars shows the existence of some of them having a small mass but with a very important orbital movement (amplitude of several km/s), but the companion does not appear in the detector instruments. If it were a normal star with such a mass it would be very easy to see. This invisible massive companion can be interpreted either as a neutron star [138] or as a black hole. In this case, astrophysicists use powerful telescopes such as CHANDRA.

- **Gravitational waves detection:** Gravitational waves, "ripples in spacetime" are disturbances in the curvature of spacetime, generated by accelerated masses, that propagate as waves outward from their source at the speed of light. Albert

Einstein predicted their existence in 1916 in his general theory of relativity. But it took a century for scientists to confirm that prediction experimentally. The first signal was detected by Laser Interferometer Gravitational Wave Observatory (LIGO) on 14 September 2015 [139], provided from the coalescence of two black holes(See figure (1.15)).

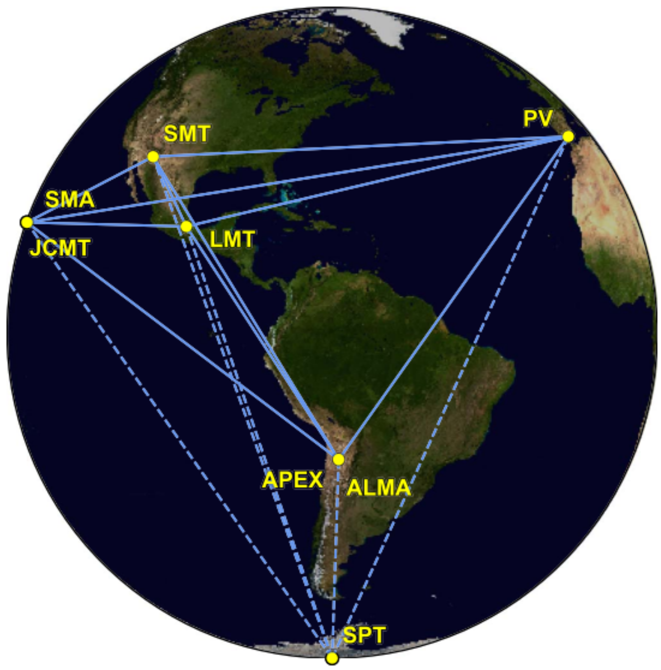

Figure 1.14: The Event Horizon Telescope(EHT Collaboration)

- **The first-ever picture of a black hole unveiled:** Despite the fact that nothing can escape from a black hole, researchers have recently obtained the image of a black hole, or more exactly the black hole's "shadow"(environment closest to the event horizon), since light cannot escape from black holes.

  This fascinating result has been obtained using the 'Event Horizon Telescope(EHT)', which is composed of many telescopes working together to create one Earth-sized observatory, all monitoring the supermassive black hole at the center of the galaxy M87, leading to the first image ever captured of a black hole(See figure (1.14)). A group of papers have been published in the Astrophysical

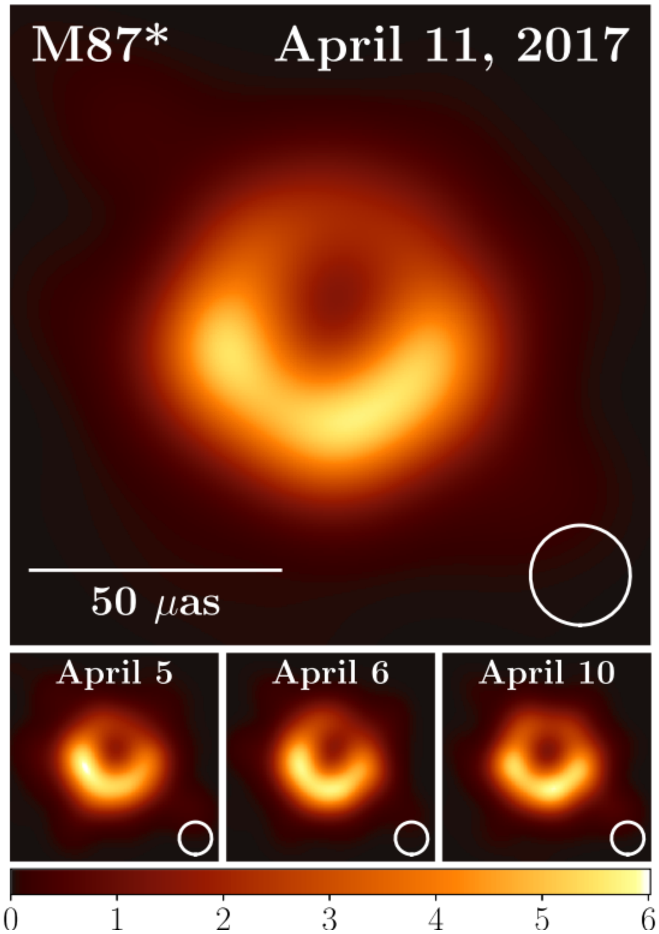

Figure 1.15: First image of the supermassive black hole of M87 Galaxy(EHT Collaboration)

Journal Letters in 2019 to describe this groundbreaking result [36–40]. The galaxy M87 is about 53 million light-years from Earth, located in the Virgo constellation. Moreover, very recently, they have published a series of articles on the first ever observed image of Sagitarius A*, the black hole inside our own galaxy [140–145].

The universe as it is known today is not made up of ordinary matter alone. Indeed, it would contain an energy that would be responsible for its accelerated expansion and the remoteness of group of galaxies, and the well known possibility to explain that is a kind of energy so-called dark energy.

1.3 Dark energy

The discovery that galaxies seem to move away from one another by Edwin Hubble in 1920 [146] has hardly affected our knowledge of the Universe. More surprisingly, observing very distant supernovae, scientists have discovered that the expansion is occurring at an accelerating rate [147]. The possible explanation of this unknown phenomenon is the presence in the universe of an energy from which certain characteristics of astrophysical observations can be deduced [148]: this energy is called dark energy.

In astrophysics, dark energy is an unknown form of energy which is responsible of the accelerated expansion of the universe [10]. In the other hand, in cosmology, dark energy is represented through the equation of state [149]

$$\epsilon \equiv \frac{P_\phi}{\rho_\phi} = \frac{\frac{1}{2}\dot{\phi} - V(\phi)}{\frac{1}{2}\dot{\phi} + V(\phi)}, \tag{1.6}$$

where ρ_ϕ is the energy density of dark energy associated with a scalar field ϕ, and the potential $V(\phi)$, and P_ϕ represents the corresponding pressure. Here, we notice that the pressure of dark energy is negative, while the density is positive.

Some candidates to be dark energy are the cosmological constant, quintessence, phantom and quintom dark energy [148, 150].

1.3.1 Cosmological constant

Denoted by the Greek letter Λ, the cosmological constant was first introduced by Einstein for the purpose of constructing a static model of the Universe. The repulsive cosmological constant was delicately fine-tuned to balance the gravitational attraction of matter [85] in order to lead to a static model. Einstein abandoned the constant in 1931 after Hubble's confirmation of the expanding universe. Today, the cosmological constant is recognized as vacuum energy, an energy assigned to empty space itself that has negative pressure and induces cosmic acceleration. It has the same value everywhere in space for all time, and it is chemically inert.

The mechanism by which this constant manifests itself remains mysterious; but what we know is that it seems inducing a sort of anti-gravity. It has the same effect as an intrinsic vacuum energy density ρ_Λ, associated with a negative pressure P_Λ. Its equation of state is expressed as

$$P_\Lambda = -\rho_\Lambda. \tag{1.7}$$

1.3.2 Quintessence dark energy

Quintessence can be defined as dynamical, evolving, spatially inhomogeneous component with negative pressure, and is a single scalar field [151]. This term was first introduced in by Robert R. Caldwell et al. [151]. It could represent the fifth dynamical component that has influenced the evolution of the Universe, in addition to the previously known baryons, leptons, photons and dark matter.

Quintessence is characterized by its equation of state

$$P_q = \epsilon\rho_q, \tag{1.8}$$

with $-1 < \epsilon \leq -\frac{1}{3}$, where P_q designates the pressure and ρ_q the energy density. Quintessence, unlike the cosmological constant, can vary in space and time. The quintessential theory also predicts an acceleration of the expansion of the universe slightly slower than the cosmological constant [152].

1.3.3 Phantom dark energy

Dark energy with $\epsilon < -1$ as defined in Eq. (1.8) is often called ”phantom dark energy.” It indicates that the energy density of dark energy increases over time. If the accelerated expansion of the universe is caused by phantom dark energy, the universe may end in a big rip, which means that the scale factor of the universe will reach infinity in a finite time from now [153].

Before the death of the universe, the phantom dark energy will rip apart all bound structures like the Milky Way, solar system, Earth, and ultimately the molecules, atoms, nuclei, and nucleons of which we are composed [154].

If we assume that the expansion of the Universe is due to phantom energy, then we will be faced with strange properties of this energy. For example, the energy density of phantom energy increases with time. It also violates the dominant-energy condition [151].

1.3.4 Quintom dark energy

Compared to phantom and quintessence models of dark energy, which are based on single scalar fields, there are also models with two fields. Especially, combining quintessence and phantom fields, one can built up the so-called "quintom models" [155].

These models, as phantom, admit the crossing of the boundary $\epsilon = -1$. There are several cosmological theories which include such a model, for example we have h-essence cosmologies [156], in which a non-canonical complex scalar field plays the role of dark energy. With h-essence type, it is found that the big rip never appears [156].

Beside dark energy, another mysterious quantity of the universe and undetected to date is dark matter, representing 23% of the content of the universe.

1.4 Dark matter

Beside dark energy, another unsolved problem on cosmology and astrophysics is dark matter, which constitutes about 23% of the total mass-energy of the universe [25] according to the Standard Model of Cosmology. Its effects are present on galaxies, where it makes the outer parts of galaxies rotate faster than expected from their starlight. The first clues to the problem appeared already in the 1930s and later, other observational arguments were raised, but the issue of the mass paradox was largely ignored by the astronomical community as a whole. In mid 1970s the amount of observational data allowed to suggest the presence of a massive and invisible population around galaxies and in clusters of galaxies [157]. However, the nature of this dark population was not clear at that time, but the hypotheses of stellar as well as of gaseous nature of the new population had serious difficulties. These difficulties disappeared when non-baryonic nature of dark matter was suggested in early 1980s [157].

Hence, many theoretical models have been proposed to be dark matter. Two of the well known are Cold Dark Matter (ΛCDM) and the Perfect fluid dark matter(PFDM).

1.4.1 Cold Dark Matter (ΛCDM/CDM)

In the CDM model, dark matter consists of non-baryonic, collisionless and cold particles. These particles are said to be cold, since they are decoupled while non-relativistic. The physical nature of CDM is currently unknown, and there are a wide variety of possibilities. Among them are Weakly Interacting Massive Particles(WIMPs) and axions [158].

Weakly Interacting Massive Particles (WIMPs) are the class of dark matter candidates that has attracted the most attention over the past four decades. WIMPs appeared for a long time as a perfect dark matter candidate, as new particles at the weak-interaction mass scale (or weak scale; approximately between 10 GeV and 1 TeV) would be produced naturally with the right relic abundance in the early Universe [159]. Presently, the best direct detection limits come from the CDMS, Edelweiss and ZEPLIN-I experiments [159]. On the other hand, axions are predicted by extensions of the Standard Model that resolve the strong CP(Charge-Parity) problem [160]. They can occur in the early Universe in the form of a Bose condensate that never comes into thermal equilibrium. Axions formed in this way are non-relativistic and can be a significant dark matter contribution if their mass is $\simeq 10^{-5} eV$.

1.4.2 Perfect fluid dark matter(PFDM)

One of the drawbacks of the CDM model is that it breaks down at small scales, as we can see in the review work in Ref. [161]. In order to account for the limits of the CDM model, warm and fuzzy dark matter models have been proposed [27,28]. These models fall into the category of perfect fluid dark matter (PFDM). The perfect fluid model has been first introduced by Kiselev, taking into account its interaction with black holes [14, 162] and then further works were putted out, such as in [163], where they study the impact of perfect fluid dark matter on galactic matter.

On this model, dark matter is described as a perfect fluid, meaning that dark matter preserves the properties of perfect fluid such as an isotropic pressure and mass density. Although simple, this model has the analytical form and the possibility of explaining the asymptotically flat rotation velocity in spiral galaxies (e.g., [162, 163]). This model of dark matter has enhanced to many work related to black holes.

Since seminal works on mathematical studies of black holes, through the Einstein theory of general relativity, black holes studies have evolved. Beside mechanical study, we have quantum, geometrical and also thermodynamic study. The last approach which will be presented in the next section.

1.5 Thermodynamics and black holes

Thermodynamics is the science that studies the relationship between heat, work, temperature, and energy [164]. In another words, thermodynamics studies the transfer of energy from one place to another and from one form to another. The key concept is that heat is a form of energy corresponding to a definite amount of mechanical work.

Until about 1798, heat was not formally recognized as a form of energy, starting by Count Rumford(Sir Benjamin Thompson [165]), a British military engineer. Rumford established the foundation of thermodynamics through observations of the proportionality between heat generated and work done. Another pioneer was the French military engineer Sadi Carnot, who introduced the concept of the heat-engine cycle and the principle of reversibility in 1824 [166]. Carnot's work concerned the limitations on the maximum amount of work that can be obtained from a steam engine operating with a high-temperature heat transfer as its driving force. Later, the German mathematician and physicist Rudolf Clausius(1822-1888), developed the first and second laws of thermodynamics, respectively [167].

1.5.1 Thermodynamic states

The applications of thermodynamic principles begins by defining a system that is in some sense distinct from its surroundings. For example, the system could be a sample of gas inside a cylinder with a movable piston, an entire steam engine, a marathon runner, the planet Earth, a neutron star, a black hole, or even the entire universe. In general, systems are free to exchange heat, work, and other forms of energy with their surroundings. Any change in value of a property does not depend on the path followed by the system from one state to another, but depends only on the initial and final states of the system. Such properties are called state functions.

1.5.2 Thermodynamic laws

Thermodynamic processes are regulated by some laws, called thermodynamic laws, which are given as follows [168]:

- **The zeroth law of thermodynamics:** When two systems are each in thermal equilibrium with a third system, the first two systems are in thermal equilibrium with each other. This property makes it meaningful to use thermometers as the "third system" and to define a temperature scale. Physically meaning, it is known that the temperature expresses hot and cold or a measure of the average of the kinetic energy of particles of a given system [169]

- **The first law of thermodynamics, or conservation of energy law:** The change in a system's internal energy is equal to the difference between heat added to the system from its surroundings and work done by the system on its surroundings.

- **The second law of thermodynamics:** Heat does not flow spontaneously from a colder region to a hotter region, or, equivalently, heat at a given temperature cannot be converted entirely into work. Consequently, the entropy of a closed system, or heat energy per unit temperature, increases over time toward some maximum value. Thus, all closed systems tend toward an equilibrium state in which entropy is at a maximum and no energy is available to make useful work. Generally speaking, the entropy is the physical quantity that is most commonly associated with a state of disorder, randomness, or uncertainty [170].

- **The third law of thermodynamics:** The entropy of a perfect crystal of an element in its most stable form tends to zero as the temperature approaches absolute zero. This allows an absolute scale for entropy to be established, and then, from a statistical point of view, the entropy determines the degree of randomness or disorder in a system.

1.5.3 Laws of black hole mechanics

In physics, black hole thermodynamics is the area of study that seeks to reconcile the thermodynamic laws with the existence of black hole event horizons.

The discovery of theoretical thermal radiation from black holes by Hawking represents a pioneering work on General relativity, even though quite a few indications of a close relationship between black hole physics and thermodynamics had emerged before this discovery [171].

The four laws of black hole mechanics, analogous to the laws of thermodynamics, where established by Brandon Carter, Stephen Hawking, and James Bardeen [172]. They are physical properties that black holes are believed to satisfy.

- **The zeroth law**: The horizon has constant surface gravity for a stationary black hole. The surface gravity, κ, of an astronomical or other object is the gravitational acceleration experienced at its surface. The surface gravity may be thought of as the acceleration due to gravity experienced by a hypothetical test particle which is very close to the object's surface and which, in order not to disturb the system, has negligible mass. For a black hole, which must be treated relativistically, one cannot define a surface gravity as the acceleration experienced by a test body at the object's surface. This is because the acceleration of a test body at the event horizon of a black hole turns out to be infinite in relativity [171]

- **The first law**: For perturbations of stationary black holes, the change of energy is related to change of area, angular momentum, and electric charge by

$$dE = \frac{\kappa}{8\pi} dA + \Omega dJ + \Phi dQ, \tag{1.9}$$

  where E is the energy, κ is the surface gravity, A is the horizon area, Ω is the angular velocity, J is the angular momentum, Φ is the electrostatic potential and Q is the electric charge. The surface gravity κ evidently plays the role of temperature. Although the quantities κ, Ω and Φ are all defined locally on the horizon, they are always constant over the horizon of a stationary black hole. [171]

- **The second law**: The horizon area is, assuming the weak energy condition, a non-decreasing function of time [171]

$$\frac{dA}{dt} \geq 0. \tag{1.10}$$

- **The third law**: It is not possible to form a black hole with vanishing surface gravity. $\kappa = 0$ is not possible to achieve. [171]

These laws mentioned above represent the foundations of thermodynamics analysis of black holes.

1.6 Conclusion

In this chapter, we presented some generalities on black holes, dark energy, dark matter, and the black hole thermodynamics. For this, we first presented how black holes can be classified. we started the classification according to their mass and ended by the classification according to the presence or not of charge and angular momentum. Afterwards, we presented black holes detection methods, and we continued with generalities on dark energy, dark matter and black hole and finally we presented the generalities on the thermodynamics of black holes, namely the thermodynamic laws of black holes. Black holes are therefore very interesting astrophysical objects for which thermodynamic study, precisely the study of phase transitions, is essential to understand their behaviour and stability. In order to achieve the goal of the thesis, we first have to present how to obtain black holes solution mathematically. To do that, we have to get the metric of charged black holes and rotating black holes, and also how to study the thermodynamics and thermodynamic stability of black holes, which is the subject of our next chapter.

Chapter II

MATERIALS AND METHODS

2.1 Introduction

The Einstein equations have led to a new way to study complex systems with strong gravity. As we know, one of the solutions of Einstein equations is black hole. Furthermore, Before making a thermodynamic study of black holes, we must present how their solutions are mathematically found. Since the first solution obtained by Schwarzschild [122], theoretical physicists obtained many other kind of solutions corresponding to black holes, either static or rotating. Since we are going to analyse the effects of quintessence dark energy, perfect fluid dark matter and rotation, we may first present how they are taken into account on the equations before solving them. Precisely, we will derive first the metric of the static nonlinear magnetic-charged AdS black hole in the quintessence field, in the background of perfect fluid dark matter. Secondly, we will put out the metric of the rotating and nonlinear magnetic-charged black hole in quintessence field. At the end, we will present some mathematical and physical tools for the thermodynamics of black holes, starting by showing how to move from the laws of black hole mechanic to the thermodynamic laws of black hole, and presenting some thermodynamic quantities such as the entropy, temperature and also how to study the thermodynamic stability of the black hole through the definition of the heat capacity.

2.2 Static charged black holes metrics

The aim of this section is to present a way to find the metric of a static charged black hole. In our case, we will derive the metric of a nonlinear magnetic-charged AdS black hole in the quintessence field, in the background of perfect fluid dark matter. We will start by the action, and then solve the Einstein-Maxwell equations.

First of all, the action corresponding to the Einstein gravity in the four-dimensional AdS spacetime is given by [56]

$$S = \int d^4x\sqrt{-g}\left[\frac{c^4}{16\pi G}(R-2\Lambda)\right], \tag{2.1}$$

where R is the scalar curvature and Λ is the cosmological constant, g is the determinant of the metric tensor $g_{\mu\nu}$, G is the Newton gravity constant and c is the light speed.

However, considering that the Einstein gravity is coupled to a nonlinear electromagnetic field, the action (2.1) becomes [56]

$$S = \int d^4x\sqrt{-g}\left[\frac{c^4}{16\pi G}(R-2\Lambda-\mathcal{L}_{\text{charge}})\right]. \tag{2.2}$$

Here, $\mathcal{L}_{\text{charge}}$ is the nonlinear electrodynamic term and is a function of the invariant $F_{\mu\nu}F^{\mu\nu}/4 \equiv F$, with $F_{\mu\nu} = \partial_\mu A_\nu - \partial_\nu A_\mu$, being the Faraday tensor of electromagnetic field, and A_ν is the gauge potential of the electromagnetic field. The expression $\mathcal{L}_{\text{charge}}$ is given by [35, 56, 173, 174]

$$\mathcal{L}_{\text{charge}} = \frac{3M}{|Q|^3}\frac{(2Q^2F)^{3/2}}{\left[1+(2Q^2F)^{3/4}\right]^2}\ , \tag{2.3}$$

where M and Q are the parameter associated with mass and magnetic charge (See III-e of the subsection (1.2.1)) of the system, respectively.

Now, taking into account the presence of quintessence energy and perfect fluid dark matter(PFDM), the action (2.2) has the form [25, 163, 175–179]

$$S = \int d^4x\sqrt{-g}\left[\frac{c^4}{16\pi G}(R-2\Lambda) - (\mathcal{L}_{\text{charge}} + 4\pi\mathcal{L}_{\text{PFDM}} - \mathcal{L}_{\text{quint}})\right], \tag{2.4}$$

The presence of PFDM in Eq. (2.4) is remarked by the term $\mathcal{L}_{\text{PDFM}}$, which is the PFDM Lagrangian density, and $\mathcal{L}_{\text{quint}}$ is the term corresponding to quintessence, which is given by [180–182]

$$\mathcal{L}_{\text{quint}} = -\frac{1}{2}\partial_\mu\phi\partial^\mu\phi - V(\phi), \tag{2.5}$$

where ϕ is the quintessential scalar field, and $V(\phi)$ is the potential.

Now, we have to apply the variational principle from Eq. (2.4), since it will allow to get the Einstein equations, that we will use in order to find the black hole metric. Making the variational principle means that we have to make the extremization of the action, with respect to the inverse of the metric $g_{\mu\nu}$. Therefore, making this mathematical calculus to the action leads to

$$0 = \frac{1}{\sqrt{-g}}\frac{\delta S(\text{action})}{\delta g^{\mu\nu}} \tag{2.6a}$$

$$= \frac{1}{\sqrt{-g}}\left\{\frac{c^4}{16\pi G}\int d^4x\frac{\delta(\sqrt{-g}(R-2\Lambda))}{\delta g^{\mu\nu}}\right. \tag{2.6b}$$

$$\left.-\left(\int d^4x\frac{\delta(\sqrt{-g}\mathcal{L}_{\text{charge}})}{\delta g^{\mu\nu}} + \int d^4x 4\pi\frac{\delta(\sqrt{-g}\mathcal{L}_{\text{PFDM}})}{\delta g^{\mu\nu}} - \int d^4x\frac{\delta(\sqrt{-g}\mathcal{L}_{\text{quint}})}{\delta g^{\mu\nu}}\right)\right\}. \tag{2.6c}$$

Now, let us compute the different derivatives present into Eq. (2.6b) and Eq. (2.6c).

Starting with the line (2.6b), we have [183]

$$\begin{aligned}
\frac{\delta(\sqrt{-g}(R-2\Lambda))}{\delta g^{\mu\nu}} &= \frac{\delta(\sqrt{-g}(R))}{\delta g^{\mu\nu}} - 2\frac{\delta(\sqrt{-g}(\Lambda))}{\delta g^{\mu\nu}} \\
&= \frac{\delta(\sqrt{-g}(g^{\alpha\beta}R_{\alpha\beta}))}{\delta g^{\mu\nu}} - 2\Lambda\frac{\delta(\sqrt{-g})}{\delta g^{\mu\nu}} \\
&= g^{\alpha\beta}R_{\alpha\beta}\frac{\delta(\sqrt{-g})}{\delta g^{\mu\nu}} + \sqrt{-g}R_{\alpha\beta}\frac{\delta(g^{\alpha\beta})}{\delta g^{\mu\nu}} + \sqrt{-g}g^{\alpha\beta}\frac{\delta(R_{\alpha\beta})}{\delta g^{\mu\nu}} \\
&- 2\Lambda\frac{\delta(\sqrt{-g})}{\delta g^{\mu\nu}}
\end{aligned}$$

$$\Rightarrow \frac{\delta(\sqrt{-g}(R-2\Lambda))}{\delta g^{\mu\nu}} = g^{\alpha\beta}R_{\alpha\beta}\frac{\delta(\sqrt{-g})}{\delta g^{\mu\nu}} + \sqrt{-g}R_{\mu\nu} + \sqrt{-g}g^{\alpha\beta}\frac{\delta(R_{\alpha\beta})}{\delta g^{\mu\nu}} - 2\Lambda\frac{\delta(\sqrt{-g})}{\delta g^{\mu\nu}} \tag{2.7}$$

Here, $R_{\mu\nu}$ is the Ricci tensor.

Before continuing, let us present how to calculate $\frac{\delta(\sqrt{-g})}{\delta g^{\mu\nu}}$.

Let start with this know property of diagonal matrix [183, 184]

$$\det(e^A) = e^{tr(A)}. \tag{2.8}$$

Then, if we define $B = e^A$, we have

$$e^A = B \Rightarrow \ln(e^A) = \ln(B) \Rightarrow A = \ln(B) \tag{2.9}$$

Hence,

$$\det(e^A) = e^{tr(A)} \Rightarrow \det(B) = e^{tr(\ln(B))} \Rightarrow \ln(\det(B)) = \ln(e^{tr(\ln(B))}), \tag{2.10}$$

$$\Rightarrow \ln(\det(B)) = tr(\ln(B)). \tag{2.11}$$

Taking the differential of both sides, we get

$$\frac{\partial(\det(B))}{\det(B)} = tr\left(\frac{\partial B}{B}\right) = tr(B^{-1} \times \partial B). \tag{2.12}$$

Coming back to the metric $g_{\alpha\beta}$, we set $B = g_{\alpha\beta}$, $B^{-1} = g^{\alpha\beta}$ and $\det(B) = g$, which allows to have

$$\frac{\delta g}{g} = g^{\alpha\beta}\delta g_{\alpha\beta}, \tag{2.13}$$

$$\Rightarrow \ \delta g = g g^{\alpha\beta}\delta g_{\alpha\beta}, \tag{2.14}$$

Therefore, we have

$$\delta(\sqrt{-g}) = -\frac{1}{2\sqrt{g}}\delta g = -\frac{1}{2\sqrt{-g}} g g^{\alpha\beta}\delta g_{\alpha\beta} = \frac{\sqrt{-g}}{2} g^{\alpha\beta}\delta g_{\alpha\beta} \tag{2.15}$$

However, we know that

$$\begin{aligned} g_{\alpha\beta}g^{\alpha\beta} &= \delta^{\alpha}_{\alpha} && (2.16)\\ \Rightarrow \ \delta(g_{\alpha\beta}g^{\alpha\beta}) &= \delta(\delta^{\alpha}_{\alpha}) = 0 && (2.17)\\ \Rightarrow \ g^{\alpha\beta}\delta g_{\alpha\beta} + g_{\alpha\beta}\delta g^{\alpha\beta} &= 0 && (2.18)\\ \Rightarrow \ g^{\alpha\beta}\delta g_{\alpha\beta} &= -g_{\alpha\beta}\delta g^{\alpha\beta}. && (2.19) \end{aligned}$$

So, we arrive at the following expression of $\delta(\sqrt{-g})$

$$\delta(\sqrt{-g}) = \frac{\sqrt{-g}}{2} g^{\alpha\beta}\delta g_{\alpha\beta} = -\frac{\sqrt{-g}}{2} g_{\alpha\beta}\delta g^{\alpha\beta} \tag{2.20}$$

$$\Rightarrow \ \frac{\delta(\sqrt{-g})}{\delta g^{\mu\nu}} = -\frac{\sqrt{-g}}{2} g_{\alpha\beta}\frac{\delta g^{\alpha\beta}}{\delta g^{\mu\nu}} = -\frac{\sqrt{-g}}{2} g_{\mu\nu}. \tag{2.21}$$

Hence, Eq. (2.7) becomes

$$\begin{aligned}\frac{\delta(\sqrt{-g}(R-2\Lambda))}{\delta g^{\mu\nu}} &= g^{\alpha\beta}R_{\alpha\beta}\left(-\frac{\sqrt{-g}}{2}g_{\mu\nu}\right)+\sqrt{-g}R_{\mu\nu}+\sqrt{-g}g^{\alpha\beta}\frac{\delta(R_{\alpha\beta})}{\delta g^{\mu\nu}}\\ &- 2\Lambda\left(-\frac{\sqrt{-g}}{2}g_{\mu\nu}\right)\\ &= -\frac{\sqrt{-g}}{2}g_{\mu\nu}R+\sqrt{-g}R_{\mu\nu}+\sqrt{-g}g^{\alpha\beta}\frac{\delta(R_{\alpha\beta})}{\delta g^{\mu\nu}}+\sqrt{-g}\Lambda g_{\mu\nu}.\end{aligned}$$

Through the boundary conditions $\nabla_\mu \delta g^{\alpha\beta}|_{\text{boundary}} = 0$ or $\delta\Gamma^\rho_{\alpha\beta}|_{\text{boundary}} = 0$, $R_{\alpha\beta}$ vanishes.

Hereby, Eq. (2.7) becomes

$$\frac{\delta(\sqrt{-g}(R-2\Lambda))}{\delta g^{\mu\nu}}=\sqrt{-g}\left(R_{\mu\nu}-\frac{1}{2}g_{\mu\nu}R+\Lambda g_{\mu\nu}\right)=\sqrt{-g}\left(G_{\mu\nu}+\Lambda g_{\mu\nu}\right), \quad (2.22)$$

where $G_{\mu\nu}$ is the Einstein tensor.

Now, we can compute the other derivatives of Eq. (2.6c).

First of all, we have

$$\begin{aligned}\frac{\delta(\sqrt{-g}\mathcal{L}_{\text{quint}})}{\delta g^{\mu\nu}} &= \sqrt{-g}\frac{\delta\mathcal{L}_{\text{quint}}}{\delta g^{\mu\nu}}+\frac{\delta\sqrt{-g}}{\delta g^{\mu\nu}}\mathcal{L}_{\text{quint}}\\ &= \sqrt{-g}\frac{\delta(-\frac{1}{2}\partial_\mu\phi\partial^\mu\phi-V(\phi))}{\delta g^{\mu\nu}}+\left(-\frac{\sqrt{-g}}{2}g_{\mu\nu}\right)\mathcal{L}_{\text{quint}}\\ &= \sqrt{-g}\left(-\frac{1}{2}\frac{\delta(g^{\mu\nu}\partial_\mu\phi\partial_\nu\phi)}{\delta g^{\mu\nu}}-\frac{1}{2}g_{\mu\nu}\mathcal{L}_{\text{quint}}\right)\\ &= \frac{\sqrt{-g}}{2}\left(-\partial_\mu\phi\partial_\nu\phi+g_{\mu\nu}(\tfrac{1}{2}\partial_\mu\phi\partial^\mu\phi+V(\phi))\right),\end{aligned} \quad (2.23)$$

$$\begin{aligned}\frac{\delta(\sqrt{-g}\mathcal{L}_{\text{charge}})}{\delta g^{\mu\nu}} &= \sqrt{-g}\frac{\delta\mathcal{L}_{\text{charge}}}{\delta g^{\mu\nu}}+\frac{\delta\sqrt{-g}}{\delta g^{\mu\nu}}\mathcal{L}_{\text{charge}}\\ &= \sqrt{-g}\frac{\delta\mathcal{L}_{\text{charge}}}{\delta F}\frac{\delta F}{\delta g^{\mu\nu}}+\left(-\frac{\sqrt{-g}}{2}g_{\mu\nu}\right)\mathcal{L}_{\text{charge}}\end{aligned} \quad (2.24)$$

However,

$$\begin{aligned}
\delta F &= \delta\left(\tfrac{1}{4}F_{\alpha\beta}F^{\alpha\beta}\right) \\
&= \tfrac{1}{4}\delta\left(g^{\alpha\rho}g^{\beta\sigma}F_{\alpha\beta}F_{\rho\sigma}\right) \\
&= \tfrac{1}{4}(\delta g^{\alpha\rho}F_{\alpha\beta}F_{\rho}{}^{\beta} + \delta g^{\beta\sigma}F_{\alpha\beta}F^{\alpha}_{\sigma}) \\
&= \tfrac{1}{4}(\delta g^{\alpha\rho}F_{\alpha\beta}F_{\rho}{}^{\beta} + \delta g^{\beta\sigma}(-F_{\beta\alpha})(-F_{\sigma}{}^{\alpha})) \\
&= \tfrac{1}{2}\delta g^{\alpha\rho}F_{\alpha\beta}F_{\rho}{}^{\beta}.
\end{aligned} \tag{2.25}$$

Hence, we get

$$\begin{aligned}
\frac{\delta(\sqrt{-g}\mathcal{L}_{\text{charge}})}{\delta g^{\mu\nu}} &= \sqrt{-g}\frac{\delta\mathcal{L}_{\text{charge}}}{\delta F}\left(\frac{1}{2}F_{\mu\beta}F_{\nu}^{\beta}\right) + \left(-\frac{\sqrt{-g}}{2}g_{\mu\nu}\right)\mathcal{L}_{\text{charge}} \\
&= \frac{\sqrt{-g}}{2}\left(\frac{\delta\mathcal{L}_{\text{charge}}}{\delta F}F_{\mu\beta}F_{\nu}^{\beta} - g_{\mu\nu}\mathcal{L}_{\text{charge}}\right)
\end{aligned}$$

Using the relation between these derivatives and the energy-momentum tensor which is given by

$$T_{\mu\nu} = \frac{2}{\sqrt{-g}}\frac{\delta(\sqrt{-g}\mathcal{L})}{\delta g^{\mu\nu}}, \tag{2.26}$$

we get [56, 182, 185]

$$T_{\mu\nu}(\text{quint}) = -\partial_\mu\phi\partial_\nu\phi + g_{\mu\nu}(\frac{1}{2}\partial_\mu\phi\partial^\mu\phi + V(\phi)) \tag{2.27}$$

$$T_{\mu\nu}(\text{charge}) = \frac{\delta\mathcal{L}_{\text{charge}}}{\delta F}F_{\mu\beta}F_{\nu}^{\beta} - g_{\mu\nu}\mathcal{L}_{\text{charge}} \tag{2.28}$$

$$T_{\mu\nu}(\text{PFDM}) = \frac{2}{\sqrt{-g}}\frac{\delta(\sqrt{-g}\mathcal{L}_{\text{PFDM}})}{\delta g^{\mu\nu}}. \tag{2.29}$$

Using this result in mind and introducing it in Eq. (2.6b) and Eq. (2.6c), the variational principle from Eq. (2.4) leads to the following equation

$$G_{\mu\nu} + \Lambda g_{\mu\nu} = \frac{8\pi G}{c^4}\left(T_{\mu\nu}(\text{charge}) + 4\pi T_{\mu\nu}(\text{PFDM}) - T_{\mu\nu}(\text{quint})\right). \tag{2.30}$$

Hence in contravariant coordinates and in units with the normalization of Newton gravity constant G, light speed c and the number π by $\frac{4\pi G}{c^4} = 1$ Eq. (2.30) becomes

$$G_\mu^\nu + \Lambda \delta_\mu^\nu = 2\left(\frac{\partial \mathcal{L}_{\text{charge}}}{\partial F} F_{\mu\rho} F^{\nu\rho} - \delta_\mu^\nu \mathcal{L}_{\text{charge}} + 4\pi T_\mu^\nu(\text{PFDM}) - T_\mu^\nu(\text{quint})\right). \quad (2.31)$$

However, $\mathcal{L}_{\text{charge}}$ is a function of the Faraday tensor of electromagnetic field, which is a solution of the Maxwell field equations, expressed as

$$\nabla_\mu \left(\frac{\partial \mathcal{L}_{\text{charge}}}{\partial F} F^{\nu\mu}\right) = 0, \quad (2.32a)$$

$$\nabla_\mu * F^{\nu\mu} = 0. \quad (2.32b)$$

Therefore, we have to make the coupling of both Einstein and Maxwell equations in order to find the tensor metric $g_{\mu\nu}$ of the black hole.

Now, since the considered dark matter is considered as a kind of perfect fluid, the energy-momentum tensor is then written as $T_\mu^\nu = \text{diag}[-\rho, p, p, p]$ [25, 163, 175], with ρ and p being the energy density and the pressure, respectively. Furthermore, in the simplest case, we assume $\frac{p}{\rho} = \delta - 1$, where δ is a constant [163].

Also, regarding the definition of a static spherically symmetric AdS black hole solution of the mass M and the magnetic charge Q in the quintessence and PFDM, the metric has to be written with ansatz [25, 173, 186]

$$ds^2 = -e^\nu dt^2 + e^\lambda dr^2 + r^2(d\theta^2 + \sin^2\theta d\phi^2) \quad (2.33a)$$

$$= -f(r)dt^2 + \frac{1}{f(r)}dr^2 + r^2(d\theta^2 + \sin^2\theta d\phi^2). \quad (2.33b)$$

Since the metric corresponds to a static spherically symmetric AdS black hole, the function $f(r)$ is chosen to have a general form which is similar to the one for the Schwarzschild metric in the AdS spacetime [56, 187].

Hence, $f(r)$ could be expressed as

$$f(r) = 1 - \frac{2P(r)}{r} - \frac{\Lambda}{3}r^2. \tag{2.34}$$

Furthermore, the ansatz used for the Maxwell field is expressed as [25, 50, 173]

$$F_{\mu\nu} = \left(\delta^\theta_\mu \delta^\varphi_\nu - \delta^\theta_\nu \delta^\varphi_\mu\right) B(r,\theta). \tag{2.35}$$

Also, the magnetic charge Q is defined through the following equation [173]

$$\frac{1}{4\pi}\int_{S_2^\infty} \boldsymbol{F} = Q, \tag{2.36}$$

with S_2^∞ being a two-sphere at the infinity.

Note furthermore that Q is the integral constant which is used to integrate the Maxwell equations (2.32a) and (2.32b), in order to find the expression of $F_{\mu\nu}$. Also, M is the integral constant which will allow to find the expression of $P(r)$. Therefore, Nam [173] has found the magnetic component of the Faraday tensor of the electromagnetic field, taking into account the Maxwell equations (2.32a), (2.32b) and (2.36), as follows

$$B(r,\theta) = Q\sin(\theta), \tag{2.37}$$

Then, due to the ansatz for the Maxwell field, we obtain the invariant F as follows

$$F = \frac{Q^2}{2r^4}. \tag{2.38}$$

Now, replacing it into Eq. (2.3), we get the nonlinear electrodynamic term as

$$\mathcal{L}_{\text{charge}} = \frac{3MQ^3}{(r^3+Q^3)^2}. \tag{2.39}$$

Considering the time component of Eq. (2.31), we get

$$G_t^t + \Lambda\delta_t^t = 2\left(\frac{\partial\mathcal{L}_{\text{charge}}}{\partial F}F_{t\rho}F^{t\rho} - \delta_t^t\mathcal{L}_{\text{charge}} + 4\pi T_t^t(\text{PFDM}) - T_t^t(\text{quint})\right). \quad (2.40)$$

Now, since the time components of energy-momentum for the PFDM and for quintessence are related to their energy density, they are expressed as follows [14, 188]

$$T_t^t(\text{PFDM}) = \frac{1}{8\pi}\frac{\alpha}{r^3}, \quad (2.41a)$$

$$T_t^t(\text{quint}) = -\frac{3\epsilon c_q}{2r^{3(\epsilon+1)}}, \quad (2.41b)$$

where α denotes the intensity of the PFDM, c_q and ϵ are the quintessence parameters.

Therefore, from Eq. (2.40), we get straightforwardly

$$G_t^t + \Lambda = -2\mathcal{L}_{\text{charge}} + \frac{\alpha}{r^3} + \frac{3\epsilon c_q}{r^{3(\epsilon+1)}}, \quad (2.42)$$

since $\delta_t^t = 1$, and $F_{t\rho}F^{t\rho} = 0$.

Before solving Eq. (2.42), we first have to find the component G_{tt} of the Einstein tensor, which is obtained using the metric Eq. (2.33). Indeed, we find

$$G_{tt} = R_{tt} - \frac{1}{2}Rg_{tt} = e^{\nu}\left[\frac{1}{r^2} - e^{-\lambda}\left(\frac{1}{r^2} - \frac{\lambda'}{r}\right)\right]. \quad (2.43)$$

Developing it, we get

$$\begin{aligned} G_{tt} &= f(r)\left[\tfrac{1}{r^2} - f(r)\left(\tfrac{1}{r^2} - \tfrac{1}{r}\left(-\tfrac{f'(r)}{f(r)}\right)\right)\right], \quad with \;\; \lambda = -\ln f(r) \\ &= f(r)\left[\tfrac{1}{r^2} - f(r)\left(\tfrac{1}{r^2} - \tfrac{1}{rf(r)}\left[2\left(\tfrac{1}{r}\tfrac{dP(r)}{dr} - \tfrac{P(r)}{r^2} + \tfrac{\Lambda}{3}r^2\right)\right]\right)\right] \\ &= f(r)\left(\tfrac{2}{r^2}\tfrac{dP(r)}{dr} + \Lambda\right). \end{aligned} \quad (2.44)$$

Therefore, the component G_t^t from Eq. (2.43) is expressed as

$$G_t^t = g^{tt}G_{tt} = (-f(r))^{-1}f(r)\left(\frac{2}{r^2}\frac{dP(r)}{dr} + \Lambda\right), \tag{2.45}$$

meaning that

$$G_t^t = -\frac{2}{r^2}\frac{dP(r)}{dr} - \Lambda. \tag{2.46}$$

Now, replacing Eq. (2.46) into Eq. (2.42), we get

$$\frac{dP(r)}{dr} = \frac{3MQ^3r^2}{(r^3+Q^3)^2} - \frac{\alpha}{2r} - \frac{3\epsilon c_q}{2r^{3\epsilon+1}}. \tag{2.47}$$

By integration, we obtain

$$P(r) = -\frac{MQ^3}{r^3+Q^3} - \frac{\alpha}{2}\ln\frac{r}{|\alpha|} + \frac{c_q}{2r^{3\epsilon}} + C^{st}. \tag{2.48}$$

Now, to find the integral constant C^{st}, we will use the boundary condition [173,188]

$$M = \lim_{r\to\infty}\left\{P(r) + \frac{\alpha}{2}\ln\frac{r}{|\alpha|} - \frac{c_q}{2r^{3\epsilon}}\right\} = \lim_{r\to\infty}\left\{-\frac{MQ^3}{r^3+Q^3} + C^{st}\right\}, \tag{2.49}$$

leading to

$$C^{st} = M. \tag{2.50}$$

Hence, the functions $P(r)$ and $f(r)$ are respectively given by

$$P(r) = \frac{Mr^3}{r^3+Q^3} - \frac{\alpha}{2}\ln\frac{r}{|\alpha|} + \frac{c_q}{2r^{3\epsilon}}, \tag{2.51}$$

$$f(r) = 1 - \frac{2Mr^2}{r^3+Q^3} + \frac{\alpha}{r}\ln\frac{r}{|\alpha|} - \frac{c_q}{r^{3\epsilon+1}} - \frac{\Lambda}{3}r^2. \tag{2.52}$$

Hereby, the spherically symmetric solution for the action (2.4) is obtained as

$$\begin{aligned} ds^2 &= -f(r)dt^2 + \tfrac{1}{f(r)}dr^2 + r^2(d\theta^2 + \sin^2\theta d\phi^2), \\ \text{with } f(r) &= 1 - \tfrac{2Mr^2}{r^3+Q^3} + \tfrac{\alpha}{r}\ln\tfrac{r}{|\alpha|} - \tfrac{c_q}{r^{3\epsilon+1}} - \tfrac{\Lambda}{3}r^2. \end{aligned} \tag{2.53}$$

Let notice first that if we replace the quintessence parameter $c = 0$ and the cosmological constant $\Lambda = 0$ into Eq. (2.53), we recover the metric of nonlinear magnetic-charged black hole surrounded by dark matter considered by Ma et *al.* [35], expressed as

$$\begin{aligned} ds^2 &= -f(r)dt^2 + \tfrac{1}{f(r)}dr^2 + r^2(d\theta^2 + \sin^2\theta d\phi^2), \\ \text{with } f(r) &= 1 - \tfrac{2Mr^2}{r^3+Q^3} + \tfrac{\alpha}{r}\ln\tfrac{r}{|\alpha|}. \end{aligned} \tag{2.54}$$

Now, using the horizon property [78, 173], and solving the following equation at the horizon

$$f(r_h) = 0, \tag{2.55}$$

leads to

$$M = \frac{(r_h^3 + Q^3)}{2r_h^2}\left(1 + \frac{\alpha}{r_h}\ln\frac{r_h}{|\alpha|} - \frac{c_q}{r_h^{3\epsilon+1}} - \frac{\Lambda}{3}r_h^2\right). \tag{2.56}$$

Eq. (2.56) gives the relation between the black hole mass and its horizon radius.

As we know, in the universe, astrophysical black holes are spinning, hence, it is interesting to find their mathematical solutions which are similar to the Kerr solutions. Now, we are going to find the mathematical solutions corresponding to rotating charged black holes.

2.3 Rotating charged black holes metrics

In this section, we will present how to get the metric of a rotating and nonlinear magnetic-charged black hole surrounded by quintessence, through the modified Newman-Janis method. Proposed by Newman and Janis [189], the Newman-Janis method method has been widely used by many authors [21, 46, 57, 190–200] in order to generate a rotational spacetime from a spherically symmetric spacetime, without sloving Einstein's field Equations. Especially, we will use the modified NJA without complexification of coordinates, proposed by Azreg-Aïnou [47, 201, 202].

To start with, let us consider a static spherically symmetric spacetime metric, expressed in Boyer-Lindquist coordinates (t, r, θ, ϕ) as

$$ds^2 = -f(r)dt^2 + g^{-1}(r)dr^2 + h(r)d\Omega^2, \ d\Omega^2 = d\theta^2 + \sin^2\theta d\phi^2. \tag{2.57}$$

From Eq. (2.57), we recall that for the static nonlinear magnetic-charged black hole in the quintessence field, we have [173]

$$g(r) = f(r) = 1 - \frac{2Mr^2}{r^3 + Q^3} - \frac{c_q}{r^{3\epsilon+1}}, \quad h(r) = r^2 \tag{2.58}$$

At the next step of the NJA, we will transform the metric above from Boyer-Lindquist coordinates (t, r, θ, ϕ) to Eddington-Finkelstein coordinates (u, r, θ, ϕ), by carrying out the following coordinate transformation

$$du = dt - \frac{dr}{\sqrt{fg}}. \tag{2.59}$$

Hence, the metric (2.57) gets the new form

$$ds^2 = -f(r)du^2 - 2\sqrt{\frac{f(r)}{g(r)}}dudr + h(r)(d\theta^2 + \sin^2\theta d\phi^2). \tag{2.60}$$

This transformation enables to obtain the non-zero components of the contravariant tensor $g^{\mu\nu}$ in terms of the null tetrad, by the following equation

$$g^{\mu\nu} = -l^{\nu}n^{\nu} - l^{\nu}n^{\mu} + m^{\mu}\bar{m}^{\nu} + m^{\nu}\bar{m}^{\mu}, \tag{2.61}$$

where

$$\begin{aligned}
l^{\mu} &= \delta^{\mu}_{r}, \\
n^{\mu} &= \sqrt{\tfrac{g(r)}{f(r)}}\delta^{\mu}_{m}u - \tfrac{f(r)}{2}\delta^{\mu}_{r}, \\
m^{\mu} &= \tfrac{1}{\sqrt{2h(r)}}\delta^{\mu}_{\theta} + \tfrac{i}{\sqrt{2h(r)}\sin\theta}\delta^{\mu}_{\phi}, \\
\bar{m}^{\mu} &= \tfrac{1}{\sqrt{2h(r)}}\delta^{\mu}_{\theta} - \tfrac{i}{\sqrt{2h(r)}\sin\theta}\delta^{\mu}_{\phi}.
\end{aligned} \tag{2.62}$$

Let recall that vectors l and n are real, while m is a complex vector and $\bar{m}$ the complex conjugate of m. Furthermore, they satisfy orthogonality, isotropic and normalization conditions [46, 189], expressed as

$$l^{\mu}m_{\mu} = l^{\mu}\bar{m}_{\mu} = n^{\mu}m_{\mu} = n^{\mu}\bar{m}_{\mu} = 0, \tag{2.63}$$

$$l^{\mu}l_{\mu} = n^{\mu}n_{\mu} = m^{\mu}m_{\mu} = \bar{m}^{\mu}\bar{m}_{\mu} = 0, \tag{2.64}$$

$$l^{\mu}n_{\mu} = 1,\ m^{\mu}\bar{m}_{\mu} = -1. \tag{2.65}$$

Now, for the next step of the NJA, let us consider a complex transformation of the $u - r$ plane, Indeed, the new coordinate system allows to study the system as a rotating one. The complex transformation is expressed in the following manner [46]

$$u \rightarrow u - ia\cos\theta,\ r \rightarrow r + ia\cos\theta, \tag{2.66}$$

with a the rotating parameter.

At the same time, we also assume that due to these transformations, the metric functions also turn into a new form [47]

$$f(r) \rightarrow F(r,a,\theta),\ g(r) \rightarrow G(r,a,\theta),\ h(r) \rightarrow \Sigma = r^2 + a^2\cos^2\theta. \tag{2.67}$$

Hence, δ^μ_ν transform as vectors [35]

$$\begin{aligned}\delta^\mu_r &\rightarrow \delta^\mu_r,\ \delta^\mu_u \rightarrow \delta^\mu_u \\ \delta^\mu_\theta &\rightarrow \delta^\mu_\theta + ia\sin\theta(\delta^\mu_u - \delta^\mu_r),\ \delta^\mu_\phi \rightarrow \delta^\mu_\phi,\end{aligned} \tag{2.68}$$

which leads the null tetrad in Eq. (2.62) to take the new form

$$\begin{aligned}l^\mu &= \delta^\mu_r, \\ n^\mu &= \sqrt{\tfrac{G}{F}}\delta^\mu_u - \tfrac{F}{2}\delta^\mu_r, \\ m^\mu &= \tfrac{1}{\sqrt{2\Sigma}}\left[\delta^\mu_\theta + ia\sin\theta(\delta^\mu_u - \delta^\mu_r) + \tfrac{i}{\sin\theta}\delta^\mu_\phi\right], \\ \bar{m}^\mu &= \tfrac{1}{\sqrt{2\Sigma}}\left[\delta^\mu_\theta - ia\sin\theta(\delta^\mu_u - \delta^\mu_r) - \tfrac{i}{\sin\theta}\delta^\mu_\phi\right].\end{aligned} \tag{2.69}$$

These new expressions of the null tetrad allow to get the components of the metric tensor $g^{\mu\nu}$ through Eq. (2.61) as follows

$$\begin{aligned}g^{uu} &= \tfrac{a^2\sin^2\theta}{\Sigma},\ g^{ur} = -\sqrt{\tfrac{G}{F}} - \tfrac{a^2\sin^2\theta}{\Sigma},\ g^{u\phi} = \tfrac{a}{\Sigma}, \\ g^{rr} &= G + \tfrac{a^2\sin^2\theta}{\Sigma},\ g^{r\phi} = -\tfrac{a}{\Sigma},\ g^{\theta\theta} = \tfrac{1}{\Sigma}, \\ g^{\phi\phi} &= \tfrac{1}{\Sigma\sin^2\theta}.\end{aligned} \tag{2.70}$$

Therefore, the covariant non-zero components in the Eddington-Finkelstein coordinates (u, r, θ, ϕ) give

$$\begin{aligned}g_{uu} &= -F,\ g_{ur} = -\sqrt{\tfrac{F}{G}},\ g_{u\phi} = a\left(F - \sqrt{\tfrac{F}{G}}\right)\sin^2\theta, \\ g_{r\phi} &= a\sqrt{\tfrac{F}{G}}\sin^2\theta,\ g_{\theta\theta} = \Sigma, \\ g_{\phi\phi} &= \sin^2\theta\left[\Sigma + a^2\left(2\sqrt{\tfrac{F}{G}} - F\right)\sin^2\theta\right].\end{aligned} \tag{2.71}$$

At the last step, we have to come back to the Boyer-Lindquist coordinates (t, r, θ, ϕ), using the following coordinate transformation [46,47]

$$du = dt + \lambda(r)dr,\ d\phi = d\phi + \chi(r)dr, \tag{2.72}$$

where $\lambda(r)$ and $\chi(r)$ are the transformation functions found using the fact that all non-diagonal components of the metric tensor, except the coefficient $g_{t\phi}(g_{\phi t})$, are equal to zero.

Hence, we have

$$\begin{aligned} \lambda(r) &= -\tfrac{k(r)+a^2}{g(r)h(r)+a^2}, \\ \chi(r) &= -\tfrac{a}{g(r)h(r)+a^2}, \end{aligned} \tag{2.73}$$

with

$$k(r) = \sqrt{\frac{g(r)}{f(r)}}h(r), \tag{2.74}$$

and

$$F(r,\theta) = \frac{(gh + a^2\cos^2\theta)\Sigma}{(k + a^2\cos^2\theta)^2},\ G(r,\theta) = \frac{(gh + a^2\cos^2\theta)}{\Sigma}. \tag{2.75}$$

Therefore, using the transformation (2.72), the tensor metric (2.71) leads to the following metric expressed in the Boyer-Lindquist coordinates (t, r, θ, ϕ)

$$\begin{aligned} ds^2 &= -\tfrac{(gh+a^2\cos^2\theta)\Sigma}{(k+a^2\cos^2\theta)^2}dt^2 + \tfrac{\Sigma}{gh+a^2}dr^2 - 2a\sin^2\theta\left[\tfrac{k-gh}{(k+a^2\cos^2\theta)^2}\right]\Sigma d\phi dt + \Sigma d\theta^2 \\ &+ \Sigma\sin^2\theta\left[1 + a^2\sin^2\theta\tfrac{2k-gh+a^2\cos^2\theta}{(k+a^2\cos^2\theta)2}\right]d\phi^2, \end{aligned} \tag{2.76}$$

where Σ is expressed in Eq. (2.67), k is defined in Eq. (2.74), while f and g are the functions present in the metric (2.57).

Since we are in the case of nonlinear magnetic-charged black hole surrounded by quintessence, we can use the definition of f, g and h expressed in Eq. (2.58), and substitute them in Eq. (2.76).

we get the metric of rotating and nonlinear magnetic-charged black hole surrounded by quintessence expressed as follows

$$\begin{aligned} ds^2 &= g_{\mu\nu}dx^\mu dx^\nu \\ &= -\left[1-\tfrac{2\rho r}{\Sigma}\right]dt^2+\tfrac{\Sigma}{\Delta}dr^2-\tfrac{4a\rho r\sin^2\theta}{\Sigma}dtd\phi \\ &+ \Sigma d\theta^2+\sin^2\theta\left[r^2+a^2+\tfrac{2a^2\rho r\sin^2\theta}{\Sigma}\right]d\phi^2, \end{aligned} \tag{2.77}$$

where

$$\begin{aligned} \Delta &= r^2-2\rho r+a^2, \\ \Sigma &= r^2+a^2\cos^2\theta, \\ 2\rho &= \tfrac{2Mr^3}{Q^3+r^3}+\tfrac{c_q}{r^{3\epsilon}}. \end{aligned} \tag{2.78}$$

Here, Q is the magnetic charge, a the rotating parameter, ϵ and c_q are quintessential parameters. Also, we can notice that this metric has been found by Benavides et *al.* [57].

In order to make a thermodynamic study of black holes, we may present some tools which will help to make a good analysis of the thermodynamic behaviour of black holes, which will be the aim of the next section.

2.4 Tools for the thermodynamic study of black holes

Considering that black holes could have thermodynamic properties leads to apprehend them in a new way. Indeed, thermodynamic study is considered as a manner to reconcile both classical and quantum theory. Therefore many studies have shown that black holes can undergo several phenomena such as Hawking radiation and second-order phase transition, hence the importance to make the thermodynamic study of black holes.

2.4.1 Black holes as thermodynamic objects

Since black holes are not terrestrial physical objects for which one can withdraw a certain quantity and make an experimental study, it is necessary to build a theoretical framework leading to appreciate how does the black hole behaves. For the thermodynamic study, it has been shown by Bekenstein that black hole should have an entropy which is proportional to the area of the event horizon A [3]. Afterwards, Hawking was able to find the proportionality factor [1]. Hence, we have

$$S = \frac{k_B A}{4 l_p^2}, \tag{2.79}$$

where k_B is the Boltzmann constant and $l_p = \sqrt{G\hbar/c^3}$ is the Planck length.

Furthermore, another outstanding result on black holes is the Hawking radiation, which would lead the black hole to emit a thermal radiation at a certain temperature(Hawking temperature). Therefore, it has been suggested that black hole may have a temperature, which is proportional to the surface gravity $\kappa(T_h = \kappa/2\pi)$. Hence, having such properties leads to have a good framework to make the thermodynamic study of black holes.

In the other hand considering this analogy allows to define the thermodynamic laws of black hole from the mechanic law of black hole defined in section (1.5.3). As an example, the first law of the black hole thermodynamic, which states the conservation of mass-energy is defined as

$$dM = T_h dS + dW, \tag{2.80}$$

where T_h is the black hole temperature and W is the work done from the exterior of the black hole.

2.4.2 Thermodynamic quantities

Here, we will present how to get some thermodynamic quantities which can be found in order to study the thermodynamic behaviour of the black hole. Therefore, as an example, we will make an application onto two types of black holes, namely a static spherically symmetric black hole and a rotating one.

Starting with the black hole mass(energy) M, for a given tensor metric $g^{\mu\nu}$ it can be found through the horizon property, defined as follows [57]

$$g^{rr} = 0. \tag{2.81}$$

Let notice that if we are in the case of static spherically symmetric black hole defined as

$$ds^2 = -f(r)dt^2 + g(r)^{-1}dr^2 + r^2(d\theta^2 + \sin^2\theta d\phi^2), \tag{2.82}$$

the horizon property becomes

$$g(r_h) = 0, \tag{2.83}$$

where r_h represents the horizon radius.

However, for a rotating black hole, which has a metric similar to Eq. (2.77), the horizon property leads to the following relation

$$\frac{\Delta(r_h)}{\Sigma(r_h)} = 0. \tag{2.84}$$

In the thermodynamics of black holes, we usually use the horizon area [46] to find the entropy. Therefore, after normalization of (2.79)($k_B = l_p = 1$) we have

$$S = \frac{A}{4} = \frac{1}{4}\int_0^{2\pi} d\phi \int_0^{\pi} d\theta \sqrt{g_{\theta\theta}g_{\phi\phi}}. \tag{2.85}$$

Then, we can compute the black hole temperature, using the definition of first law of black hole thermodynamics in Eq. (2.80). Indeed, we have [173]

$$T_h = \frac{\partial M}{\partial S}. \tag{2.86}$$

However, in the particular case of regular Bardeen black holes with a tensor metric $g^{\mu\nu}$, the entropy is found on a different manner, since we have a nonlinear distribution of the electromagnetic field. Indeed, we have to start deriving the temperature from the surface gravity definition [49] as follows

$$T_h = \frac{\kappa}{2\pi} = \frac{1}{4\pi}\frac{d\{g^{rr}\}}{dr}. \tag{2.87}$$

Therefore, using the first law equation (2.80), we find the entropy through the following equation

$$S_h = \int \frac{1}{T_h}\frac{\partial M}{\partial r_h} dr_h. \tag{2.88}$$

Now, the enthalpy is usually defined as the black hole mass($H = M$). However, if we are for example in the case of the AdS (Anti de Sitter) spacetime, where we have the cosmological constant which plays the role of the pressure, we have

$$H = M(S, P), \tag{2.89}$$

where S is the entropy.

Moreover, with this in mind one can calculate the Gibbs free energy or the free enthalpy using this formula

$$G = H - TS, \tag{2.90}$$

and the thermodynamic volume as follows

$$V = \left(\frac{\partial H}{\partial P}\right)_S. \tag{2.91}$$

2.5 Phase transitions

2.5.1 Definition

In physics, phase transition can be defined as a physical transformation of a system from one phase to another, induced by the variation of an external control parameter (temperature, magnetic field, etc.). Phase transitions are ubiquitous in nature, and one of the well known from which we are all familiar is about the phases of water(vapour, liquid and ice), and with the change from one to the other. Phase transition is a vast subject, and a lot of research effort is still being dedicated to it, both from experimental and theoretical points of view. The first microscopically-based understanding of phase transitions was made in 1873 by van der Waals [203], where he presented a primitive theory of the liquid-gas transition. In his doctoral thesis he found an equation of state and he presented a way to link the equation of state parameters to a molecular model. Thereby, he laid down the basic ideas on which the modern theoretical understanding has emerged. Later, Landau [204] (1937) proposed a phenomenological (not fully microscopic) approach that was crucial to understand second-order phase transitions. And further, Wilson [205] (1971) and others, developed a powerful and unifying set of concepts for second-order phase transitions.

2.5.2 Classification of phase transitions

When talking about phase transitions, we must first know how we can classify them.

A) Ehrenfest classification of phase transitions

The best adapted thermodynamic function used to the study of these transformations is the free enthalpy G defined as follows [206]

$$dG = -SdT + VdP \quad \text{or} \quad dg = -sdT + vdP. \tag{2.92}$$

Here, g is the free mass enthalpy function, S the entropy s the mass entropy, V the volume, v the mass volume, T the temperature and P is the pressure.

Therefore, the first derivatives of the free enthalpy G are from Eq. (2.92) in the following form

$$\left(\frac{\partial G}{\partial T}\right)_P = -S \quad \text{and} \quad \left(\frac{\partial G}{\partial P}\right)_T = V, \tag{2.93}$$

while the three second derivatives are expressed as

$$\begin{cases} \left(\frac{\partial^2 G}{\partial T^2}\right)_P &= -\left(\frac{\partial S}{\partial T}\right)_P, \\ \left(\frac{\partial^2 G}{\partial P^2}\right)_T &= \left(\frac{\partial V}{\partial P}\right)_T, \\ \left(\frac{\partial^2 G}{\partial T \partial P}\right) &= \left(\frac{\partial V}{\partial T}\right)_P = -\left(\frac{\partial S}{\partial P}\right)_T. \end{cases} \tag{2.94}$$

Taking into account the definitions of the heat capacity at constant pressure C_p, the isothermal compressibility coefficient κ_T, and the isobaric expansion coefficient β_p, we conclude that we have finally [206]

$$\begin{cases} \left(\frac{\partial^2 G}{\partial T^2}\right)_P &= -\frac{C_P}{T}, \\ \left(\frac{\partial^2 G}{\partial P^2}\right)_T &= -V\kappa_T, \\ \left(\frac{\partial^2 G}{\partial P \partial T}\right) &= V\beta_P. \end{cases} \tag{2.95}$$

Here, we recall that the heat capacity is defined as the amount of heat to be supplied to an object to produce a unit change in its temperature [207].

In the modern classification scheme provided from the definition of the free enthalpy, phase transitions are divided into two categories, named similarly to the Ehrenfest classes:

- **First-order phase transitions** are those that involve a latent heat. During such a transition, a system either absorbs or releases a fixed (and typically large) amount of energy per volume. As heat is added during this process, the temperature of the system will stay constant, meaning that the system is in a "mixed-phase regime" in which some parts of the system have completed the transition and others have not. As an example, we have the smelting of ice or the boiling of water (the water does not instantly turn into vapor, but forms a turbulent mixture of liquid water and vapor bubbles) [208].

  First-order phase transitions are identified from the plot of the first derivatives of G like the entropy(See Eq. (2.93)), for which we see a discontinuity [209].

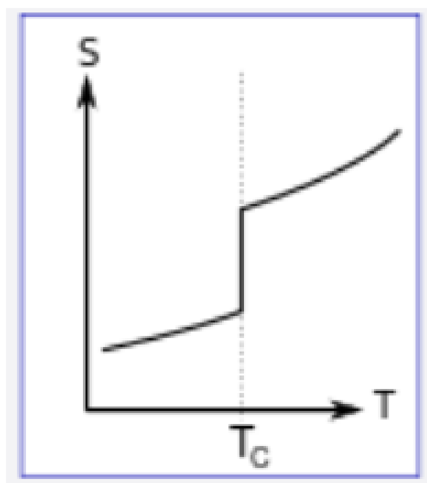

Figure 2.1: Illustration of first-order phase transition, with the plot of the entropy

- **Second-order phase transitions**. Also called continuous phase transitions, they are characterized by the absence of latent heat associated, and by the gigantic fluctuations in the system. As an example of second-order phase transitions we have the Ferromagnetic-paramagnetic transition, superconducting transition(Superconductivity is a set of physical properties observed in certain materials where electrical resistance vanishes and magnetic flux fields are expelled from the material) and the superfluid transition(a superfluid is a state of matter in which matter behaves like a zero-viscosity fluid.) [208].

Second order transitions are localized through discontinuities in plot of the second derivatives of G like the heat capacity C(See Eq. (2.95)) [206, 209].

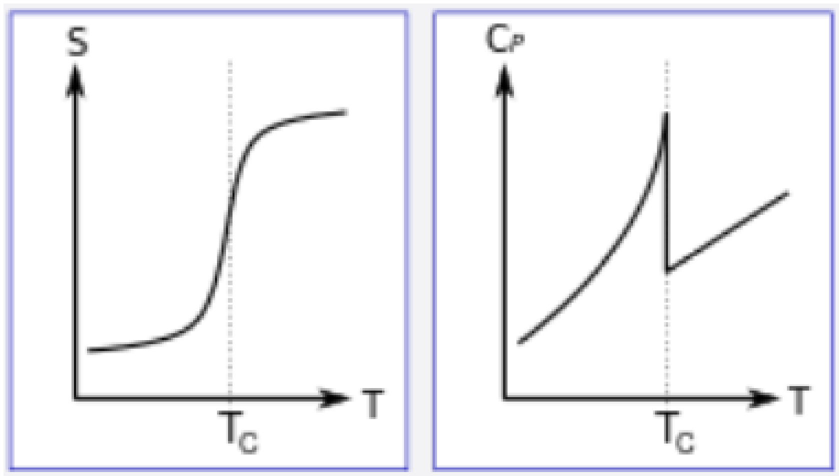

Figure 2.2: Illustration of second-order phase transition, with the plot of the entropy and heat capacity

B) van der Waals Phase transition in fluids

One of the used model describing real conditions for liquid-gas phase transition is the van der Waals model. Instead of the ideal gas model with the equation of state $Pv = RT$, where P is the molar pressure, v is the molar volume, T is the temperature and R is the universal gas constant, the one corresponding to the van der Waals is expressed as [210, 211]

$$\left(P + \frac{a}{v^2}\right)(v - b) = RT. \tag{2.96}$$

A plot of the $P - v$ diagram(See figure (2.3) [212]) through this equation with given constant values of temperature(isothermal cures), shows the existence of a critical temperature (T_c), from which we are able to see two types of curves, which conduct respectively to different behaviours of the system.

- For a given temperature $T > T_c$, the van der Waals equation only associates

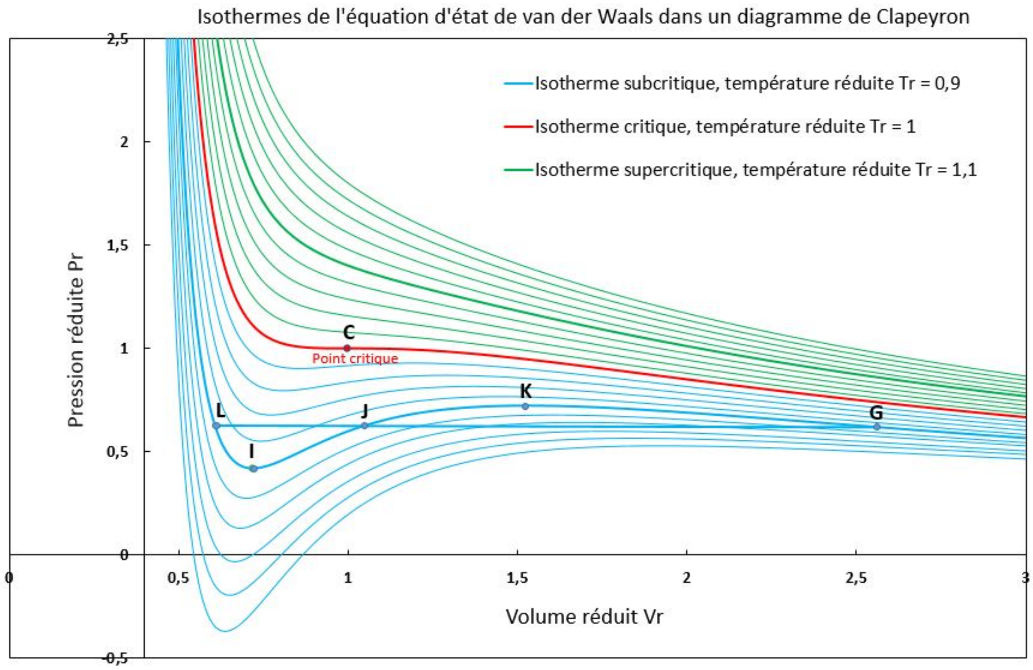

Figure 2.3: Illustration of $P-V$ isotherms of the van der Waals equation of state

a single volume with a given pressure (green curves in figure (2.3)): the cubic equation of state produces only a single real root (a single molar volume) whatever the value of the pressure.

- For a given temperature $T < T_c$, the behaviour is more complex (turquoise blue curves in figure (2.3)): the cubic equation of state can produce, depending on the pressure, a single real root (a single molar volume) or three real roots (three molar volumes).

Let recall that the curve for the temperature $T = T_c$ represents the boundary of both behaviour previously mentioned. Also the critical values are obtained through the following equations

$$\left(\frac{\partial P}{\partial v}\right)_{T_c} = 0, \quad \left(\frac{\partial^2 P}{\partial v^2}\right)_{T_c} = 0. \tag{2.97}$$

Those equations lead to get T_c and v_c. Afterwards, when replacing them into Eq.

(2.96), we find P_c.

2.6 Conclusion

Our aim in this chapter was essentially focused on presenting how to get the metric of black holes necessary for our study, and to present some tools for the black holes thermodynamics. Especially, we started by obtaining the metric of the static nonlinear magnetic-charged AdS black hole surrounded by quintessence and perfect fluid dark matter, by coupling the Einstein equations with the Maxwell equations. To do that, we defined the corresponding action, and applied its extermination with respect to the inverse of the metric. This led to get the Einstein-Maxwell equations that we solved to find the metric. In the second part, we putted out the metric for the rotating and nonlinear magnetic charged black hole in the quintessence, by using the modified Newman-Janis algorithm, which is the common way used to get rotating solutions. Afterwards, in the last part, we presented some tools related to the thermodynamic study of black holes such as temperature, entropy and heat capacity, and therefore we presented a way to study the thermodynamic stability of a given black hole. Now, in the next chapter, we will study the effects of perfect fluid dark matter, quintessence dark energy and rotation, by making the thermodynamic study of a nonlinear magnetic-charged black hole we found. Especially, we will find various thermodynamic quantities provided from this black hole and taking into account perfect fluid dark matter, quintessence dark energy and rotation. Therefore, we will analyse their curves in order to appreciate their impact on the black hole.

Chapter III

RESULTS AND DISCUSSION

3.1 Introduction

Black hole thermodynamics is an interesting subject widely studied in modern cosmology and is the area of study which seeks to reconcile the laws of thermodynamics with the existence of black hole event horizon, by seeking to join the general relativity with the quantum field theory. Studying thermodynamic of black holes allows to apprehend several properties of black holes, from their stability to the evolution of their entropy and Hawking temperature. Black holes become hence real laboratories for extracting thermodynamic properties. Our aim in this chapter is to study the effects of dark energy, dark matter and rotation onto the thermodynamics of the nonlinear magnetic-charged black hole. To do that, first of all, we will study the effects of dark energy, by computing various thermodynamic quantities of the nonlinear magnetic-charged black hole surrounded by quintessence dark energy. Then, we will analyse the impact of dark matter, precisely the perfect fluid dark matter, on the thermodynamics of the nonlinear magnetic-charged black hole. Afterwards, we will investigate what could happen if quintessence dark energy and perfect fluid dark matter are considered simultaneously. Let notice that in this study, we consider that the black hole is under an AdS spacetime. At the end, we will study how rotation and quintessence energy can impact the behaviour of the black hole, this is why we focus the study here on the rotating and nonlinear magnetic charged black hole surrounded by quintessence. In all of this study, we will be able to identify at which conditions black holes become stable or unstable, and also if they can undergo a second order phase transition, recognized by the presence of a discontinuity in the plot of the heat capacity.

3.2 Effects of dark energy on the thermodynamics of black hole

Here, in order to study the effects of dark energy, we will choose the metric of a non-linear magnetic-charged black hole surrounded by quintessence. It can be obtained through the metric (2.77), by fixing the rotating parameter $a = 0$. Therefore, we get the following metric

$$\begin{aligned} ds^2 &= -f(r)dt^2 + \tfrac{1}{f(r)}dr^2 + r^2(d\theta^2 + \sin^2\theta d\phi^2), \\ \text{with } f(r) &= 1 - \tfrac{2Mr^2}{r^3+Q^3} - \tfrac{c_q}{r^{3\epsilon+1}}, \end{aligned} \tag{3.1}$$

where c_q and ϵ are the quintessence parameters.

Using the horizon property [78, 173], and solving the following equation at the horizon

$$f(r_h) = 0, \tag{3.2}$$

leads to

$$M = \frac{(r_h^3 + Q^3)}{2r_h^2}\left(1 - \frac{c_q}{r_h^{3\epsilon+1}}\right). \tag{3.3}$$

Eq. (3.3) gives the relation between the black hole mass and its horizon radius.

3.2.1 Temperature and entropy

In order to study the thermodynamic analysis of the black hole, we will focus on the event horizon r_h. Through the surface gravity definition at the horizon showed in Eq. (2.87), the Hawking temperature is given by

$$\begin{aligned}
T_h &= \tfrac{\kappa}{2\pi} = \tfrac{f'(r_h)}{4\pi} \\
&= \tfrac{1}{4\pi}\left\{-2M\left(\tfrac{2r_h(r_h^3+Q^3)-3r^4}{(r_h^3+Q^3)^2}\right)+\tfrac{(3\epsilon+1)c_q}{r_h^{3\epsilon+2}}\right\} \\
&= \tfrac{1}{4\pi}\left\{2\left[\tfrac{r_h^3+Q^3}{2r_h^2}\left(1-\tfrac{c_q}{r_h^{3\epsilon+1}}\right)\right]\left[\tfrac{r_h(r_h^3-2Q^3)}{(r_h^3+Q^3)^2}\right]+\tfrac{3\epsilon+1}{r_h^{3\epsilon+2}}c_q\right\} \\
&= \tfrac{1}{4\pi}\left\{\tfrac{1}{r_h(r_h^3+Q^3)}\left(1-\tfrac{c_q}{r_h^{3\epsilon+1}}\right)(r_h^3-2Q^3)+\tfrac{(3\epsilon+1)(r_h^3+Q^3)c_q}{(r_h^3+Q^3)r_h^{3\epsilon+2}}\right\}.
\end{aligned}$$

Therefore, we obtain

$$T_h = \frac{1}{4\pi(r_h^3+Q^3)}\left[\frac{r_h^3-2Q^3}{r_h}+\frac{3c_q\epsilon}{r_h^{3\epsilon+2}}\left(r_h^3+Q^3\left(\frac{\epsilon+1}{\epsilon}\right)\right)\right]. \tag{3.4}$$

Here, we notice that, the temperature obtained corresponds to the one obtained by Nam in Ref. [173].

In this case, the first law of the thermodynamics is established as [173].

$$dM = T_h dS + \Phi_h dQ + C_h dc_q, \tag{3.5}$$

where the entropy S, the magnetic charge Q and the quintessence parameter c_q form a complete set of extensible variables. Here, Φ_h is the Potential provided from the magnetic charge and C_h the conjugating quantity corresponding to the quintessence.

Now, let us compute the entropy of the black hole. To having it, we can write first the differential of $M(S, Q, c_q)$ as

$$dM(S,Q,c_q) = \left.\frac{\partial M}{\partial S}\right|_{Q,c_q} dS + \left.\frac{\partial M}{\partial Q}\right|_{S,c_q} dQ + \left.\frac{\partial M}{\partial c_q}\right|_{S,Q} dc_q. \tag{3.6}$$

Proceeding by identification between (3.6) and (3.5), we have

$$\Phi_h = \left.\frac{\partial M}{\partial Q}\right|_{S,c_q} \text{ and } C_h = \left.\frac{\partial M}{\partial c_q}\right|_{S,Q}. \tag{3.7}$$

However, the mass $M(r_h, Q, c_q)$ expressed in Eq. (3.3) can be differentiated as

$$dM(r_h, Q, c_q) = \left.\frac{\partial M}{\partial r_h}\right|_{Q,c_q} dr_h + \left.\frac{\partial M}{\partial Q}\right|_{r_h,c_q} dQ + \left.\frac{\partial M}{\partial c_q}\right|_{r_h,Q} dc_q. \tag{3.8}$$

Therefore, since (3.8) and (3.5) are equal, we straightforwardly obtain the following equation

$$T_h dS - \left.\frac{\partial M}{\partial r_h}\right|_{Q,c_q} dr_h + \left(\Phi_h - \left.\frac{\partial M}{\partial Q}\right|_{r_h,c_q}\right) dQ + \left(C_h - \left.\frac{\partial M}{\partial c_q}\right|_{r_h,Q}\right) dc_q = 0. \tag{3.9}$$

However, taking into account (3.7) leads us to have

$$T_h dS = \frac{\partial M}{\partial r_h} dr_h. \tag{3.10}$$

Finally, the entropy can be computed through the following equation

$$S = \int \frac{1}{T_h}\frac{\partial M}{\partial r_h} dr_h. \tag{3.11}$$

Now, in order to get the entropy of the black hole, let us find $\frac{\partial M}{\partial r_h}$, through the definition of the mass at the event horizon in Eq. (3.3).

Therefore, we have

$$\begin{aligned}
\frac{\partial M}{\partial r_h} &= \frac{1}{2}\left\{\frac{3r_h^3 - 2(r_h^3+Q^3)}{r_h^3}\left(1 - \frac{c_q}{r_h^{3\epsilon+1}}\right) + \left(\frac{r_h^3+Q^3}{r_h^2}\right)\left(\frac{(3\epsilon+1)c_q}{r^{3\epsilon+2}}\right)\right\} \\
&= \frac{1}{2}\left\{3 - \frac{3c_q}{r_h^{3\epsilon+1}} - \frac{2}{r_h^3}(r^3+Q^3) + \frac{2(r^3+Q^3)c_q}{r_h^{3\epsilon+4}} + \frac{(r^3+Q^3)(3\epsilon+1)c_q}{r_h^{3\epsilon+4}}\right\} \\
&= \frac{1}{2}\left\{3 - \frac{3c_q}{r_h^{3\epsilon+1}} - \frac{2}{r_h^3}(r^3+Q^3) + \frac{2(r^3+Q^3)(3\epsilon+3)c_q}{r_h^{3\epsilon+4}}\right\} \\
&= \frac{1}{2}\left\{3 + \frac{3(\epsilon r^3 + Q^3(\epsilon+1))c_q}{r^{3\epsilon+4}} - 2 - \frac{2Q^3}{r^3}\right\} \\
&= \frac{1}{2}\left\{1 + \frac{3c_q}{r^{3\epsilon+4}}(\epsilon r^3 + Q^3(\epsilon+1)) - \frac{2Q^3}{r^3}\right\}.
\end{aligned}$$

Therefore, we get

$$\frac{\partial M}{\partial r_h} = \frac{1}{2r^2}\left\{\frac{r_h^3 - 2Q^3}{r_h} + \frac{3c_q\epsilon}{r_h^{3\epsilon+2}}\left(r_h^3 + Q^3\left(\frac{\epsilon+1}{\epsilon}\right)\right)\right\}. \tag{3.12}$$

Now, we can easily see the correspondence between T_h and $\frac{\partial M}{\partial r_h}$, hence, Eq. (3.11) becomes

$$S = 2\pi \int \left(\frac{r_h^3 + Q^3}{r_h^2}\right) dr = \pi r_h^2 \left(1 - \frac{2Q^3}{r_h^3}\right). \tag{3.13}$$

Here, we can notice that the entropy depends only on one extensive thermodynamic variable, namely Q. Hereby, we can say that quintessence dark energy does not affect the evolution of the black hole entropy.

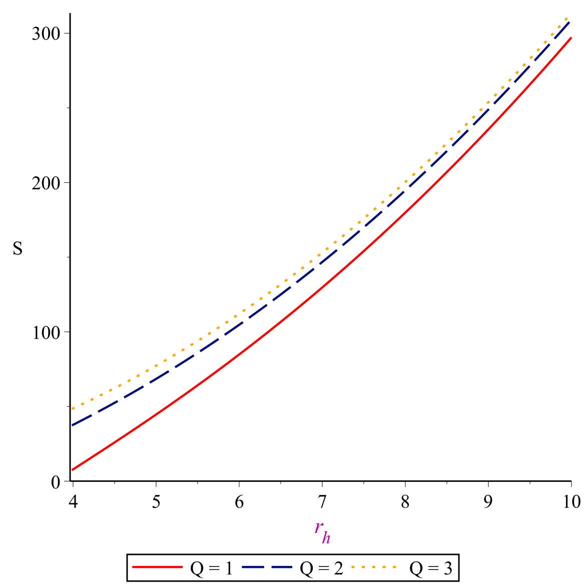

Figure 3.1: Change of the black hole entropy S. Here, $Q = 1$ corresponds to red continuous line, $Q = 2$ to blue dash and $Q = 3$ to orange dot.

The change of entropy S, in term of the event horizon r_h is plotted in figure (3.1). Here, we see that whatever the value of the magnetic charge Q, the entropy is always growing up, when the event horizon r_h increases. This result tells that a larger and more charged black hole has a higher entropy. Furthermore, we notice that if we increase the value of the magnetic charge Q, the entropy seems to be higher.

Furthermore, from Eq. (3.4), we are able to plot the behaviour of the Hawking temperature, and then, appreciate the effect of dark energy. This has been done in figure (3.2)

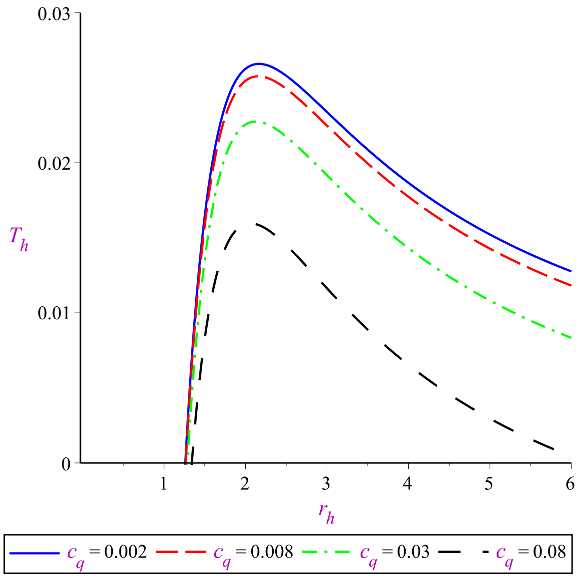

(a) for $Q = 1$

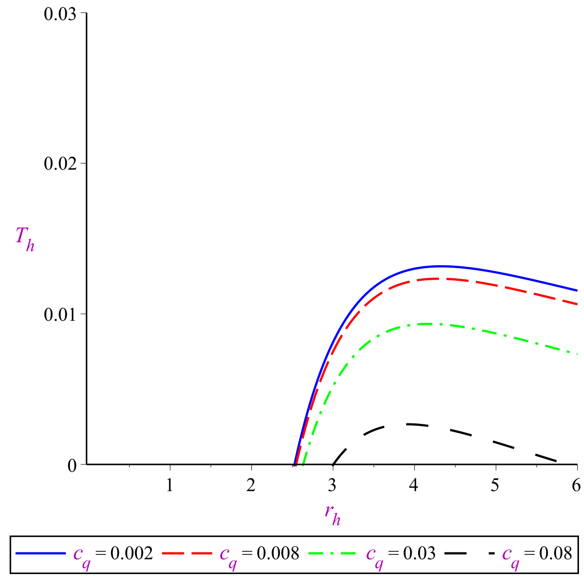

(b) for $Q = 2$

Figure 3.2: Change of the black hole temperature T_h in the presence of quintessence dark energy with characteristics $\epsilon = -2/3$.

Looking at figure (3.2), we see that the temperature starts increasing, and then decreases towards zero. More precisely, subfigure (3.2)(a) shows that the maximum of temperature is shifted to lower values as we increase the value of quintessence parameter c_q. This leads to say that a black hole with a higher value of c_q decreases the maximum of temperature. Also, looking at subfigure (3.2)(b), we see the same behaviour but with one difference. indeed, here the magnetic charge Q is greater than the one for (3.2)(a), and we see that the maximum of temperature is truly affected, and then appears smaller as we increase the magnetic charge.

3.2.2 Thermodynamic potential

For the next step of our thermodynamic analysis, we will derive another conjugating quantity which is the thermodynamic potential Φ_h [173]. Hence, regarding Eq. (3.13), we can see that the event horizon radius r_h is a function of the extensive thermodynamic variables S and Q. Also, Eq. (3.3), leads to determine the mass as follows

$$M(S, Q, c_q) = M(r_h(S, Q), Q, c_q). \tag{3.14}$$

Hence, the thermodynamic potential Φ_h reads

$$\begin{aligned}\Phi_h &= \frac{\partial M}{\partial Q} + \frac{\partial M}{\partial r_h}\frac{\partial r_h}{\partial Q} \\ &= \frac{\partial M}{\partial Q} + \frac{\partial M}{\partial r_h}\left(\frac{\partial r_h}{\partial S}\frac{\partial S}{\partial Q}\right).\end{aligned}$$

However,

$$\begin{aligned}\frac{\partial S}{\partial r_h} &= \pi\frac{\partial}{\partial r_h}\left[r_h^2\left(1-\frac{2Q^3}{r_h^3}\right)\right] \\ &= \pi\left[2r_h\left(1-\frac{2Q^3}{r_h^3}\right)+\frac{6Q^3}{r_h^4}r_h^2\right] \\ &= \pi\left[2r_h-\frac{4Q^3}{r_h^2}+\frac{6Q^3}{r_h^2}\right] \\ &= \pi\left[2r_h+\frac{2Q^3}{r_h^2}\right] \\ &= \pi\left[\frac{2r_h^3+2Q^3}{r_h^2}\right] \\ &= 2\pi\left[\frac{r_h^3+Q^3}{r_h^2}\right],\end{aligned}$$

and

$$\frac{\partial S}{\partial Q} = -\frac{2\pi r_h^2}{r_h^3} \times 3Q^2 = -\frac{6\pi Q^2}{r_h}.$$

Therefore, taking also Eq. (3.12), the potential becomes

$$\begin{aligned}
\Phi_h &= \frac{\partial M}{\partial Q} + \frac{\partial M}{\partial r_h}\left(\frac{\partial r_h}{\partial S}\frac{\partial S}{\partial Q}\right) \\
&= \frac{3Q^2}{2r_h^2}\left(1 - \frac{c_q}{r_h^{3\epsilon+1}}\right) \\
&+ \frac{1}{2r_h}\left\{\frac{r_h^3 - 2Q^3}{r_h^2} + \frac{3c_q}{r_h^{3(\epsilon+1)}}\left(\epsilon r_h^3 + Q^3(\epsilon+1)\right)\right\}\left(-\frac{3r_h Q^2}{r_h^3 + Q^3}\right) \\
&= \frac{3Q^2}{2(r_h^3+Q^3)}\left[\frac{r_h^3+Q^3}{r_h^2}\left(1 - \frac{c_q}{r_h^{3\epsilon+1}}\right) - \frac{r_h^3 - 2Q^3}{r_h^2} - \frac{3c_q}{r_h^{3(\epsilon+1)}}\left(\epsilon r_h^3 + Q^3(\epsilon+1)\right)\right] \\
&= \frac{3Q^2}{2(r_h^3+Q^3)}\left[\frac{r_h^3 - r_h^3 + Q^2 + 2Q^3}{r_h^2} - \frac{c_q}{r_h^{3(\epsilon+1)}}(r_h^3 + Q^3 + 3\epsilon r_h^3 + 3\epsilon Q^3 + 3Q^3)\right],
\end{aligned}$$

Hence, we have

$$\Phi_h = \frac{3Q^2}{2(r_h^3+Q^3)}\left[\frac{3Q^3}{r_h^2} - \frac{c_q}{r_h^{3(\epsilon+1)}}[(1+3\epsilon)(r_h^3+Q^3) + 3Q^3]\right]. \quad (3.15)$$

Here, we can notice that the thermodynamic potential of the black hole appears different from the Nam result in Ref. [173]. Indeed, he found

$$\Phi_h = \frac{3Q^2}{2(r_h^3+Q^3)}\left[\frac{2r_h^3 - Q^3}{r_h^2} - \frac{c_q}{r_h^{3(\epsilon+1)}}[(-1+3\epsilon)(r_h^3+Q^3) + 3Q^3]\right].$$

Now, we are going to plot the thermodynamic potential expressed in Eq. (3.15), in order to appreciate the effects of quintessence dark energy. In figure (3.3), we depicted the variation of the black hole potential. Regarding this figure, we can say that the potential still decreases towards zero, then stay positive. Furthermore, we

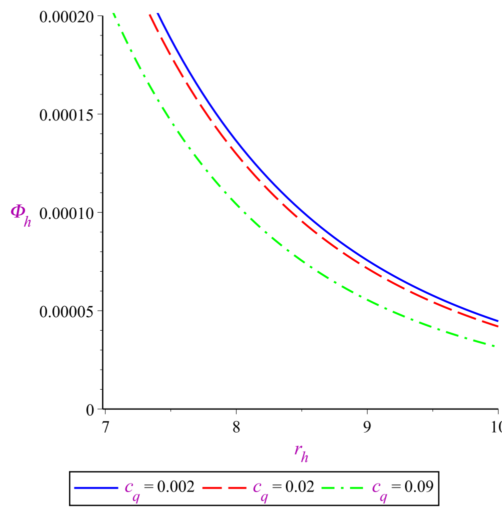

Figure 3.3: Variation of the black hole potential Φ_h for different values of the quintessence parameter c_q, with $\epsilon = -2/3$ and $Q = 1$.

notice that the potential has lower values as we increase the quintessence parameter c_q. This result implies that quintessence acts as negative energy which allows the lost of black hole potential.

3.2.3 Phase transition and analysis of the stability of the black hole

In order to study the thermodynamic stability of the black hole, we will compute and plot the heat capacity of the black hole, which is given by

$$Ca = T_h \left(\frac{\partial S}{\partial T_h} \right)_{Q,c_q} = T_h \left(\frac{\partial S}{\partial r_h} \frac{\partial r_h}{\partial T_h} \right)_{Q,c_q}. \quad (3.16)$$

After computing it, we get the following expression

$$Ca = -\frac{2\,\pi\,\left(Q^3 + r^3\right)^2 \left(-r^{4+3\,\epsilon} + 2\,r^{3\,\epsilon+1} Q^3 - 3\,cQ^3\epsilon - 3\,r^3 c\epsilon - 3\,cQ^3\right)}{A}, \quad (3.17)$$

where

$$A = r\left(2\,Q^6 r^{3\,\epsilon+1} + 10\,Q^3 r^{4+3\,\epsilon} - r^{7+3\,\epsilon} - 9\,Q^6 c\epsilon^2 - 18\,r^3 Q^3 c\epsilon^2 - 9\,r^6 c\epsilon^2\right.$$
$$\left. -15\,Q^6 c\epsilon - 21\,r^3 Q^3 c\epsilon - 6\,r^6 c\epsilon - 6\,Q^6 c - 15\,r^3 Q^3 c\right).$$

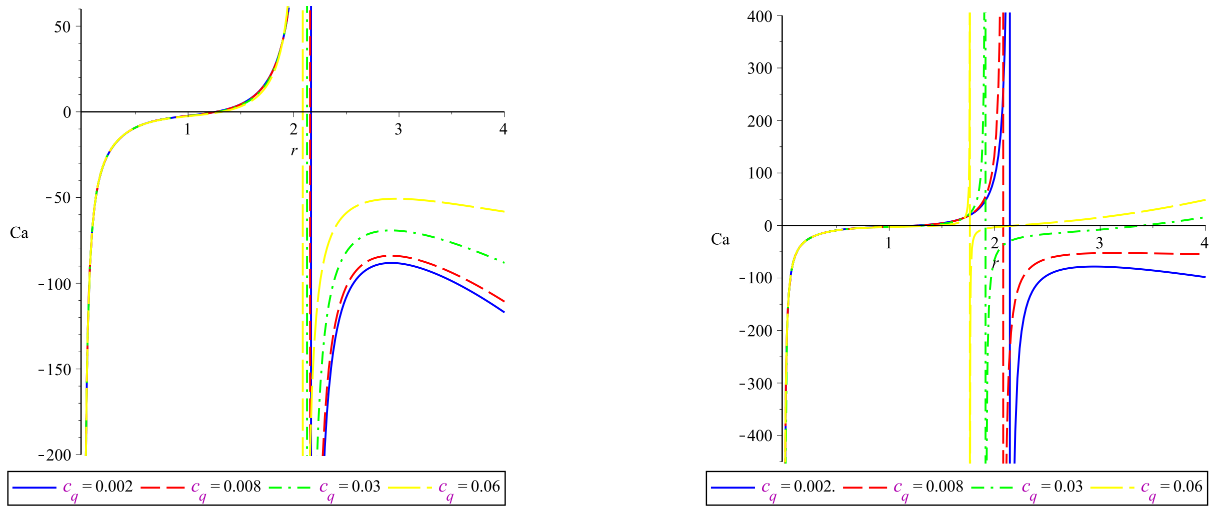

(a) for $\epsilon = -2/3$ (b) for $\epsilon = -0.98$

Figure 3.4: Change of the black hole heat capacity Ca in the presence of quintessence dark energy with the magnetic charge $Q = 1$.

In figure (3.4), we depicted the black hole heat capacity, and analysing this plot, a good appreciation of black hole behaviour can be done. Indeed, we can see that the heat capacity moves from the negative region and then becomes positive without discontinuity. Physically, this result means that the black hole moves from the unstable phase to stable phase without any second-order phase transition. Also, this behaviour happens in both subfigures (3.4)(a) and (b). Furthermore, this result is similar to the plot of the heat capacity of the Reissner-Nordstöm black hole surrounded by quintessence, which corresponds to a linear distribution of the electric charge [17].

Furthermore, we notice that after being stable, the black hole becomes back unstable, but this time through a second-order phase transition, identified by the presence of discontinuity in the plot.

In the other hand, comparing subfigures (3.4)(a) and (b), we can see that in subfigure (3.4)(a) which corresponds to $\epsilon = -2/3$, the behaviour remains almost unchangeable before the second-order phase transition. However, it is not the case in subfigure (3.4)(b) which corresponds to $\epsilon = -0.98$, where we see that the second order phase transition appears as later as we decrease the quintessence parameter c_q.

Also comparing these subfigures leads to say that a smaller value of ϵ allows the black hole to become stable again after the second-order phase transition at certain values of c_q(See subfigure (3.4)(b)). However, this is not the case for higher values of the quintessence parameter ϵ (See subfigure (3.4)(a)).

After having studied the effects of dark energy on the thermodynamics of black hole, in the next section, we are going to analyse the impact of dark matter, especially the perfect fluid model, onto the thermodynamics of the black hole.

3.3 Effects of dark matter on the thermodynamics of black hole

In this section, in order to study the effects of dark matter, we will choose the metric of a nonlinear magnetic-charged AdS black hole in the background of perfect fluid dark matter, which can be found by choosing $c_q = 0$ and $\Lambda = 0$ into Eq. (2.53). Therefore, we have

$$\begin{aligned} ds^2 &= -f(r)dt^2 + \tfrac{1}{f(r)}dr^2 + r^2(d\theta^2 + \sin^2\theta d\phi^2), \\ \text{with } f(r) &= 1 - \tfrac{2Mr^2}{r^3+Q^3} + \tfrac{\alpha}{r}\ln\tfrac{r}{|\alpha|}. \end{aligned} \tag{3.18}$$

Using the horizon property [78, 173], and solving the following equation at the horizon

$$f(r_h) = 0, \tag{3.19}$$

leads to

$$M = \frac{(r_h^3 + Q^3)}{2r_h^2}\left(1 + \frac{\alpha}{r_h}\ln\frac{r_h}{|\alpha|}\right). \tag{3.20}$$

Eq. (3.20) gives the relation between the black hole mass and its horizon radius. Now, we will focus on the event horizon to make the thermodynamic analysis.

3.3.1 Temperature and entropy

Through the surface gravity definition at the horizon showed in Eq. (2.87), the Hawking temperature T_h is given by

$$\begin{aligned}
T_h &= \tfrac{\kappa}{2\pi} = \tfrac{f'(r_h)}{4\pi} \\
&= \tfrac{1}{4\pi}\left\{-2M\left(\tfrac{2r_h(r_h^3+Q^3)-3r^4}{(r_h^3+Q^3)^2}\right) - \tfrac{\alpha}{r_h^2}\ln\left(\tfrac{r_h}{|\alpha|}\right) + \tfrac{\alpha}{r_h}\times\tfrac{\frac{1}{|\alpha|}}{\frac{r_h}{|\alpha|}}\right\} \\
&= \tfrac{1}{4\pi}\left\{2\left[\tfrac{r_h^3+Q^3}{2r_h^2}\left(1+\ln\left(\tfrac{r_h}{|\alpha|}\right)\right)\right]\left[\tfrac{r_h(r_h^3-2Q^3)}{(r_h^3+Q^3)^2}\right] + \tfrac{\alpha}{r_h^2}\left(1-\ln\left(\tfrac{r_h}{|\alpha|}\right)\right)\right\} \\
&= \tfrac{1}{4\pi}\left\{\tfrac{1}{r_h(r_h^3+Q^3)}\left(1+\ln\left(\tfrac{r_h}{|\alpha|}\right)\right)(r_h^3-2Q^3) + \tfrac{\alpha}{r_h^2}\left(1-\ln\left(\tfrac{r_h}{|\alpha|}\right)\right)\right\} \\
&= \tfrac{1}{4\pi(r_h^3+Q^3)}\left\{\tfrac{r_h^3-2Q^3}{r_h} + \tfrac{\alpha}{r_h^2}(r_h^3+Q^3)\ln\left(\tfrac{r_h}{|\alpha|}\right) + \tfrac{\alpha}{r_h^2}(r_h^3+Q^3)\left(1-\ln\left(\tfrac{r_h}{|\alpha|}\right)\right)\right\} \\
&= \tfrac{1}{4\pi(r_h^3+Q^3)}\left\{\tfrac{r_h^3-2Q^3}{r_h} + \tfrac{\alpha}{r_h^2}\left((r_h^3-2Q^3-r_h^3-Q^3)\ln\left(\tfrac{r_h}{|\alpha|}\right) + r_h^3+Q^3\right)\right\}.
\end{aligned}$$

Therefore, we obtain the following Hawking temperature

$$T_h = \frac{1}{4\pi(r_h^3+Q^3)}\left[\frac{r_h^3-2Q^3}{r_h} + \frac{\alpha}{r_h^2}\left(r_h^3+Q^3-3Q^3\ln\left(\frac{r_h}{|\alpha|}\right)\right)\right]. \tag{3.21}$$

In figure (3.5), we plotted the temperature of the nonlinear magnetic-charged black hole surrounded by perfect fluid dark matter. On the plots of figure (3.5), we can see that the black hole temperature increases and reaches a maximum, and

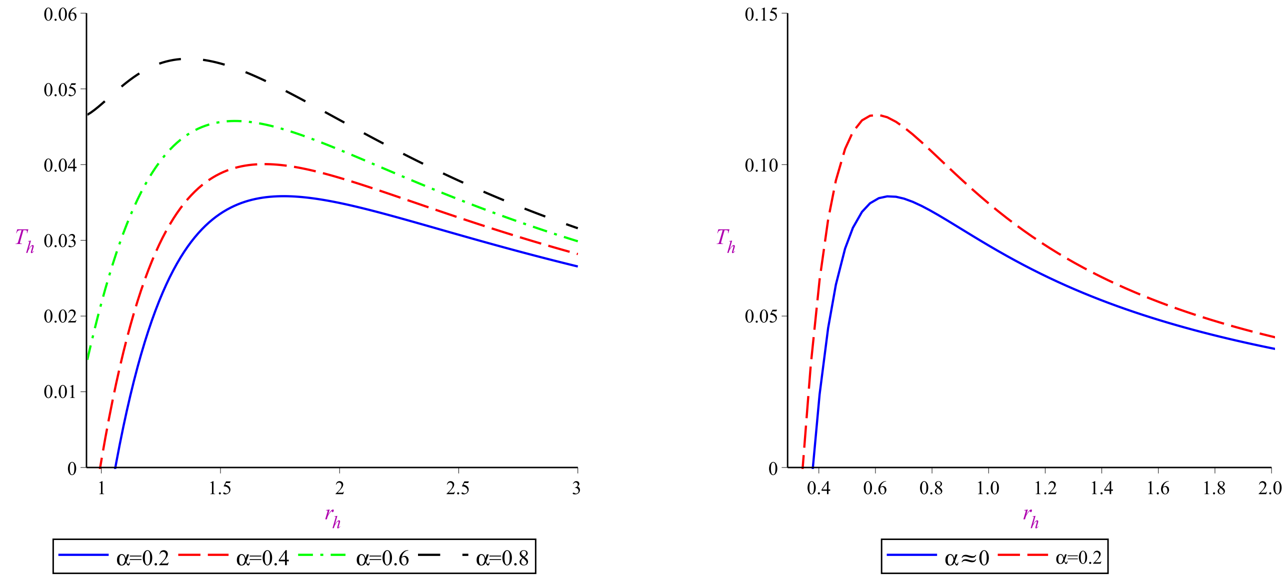

(a)For different values of dark matter parameter for $Q = 0.8$

(b)In the presence or not of dark matter for $Q = 0.3$

Figure 3.5: Change of the black hole temperature T_h.

then decreases, which is similar to the behaviour of the temperature of the nonlinear magnetic-charged black hole surrounded by quintessence, plotted in Figure (3.2). Furthermore looking at subfigure (3.5)(a), we see that this maximum increases for higher values of dark matter parameter. However, subfigure (3.5)(b) shows that for a given value of the magnetic charge Q, the dark matter leads the maximum of temperature to be higher.

In the other hand, comparing figure (3.2) and subfigure (3.5)(a), we notice that the maximum of the temperature shifts to lower values as we increase the quintessence parameter c_q and decrease the perfect fluid dark matter parameter α.

Now, the first law of the thermodynamic reads

$$dM = T_h dS + \Phi_h dQ + \beta_h d\alpha, \tag{3.22}$$

where the entropy S, the magnetic charge Q and the dark matter parameter α form a complete set of extensible variables. Let notice that T_h is the Hawking temperature at the horizon, Φ_h is the potential, and β_h is the conjugating quantity of the dark matter parameter α.

After that, in order to find the entropy, we can proceed in the same way than Section(3.2). Hence, we have

$$S = \int \frac{1}{T_h}\frac{\partial M}{\partial r_h} dr_h. \tag{3.23}$$

To compute this, we have to find $\frac{\partial M}{\partial r_h}$ from Eq. (3.20), on that way:

$$\begin{aligned}
\frac{\partial M}{\partial r_h} &= \frac{1}{2}\left\{\frac{3r_h^3-2(r_h^3+Q^3)}{r_h^3}\left(1+\ln\left(\frac{r_h}{|\alpha|}\right)\right)+\left(\frac{r_h^3+Q^3}{r_h^2}\right)\left(-\frac{\alpha}{r_h^2}\ln\left(\frac{r_h}{|\alpha|}\right)+\frac{\alpha}{r_h}\times\frac{\frac{1}{|\alpha|}}{\frac{r_h}{|\alpha|}}\right)\right\} \\
&= \frac{1}{2}\left\{3+3\frac{\alpha}{r_h}\ln\left(\frac{r_h}{|\alpha|}\right)-2-\frac{2Q^3}{r_h^3}-\frac{3\alpha(r_h^3+Q^3)}{r_h^4}\ln\left(\frac{r_h}{|\alpha|}\right)+\frac{\alpha(r_h^3+Q^3)}{r_h^4}\right\} \\
&= \frac{1}{2}\left\{1-\frac{2Q^3}{r_h^3}+\frac{\alpha}{r_h^2}\left[\frac{r_h^3+Q^3}{r_h^2}-\frac{3Q^3}{r_h^2}\ln\left(\frac{r}{|\alpha|}\right)\right]\right\}.
\end{aligned}$$

Hereby, the first derivative of the black hole mass is found as

$$\frac{\partial M}{\partial r_h} = \frac{1}{2r_h^2}\left\{\frac{r_h^3-2Q^3}{r_h}+\frac{\alpha}{r_h^2}\left[r_h^3+Q^3-3Q^3\ln\left(\frac{r_h}{|\alpha|}\right)\right]\right\}. \tag{3.24}$$

Introducing Eq.(3.24) and (3.21) into Eq. (3.23), we get the entropy of the nonlinear magnetic-charged black hole in the background of perfect fluid dark matter expressed as

$$S = 2\pi\int\left(\frac{r_h^3+Q^3}{r_h^2}\right)dr = \pi r_h^2\left(1-\frac{2Q^3}{r_h^3}\right). \tag{3.25}$$

Here, we can notice that the entropy is the same than the one obtained in the presence of quintessence dark energy, found in Eq. (3.11). Hereby, we can say that perfect fluid dark matter does not affect the evolution of entropy.

3.3.2 Thermodynamic potential

Now, we are going to compute the thermodynamic potential, which is found using the procedure we developed in the subsection (3.2.2), and the result gives

$$\begin{aligned}\Phi_h &= \frac{\partial M}{\partial Q} + \frac{\partial M}{\partial r_h}\frac{\partial r_h}{\partial Q} \\ &= \frac{\partial M}{\partial Q} + \frac{\partial M}{\partial r_h}\left(\frac{\partial r_h}{\partial S}\frac{\partial S}{\partial Q}\right).\end{aligned}$$

However,

$$\begin{aligned}\frac{\partial S}{\partial r_h} &= \pi\frac{\partial}{\partial r_h}\left[r_h^2\left(1-\frac{2Q^3}{r_h^3}\right)\right] \\ &= \pi\left[2r_h\left(1-\frac{2Q^3}{r_h^3}\right)+\frac{6Q^3}{r_h^4}r_h^2\right] \\ &= \pi\left[2r_h-\frac{4Q^3}{r_h^2}+\frac{6Q^3}{r_h^2}\right] \\ &= \pi\left[2r_h+\frac{2Q^3}{r_h^2}\right] \\ &= \pi\left[\frac{2r_h^3+2Q^3}{r_h^2}\right] \\ &= 2\pi\left[\frac{r_h^3+Q^3}{r_h^2}\right],\end{aligned}$$

and

$$\frac{\partial S}{\partial Q} = -\frac{2\pi r_h^2}{r_h^3}\times 3Q^2 = -\frac{6\pi Q^2}{r_h}.$$

Therefore, taking also Eq. (3.24), the potential becomes

$$\begin{aligned}
\Phi_h &= \frac{\partial M}{\partial Q}+\frac{\partial M}{\partial r_h}\left(\frac{\partial r_h}{\partial S}\frac{\partial S}{\partial Q}\right)\\
&= \frac{3Q^2}{2r_h^2}\left(1+\ln\left(\frac{r_h}{|\alpha|}\right)\right)\\
&\quad +\frac{1}{2r_h}\left\{\frac{r_h^3-2Q^3}{r_h^2}+\frac{\alpha}{r_h^3}\left[r_h^3+Q^3-3Q^3\ln\left(\frac{r_h}{|\alpha|}\right)\right]\right\}\left(-\frac{3r_hQ^2}{r_h^3+Q^3}\right)\\
&= \frac{3Q^2}{2(r_h^3+Q^3)}\left[\frac{r_h^3+Q^3}{r_h^2}\left(1+\ln\left(\frac{r_h}{|\alpha|}\right)\right)-\frac{r_h^3-2Q^3}{r_h^2}-\frac{\alpha}{r_h^3}\left[r_h^3+Q^3\right.\right.\\
&\quad \left.\left.-3Q^3\ln\left(\frac{r_h}{|\alpha|}\right)\right]\right]\\
&= \frac{3Q^2}{2(r_h^3+Q^3)}\left[\frac{r_h^3-r_h^3+Q^2+2Q^3}{r_h^2}-\frac{\alpha}{r_h^3}\left[r_h^3+Q^3-(r_h^3+Q^3+3Q^3)\ln\left(\frac{r_h}{|\alpha|}\right)\right]\right].
\end{aligned}$$

Therefore, the potential has the following expression

$$\Phi_h=\frac{3Q^2}{2(r_h^3+Q^3)}\left\{\frac{3Q^3}{r_h^2}-\frac{\alpha}{r_h^3}\left[r_h^3+Q^3-(r_h^3+4Q^3)\ln\left(\frac{r_h}{|\alpha|}\right)\right]\right\}. \tag{3.26}$$

Plotting the thermodynamic potential found in Eq. (3.26) leads to appreciate the effects of dark matter. Indeed, we can remark that black hole potential decreases towards zero, and it seems lower when the dark matter parameter decreases. Therefore, we can say that dark matter reduces the potential of the black hole. Let notice that the dark energy induces the same behaviour, as it was presented in figure (3.3).

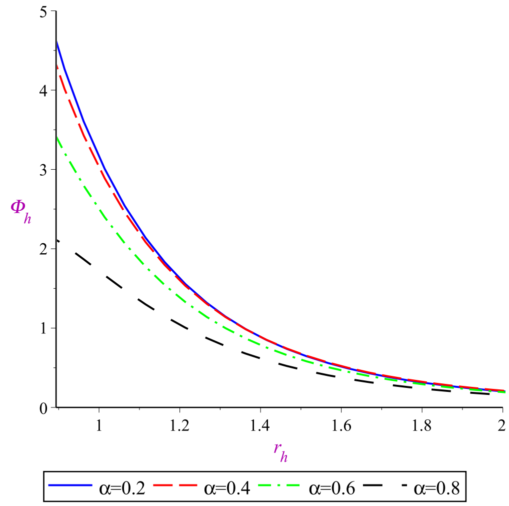

Figure 3.6: Variation of the black hole potential Φ_h for different values of the perfect fluid dark matter α, with $Q = 1$.

3.3.3 Specific heat and phase transition

Here, the thermodynamic stability of the black hole, will be studied through the calculus and the plot of the corresponding heat capacity, which is expressed as

$$C = T_h \left(\frac{\partial S}{\partial T_h}\right)_{Q,\alpha} = T_h \left(\frac{\partial S}{\partial r_h}\frac{\partial r_h}{\partial T_h}\right)_{Q,\alpha}. \tag{3.27}$$

After computing it, we get the following expression

$$C = -\frac{2\left(3\ln(|\alpha|)\,Q^3\alpha - 3\ln(r)\,Q^3\alpha + Q^3\alpha - 2\,Q^3 r + \alpha\,r^3 + r^4\right)\pi\,\left(Q^3 + r^3\right)^2}{A}, \tag{3.28}$$

where

$$A = r(6\,Q^6\alpha\,\ln(|\alpha|) + 15\,Q^3\alpha\,r^3\ln(|\alpha|) - 6\,Q^6\alpha\,\ln(r) - 15\,Q^3\alpha\,r^3\ln(r)$$
$$+5\,Q^6\alpha - 2\,Q^6 r + 7\,Q^3\alpha\,r^3 - 10\,Q^3 r^4 + 2\,\alpha\,r^6 + r^7).$$

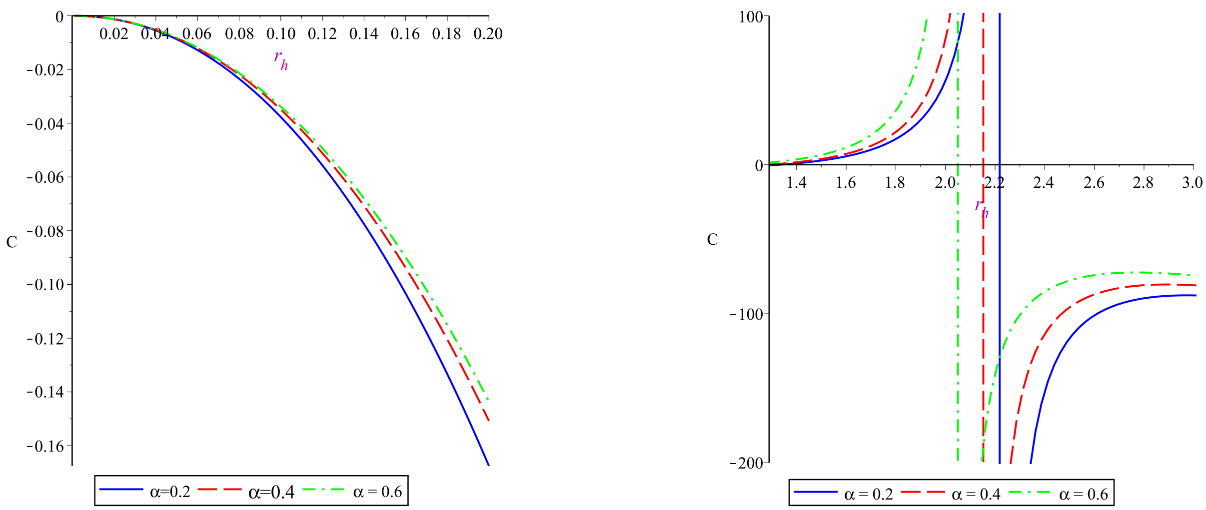

(a) for $Q = 0$ (b) for $Q = 1$

Figure 3.7: Change of the heat capacity C of the nonlinear magnetic-charged black hole in the background of perfect fluid dark matter.

In figure (3.7), we plotted the heat capacity C of the nonlinear magnetic-charged black hole in the background of perfect fluid dark matter. Analysing its plot, especially subfigure (3.7)(a), we see that in the absence of the magnetic charge, the heat capacity is negative, meaning that the black hole is unstable in the absence of magnetic charge, even when the black hole is surrounded by perfect fluid dark matter. On the contrary, taking into account magnetic charge(see subfigure (3.7)(b)), we can see the presence of a discontinuity for each dark matter parameter α. Physically meaning, that is to say that the black hole undergoes a second-order phase transition. Moreover, this second-order phase transition leads the black hole to move from the stable phase($C > 0$) to unstable phase($C < 0$).

Now, in the next section, we are going to study the thermodynamic of black hole when both dark matter and dark energy are considered simultaneously.

3.4 Simultaneous effects of dark matter and dark energy on the thermodynamics of black hole

The metric of the nonlinear magnetic-charged AdS black hole surrounded by quintessence and in the background of PFDM has been found in the previous chapter, especially in Eq. (2.53), which is given as

$$\begin{aligned} ds^2 &= -f(r)dt^2 + \tfrac{1}{f(r)}dr^2 + r^2(d\theta^2 + \sin^2\theta d\phi^2), \\ \text{with } f(r) &= 1 - \tfrac{2Mr^2}{r^3+Q^3} + \tfrac{\alpha}{r}\ln\tfrac{r}{|\alpha|} - \tfrac{c_q}{r^{3\epsilon+1}} - \tfrac{\Lambda}{3}r^2. \end{aligned}$$

On that metric, we can see that the function $f(r)$ depends also on the black hole mass M. This solution will help to study the impact of both dark matter and dark energy. Through the metric function $f(r)$, we will be able to derive the mass at the event horizon, and then we will start the thermodynamic study.

3.4.1 Temperature and entropy

For the first step, we will get the isothermal $P - r_h$ diagram, and to do that, we consider that the cosmological constant term Λ will act as a dynamical pressure. Thus, we could write [65–73]

$$P = -\frac{\Lambda}{8\pi}. \tag{3.29}$$

Therefore, substituting Λ from Eq. (3.29) into Eq. (2.56), we readily find

$$M = \frac{(r_h^3 + Q^3)}{2r_h^2}\left(1 + \frac{\alpha}{r_h}\ln\frac{r_h}{|\alpha|} - \frac{c_q}{r_h^{3\epsilon+1}} + \frac{8\pi P}{3}r_h^2\right). \tag{3.30}$$

The Hawking temperature is found through the surface gravity definition at the horizon [173]

$$\begin{aligned} T_h &= \tfrac{\kappa}{2\pi} = \tfrac{f'(r_h)}{4\pi} \\ &= \tfrac{1}{4\pi}\left\{-2M\left[\tfrac{2r_h(r_h^3+Q^3)-3r^4}{(r_h^3+Q^3)^2}\right] - \tfrac{\alpha}{{r_h}^2}\ln\tfrac{r_h}{|\alpha|} + \tfrac{\alpha}{{r_h}^2} + \tfrac{c_q(3\epsilon+1)}{{r_h}^{3\epsilon+2}} + \tfrac{16\pi P}{3}r_h\right\}. \end{aligned} \tag{3.31}$$

Thus, using Eq. (3.30), Eq. (3.31) may become as

$$\begin{aligned} T_h \;=\; & \tfrac{1}{4\pi(r_h^3+Q^3)}\left[\tfrac{r_h^3-2Q^3}{r_h}+\tfrac{3c_q\epsilon}{r_h^{3\epsilon+2}}\left(r_h^3+Q^3\left(\tfrac{\epsilon+1}{\epsilon}\right)\right)+\tfrac{\alpha Q^3}{r_h^2}\left(1-3\ln\tfrac{r_h}{|\alpha|}\right)\right. \\ & \left.+\alpha r_h+8\pi P r_h^4\right]. \end{aligned} \tag{3.32}$$

For $\alpha \approx 0$ and $P = 0$, meaning that in the absence of dark matter and cosmological constant, we find the Hawking temperature of the nonlinear magnetic-charged black hole surrounded by quintessence which has been found previously in Eq. (3.4), given by

$$T_h = \frac{1}{4\pi(r_h^3+Q^3)}\left[\frac{r_h^3-2Q^3}{r_h}+\frac{3c_q\epsilon}{r_h^{3\epsilon+2}}\left(r_h^3+Q^3\left(\frac{\epsilon+1}{\epsilon}\right)\right)\right]. \tag{3.33}$$

Now, the first law of the thermodynamic has the following form

$$dM = T_h dS + \Phi_h dQ + C_h dc_q + \beta_h d\alpha, \tag{3.34}$$

where the entropy S, the magnetic charge Q, the quintessence parameter c_q and the dark matter parameter α form a complete set of extensible variables. Let notice that T_h is the Hawking temperature at the horizon, Φ_h is the potential, and β_h is the conjugating quantity of the dark matter parameter α.

After that, in order to find the entropy, we can proceed in the same way than Section(3.2). Hence, we have

$$S = \int \frac{1}{T_h}\frac{\partial M}{\partial r_h} dr_h. \tag{3.35}$$

From Eq. (3.30), we have obtained the first derivative of the mass with respect to the horizon radius as

$$\begin{aligned}\frac{\partial M}{\partial r_h} &= \tfrac{1}{2r^2}\Big[\tfrac{r_h^3-2Q^3}{r_h}+\tfrac{3c_q\epsilon}{r_h^{3\epsilon+2}}\left(r_h^3+Q^3\left(\tfrac{\epsilon+1}{\epsilon}\right)\right)+\tfrac{\alpha Q^3}{r_h^2}\left(1-3\ln\tfrac{r_h}{|\alpha|}\right)\\ &\quad +\alpha r_h+8\pi P r_h^4\Big].\end{aligned} \tag{3.36}$$

Hence, from Eq. (3.32) and (3.36), the entropy of the black hole in Eq. (3.35), is straightforwardly obtained as

$$S=\pi r_h^2\left(1-\frac{2Q^3}{r_h^3}\right). \tag{3.37}$$

3.4.2 $P-r_h$ diagram and Gibbs free energy

In order to examine the possible phase transition, we are going to derive the expression of the pressure P as a function of T and r_h, then ending by analysing the critical behaviour of $P-r_h$ diagram. Afterwards, we will compute the heat capacity of the black hole and analyse its plot

Indeed, from Eq. (3.32), one can explicitly express the pressure P as a function of T and r_h as

$$\begin{aligned}P &= \tfrac{1}{8\pi r_h^4}\Big[4\pi(r_h^3+Q^3)T-\tfrac{r_h^3-2Q^3}{r_h}-\tfrac{3c_q\epsilon}{r_h^{3\epsilon+2}}\left(r_h^3+Q^3\left(\tfrac{\epsilon+1}{\epsilon}\right)\right)\\ &\quad -\tfrac{\alpha Q^3}{r_h^2}\left(1-3\ln\tfrac{r_h}{|\alpha|}\right)-\alpha r_h\Big].\end{aligned} \tag{3.38}$$

Since the black hole mass M is most naturally associated with the enthalpy H of the black hole in the extended phase space [78], the expression of the volume can be expressed as follows

$$V=\left(\frac{\partial H}{\partial P}\right)_{r_h,Q}=\left(\frac{\partial M}{\partial P}\right)_{r_h,Q}=\frac{4}{3}\pi(r_h^3+Q^3). \tag{3.39}$$

However, given that the expression of pressure would be less complex if we express it in term of horizon radius rather than volume, we will make our thermodynamic

α	r_{h_c}	T_c	P_c
0.01	2.7109	0.0126	0.0032
0.05	2.7546	0.0127	0.0032
0.1	2.7756	0.0132	0.0033
0.2	2.7763	0.0148	0.0034
0.4	2.7090	0.0190	0.0039
0.6	2.5947	0.0240	0.0045
0.8	2.4418	0.0308	0.0054

Table 3.1: Critical values for $(Q, c_q, \epsilon) = (1, 0.2, -2/3)$ for different dark matter parameters α.

analysis with the isothermal $P - r_h$ diagram. Therefore, we putted out in table 3.1 critical values which leads to have an inflexion point in the isothermal $P - r_h$ diagram. They are found through the following system of equations

$$\left(\frac{\partial P}{\partial r_h}\right)_{T_c} = 0, \quad \left(\frac{\partial^2 P}{\partial r_h^2}\right)_{T_c} = 0. \tag{3.40}$$

Next, we investigate Eq. (3.40) numerically in order to get the table 3.1, since it is not a trivial task to solve it analytically.

Therefore, it is shown in the present calculation(see table 3.1) the impact of PFDM on the critical values. remarkably, we can notice that when increasing the PFDM parameter α, we see that r_{h_c} increases for $\alpha < 0.2$ and then decreases when $\alpha > 0.2$. At the same time, we notice that T_c and P_c increase as we increase α.

In figure 3.8, we plotted the $P - r_h$ diagrams. Analysing these plots, we observe a van der Waals like behaviour. This means that a small/large black hole first-order phase transition occurs, moving from $T < T_c$ to $T > T_c$. Here, the first region($T < T_c$) is remarked by one value of the horizon radius for a high pressure, and two or three horizon radii for low pressure, and the second region ($T > T_c$) is remarked by only one horizon radius, for any value of pressure P. Furthermore, we can see that this van der Waals like behaviour occurs whatever the value of PFDM parameter α.

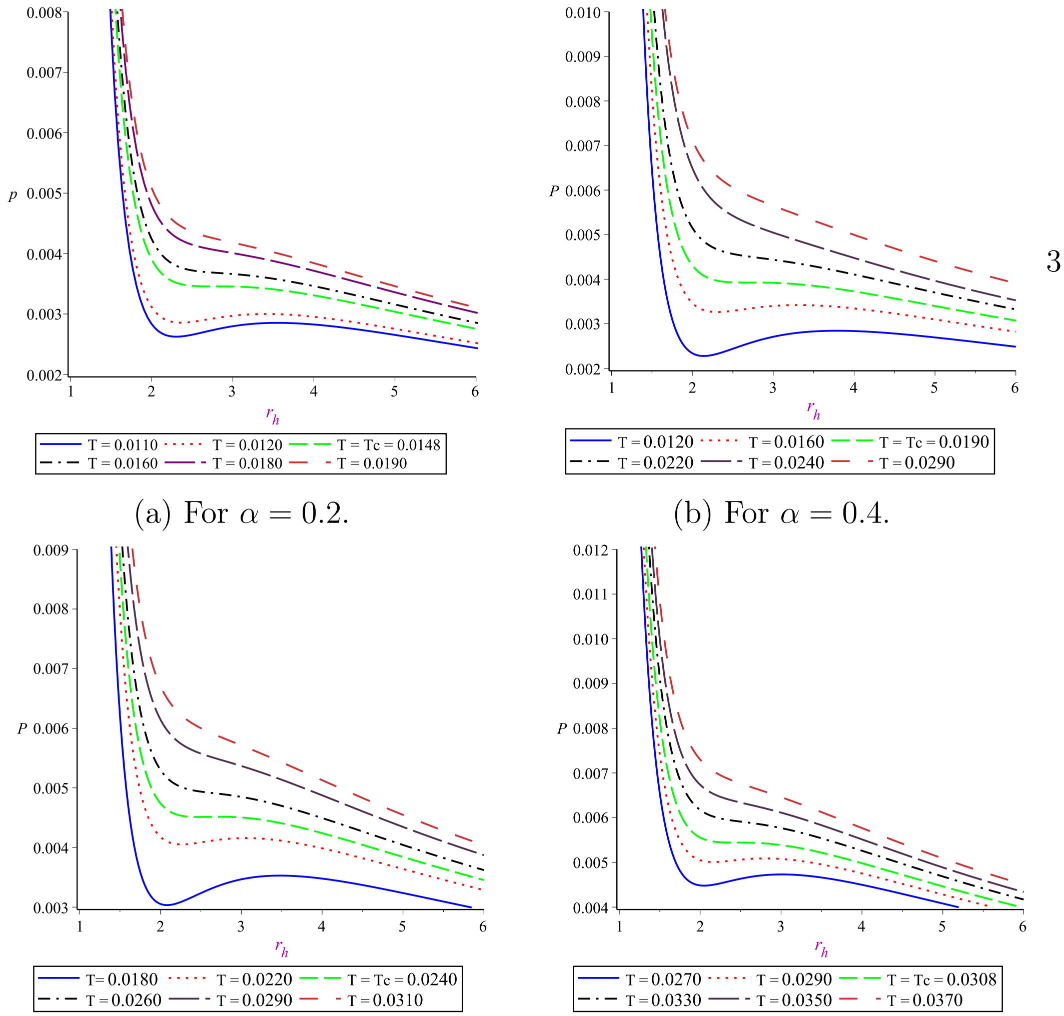

(a) For $\alpha = 0.2$. (b) For $\alpha = 0.4$.

(c) For $\alpha = 0.6$. (d) For $\alpha = 0.8$.

Figure 3.8: Variation of pressure for different values of α, with $(Q, c_q, \epsilon) = (1, .2, -2/3)$.

On the other hand, one can get the Gibbs free energy G, through the following relation

$$G = H - TS, \tag{3.41}$$

where the enthalpy H is considered as the black hole mass. In figure 3.9, we depicted the behaviour of the Gibbs free energy. Here, we can see that the plot presents the swallow tail characteristic, which appears below the critical temperature and critical pressure(we can see the corresponding critical values for $\alpha = 0.4$ on the table 3.1), and hence confirms the existence of first order phase transition. Furthermore, in

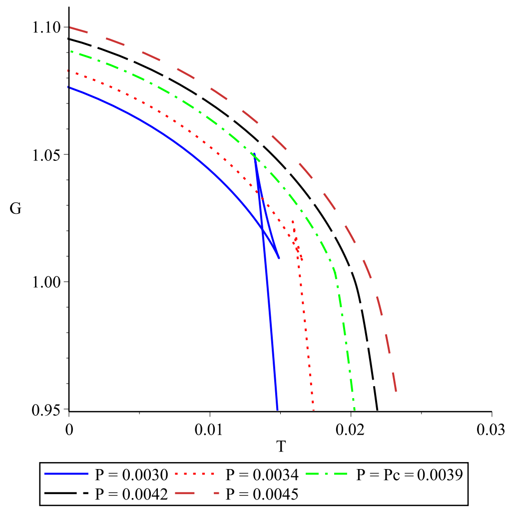

Figure 3.9: Variation of the Gibbs free energy G for different values of P, with $(Q, c_q, \epsilon, \alpha) = (1, 0.2, -2/3, 0.4)$.

figure 3.9, the swallow tail behaviour disappears, for higher values of the pressure and temperature.

3.4.3 Heat capacity and phase transition

To get more information about phase transition, we have also studied the heat capacity C, and see how the presence of PFDM and quintessence impact the behaviour of the black hole. This heat capacity is expressed as

$$C = T\left(\frac{\partial S}{\partial T}\right)_{Q,c_q,\epsilon,P}. \tag{3.42}$$

Substituting Eqs. (3.31) and (3.37) into Eq. (3.42) , we obtain

$$C = \frac{2\pi(Q^3 + r_h^3)^2}{r_h}\left(\frac{A}{B - D}\right), \tag{3.43}$$

with

$$\begin{aligned} A &= -3r_h^{3\epsilon}\alpha Q^3\ln(\tfrac{r_h}{\alpha}) + r_h^{3\epsilon}\alpha Q^3 - 2r_h^{3\epsilon+1}Q^3 + 3c_q\epsilon Q^3 + 3r_h^3 c_q\epsilon + 8\pi P r_h^{3\epsilon+6} \\ &\quad +3c_q Q^3 + \alpha r^{3\epsilon+3} + r^{3\epsilon+4}, \end{aligned} \tag{3.44}$$

$$\begin{aligned} B &= 32\pi P Q^3 r_h^{3\epsilon+6} + 8\pi P r_h^{3\epsilon+9} + 6r_h^{3\epsilon}\alpha Q^6\ln(\tfrac{r_h}{\alpha}) + 15Q^3\alpha r_h^{3\epsilon+3}\ln(\tfrac{r_h}{\alpha}) \\ &\quad -5r_h^{3\epsilon}\alpha Q^6 + 2Q^6 r_h^{3\epsilon+1} - 7Q^3\alpha r_h^{3\epsilon+3}, \end{aligned} \tag{3.45}$$

and

$$\begin{aligned} D &= 10Q^3 r_h^{3\epsilon+4} - 2\alpha r_h^{3\epsilon+6} - r_h^{3\epsilon+7} - 9Q^6 c_q\epsilon^2 - 18r_h^3 Q^3 c_q\epsilon^2 - 9r_h^6 c_q\epsilon^2 \\ &\quad -15Q^6 c_q\epsilon - 21r_h^3 Q^3 c_q\epsilon - 6r_h^6 c\epsilon - 6Q^6 c_q - 15r_h^3 Q^3 c_q. \end{aligned} \tag{3.46}$$

With this in mind, in subfigure 3.10 (a) and (b), the heat capacity is reported for different values of PFDM parameter α. In these plots, it comes that the black hole moves from stable phase to unstable one through a second-order phase transition. Here, the unstable phase is remarked by the negative heat capacity($C < 0$), the stable one by the positive heat capacity($C > 0$) and the discontinuity on the plot of heat capacity is identified as the second-order phase transition(see subfigure 3.10 (a) and (c)). Also, notice that this phase transition is shifted towards higher values of the horizon radius as the PFDM parameter increases(see subfigure 3.10 (a)). Furthermore, for higher values of the horizon radius(see subfigure 3.10 (b)), we can see that the black hole moves from unstable phase to stable phase without any second-order phase transition. The same behaviour is noticed before the appearance of the phase transition in subfigure 3.10 (a).

On the other hand, in order to get more informations about the stability of the black hole, in subfigure 3.10 (c) and (d), the heat capacity is plotted for different values of the quintessence parameter c. Analysing these plots, we observe that a second-order phase transition occurs for lower values of the horizon radius. Also, notice that this phase transition is shifted towards higher values of the horizon radius as the quintessence parameter increases. Furthermore for higher values of the horizon radius, the black hole moves from unstable phase to stable phase without second-order phase transition(see subfigure 3.10 (d)).

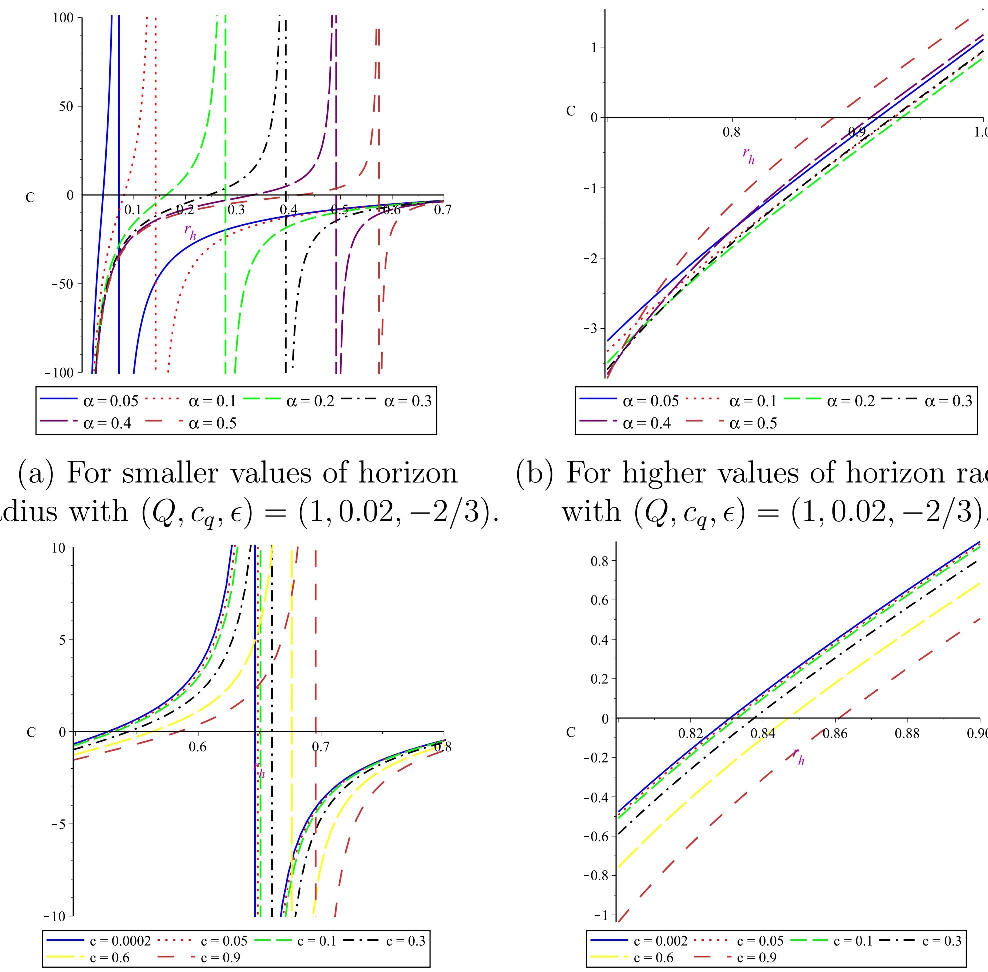

(a) For smaller values of horizon radius with $(Q, c_q, \epsilon) = (1, 0.02, -2/3)$.

(b) For higher values of horizon radius with $(Q, c_q, \epsilon) = (1, 0.02, -2/3)$.

(c) For smaller values of horizon radius with $(Q, \alpha, \epsilon) = (1, 0.6, -2/3)$.

(d) For higher values of horizon radius with $(Q, \alpha, \epsilon) = (1, 0.6, -2/3)$.

Figure 3.10: Variation of Heat capacity C in term of horizon radius.

Next, let us consider the relationship between the density of PFDM and quintessence in term of α and c_q, respectively. From Eq. (2.41), they are expressed as $\rho_{\text{PFDM}} = -\frac{1}{8\pi}\frac{\alpha}{r^3}$ and $\rho_{\text{quint}} = -\frac{3\epsilon c_q}{2r^{3(\epsilon+1)}}$. Then we study their impact on the behaviour of the black hole. These relations clearly show that the second-order phase transition occurs in the presence of both PFDM and quintessence dark energy, and this phase transition is shifted towards higher values of horizon radius as we decrease the PFDM density and increase the quintessence density. This result means that if we are in a presence of strong dark energy and dark matter, meaning that they have high values, the black hole would be more impacted by dark energy rather than dark matter.

After having considered both dark energy and dark matter, let us now study how the thermodynamic of the black hole is influenced by rotation and dark energy, when they are considered at the same time.

3.5 Simultaneous effects of rotation and dark energy on the thermodynamics of black hole

The rotating and nonlinear magnetic-charged black hole in the quintessence field we study here can be identified as a fusion of two metrics, namely the metric of a rotating black hole and the one for a nonlinear magnetic-charged black hole in the quintessence field, as we presented in the chapter (2) and obtained in 2.77. It is expressed as

$$\begin{aligned} ds^2 &= g_{\mu\nu}dx^\mu dx^\nu \\ &= -\left[1-\tfrac{2\rho r}{\Sigma}\right]dt^2+\tfrac{\Sigma}{\Delta}dr^2-\tfrac{4a\rho r\sin^2\theta}{\Sigma}dtd\phi \\ &+ \Sigma d\theta^2+\sin^2\theta\left[r^2+a^2+\tfrac{2a^2\rho r\sin^2\theta}{\Sigma}\right]d\phi^2, \end{aligned} \tag{3.47}$$

where

$$\begin{aligned} \Delta &= r^2-2\rho r+a^2, \\ \Sigma &= r^2+a^2\cos^2\theta, \\ 2\rho &= \tfrac{2Mr^3}{Q^3+r^3}+\tfrac{c_q}{r^{3\epsilon}}. \end{aligned} \tag{3.48}$$

Here, Q is the magnetic charge, a the rotating parameter, ϵ and c_q are quintessential parameters.

Using that metric, we will be able to make the thermodynamic study.

3.5.1 Entropy of the black hole

In the case of rotating and nonlinear magnetic-charged black hole, we have the presence of three horizons: the inner horizon r_-, the event or outer horizon $r_h(\geq r_-)$ and the quintessence or cosmological horizon $r_q(\geq r_h)$ [56, 57]. In our work, we will focus on the event horizon radius and make a thermodynamic analysis. The expression of the entropy is found throughout the horizon area [46]. Therefore, we have

$$S = \frac{A}{4} = \frac{1}{4}\int_0^{2\pi} d\phi \int_0^{\pi} d\theta \sqrt{g_{\theta\theta}g_{\phi\phi}}, \tag{3.49}$$

which gives, for the rotating black hole in the metric 2.77,

$$\begin{aligned} S &= \frac{\pi}{2}\int_0^{\pi} d\theta \sqrt{\Sigma \sin^2\theta \left[r_h^2 + a^2 + \frac{2a^2\rho r_h \sin\theta}{\Sigma}\right]} \\ &= \pi(r_h^2 + a^2) \\ &= \pi(r_h^2 + \frac{J^2}{M^2}),\ with\ \ a = \frac{J}{M}. \end{aligned}$$

Hence, we have

$$S = \pi(r_h^2 + \frac{J^2}{M^2}). \tag{3.50}$$

The change of entropy S, in term of J and with $M = 1$ is plotted in figure (3.11).

Here, we see that whatever the value of r_h, the entropy is always growing up, when the angular momentum J increases. Furthermore, we notice that if we increase the value of the event horizon radius r_h, the entropy seems to increase. This result tells that a larger and more rotating black hole has a higher entropy. Consequently, supermassive black holes have a high entropy at their event horizons, due to their rotation and their width.

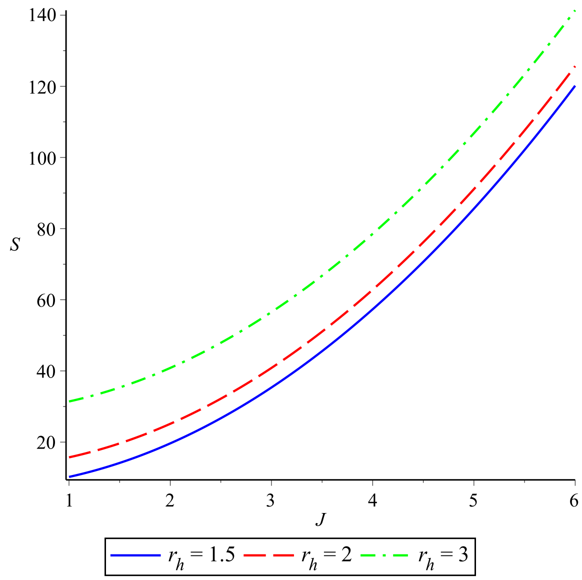

Figure 3.11: Change of the entropy S in the presence of quintessence dark energy. Here, $r_h = 1.5$ corresponds to blue continuous line, $r_h = 2$ to red dash and $r_h = 3$ to green dash-point.

3.5.2 Black hole mass, temperature and potential

To compute the mass M, we will use the event horizon property [57], then solving the following equation

$$g^{rr} = 0 \Rightarrow \frac{\Delta}{\Sigma} = 0, \quad \text{with } r = r_h. \tag{3.51}$$

From (3.51), we have

$$M = \frac{1}{2}(Q^3 + r_h^3)\left(\frac{1}{r_h^2} + \frac{a^2}{r_h^4} - \frac{c}{r_h^{3\epsilon+3}}\right). \tag{3.52}$$

When $a = 0$ and $\epsilon = -\frac{2}{3}$, we obtain the same result as Nam [56], for the magnetic-charged black hole in the quintessence expressed as

$$M = \frac{Q^3 + r^3}{2r_h^2}\left(1 - cr_h\right). \tag{3.53}$$

Moreover, if we have $Q = 0$ and $\epsilon = -\frac{2}{3}$, we obtain the same result as Toshmatov [46], for the rotating black hole with quintessence expressed in the following form

$$M = \frac{1}{2}\left(r_h + \frac{a^2}{r_h} - cr_h^2\right). \tag{3.54}$$

Then, in term of S, the mass M in Eq. (3.52) becomes

$$\begin{aligned} M &= \tfrac{1}{2}\left(Q^3 + \left(\tfrac{S}{\pi} - a^2\right)^{\frac{3}{2}}\right)\left(\tfrac{1}{\left(\frac{S}{\pi}-a^2\right)} + \tfrac{a^2}{\left(\frac{S}{\pi}-a^2\right)^2}\right. \\ &- \left.\tfrac{c}{\left(\frac{S}{\pi}-a^2\right)^{\frac{3\epsilon+3}{2}}}\right). \end{aligned} \tag{3.55}$$

Now, let us compute the temperature T, the potential Φ and the free enthalpy. Their formulas are respectively [56, 67]

$$T = \left(\frac{\partial M}{\partial S}\right), \tag{3.56}$$

$$\Phi = \left(\frac{\partial M}{\partial Q}\right). \tag{3.57}$$

Developing Eq. (3.56), we get

$$\begin{aligned} T &= \tfrac{3}{4}\frac{\sqrt{\frac{S}{\pi}-a^2}\left(\frac{1}{\frac{S}{\pi}-a^2} + \frac{a^2}{\left(\frac{S}{\pi}-a^2\right)^2} - \frac{c}{\left(\frac{S}{\pi}-a^2\right)^{\frac{3\epsilon+3}{2}}}\right)}{\pi} \\ &+ B\left(-\frac{1}{\pi\left(\frac{S}{\pi}-a^2\right)^2} - \frac{2a^2}{\pi\left(\frac{S}{\pi}-a^2\right)^3} + \frac{c\left(\frac{3\epsilon+3}{2}\right)}{\pi\left(\frac{S}{\pi}-a^2\right)^{\frac{3\epsilon+5}{2}}}\right), \end{aligned} \tag{3.58}$$

with

$$B = \frac{1}{2}\left(Q^3 + \left(\frac{S}{\pi} - a^2\right)^{\frac{3}{2}}\right).$$

In figure (3.12), we plotted the behaviour of the temperature for $Q = 1$. It shows that the temperature T starts increasing, and then decreases towards zero.

Especially, looking at subfigure (3.12)(a), the plot of temperature shows that as we increase the value of rotating parameter a, the maximum of temperature is shifted to lower values. This implies that temperature of a black hole with a stronger rotation has a lower value of maximum.

In addition, regarding subfigure (3.12)(b), we see that the maximum of temperature without quintessence ($c = 0$) is greater than the one with quintessence($c \neq 0$). Furthermore, increasing the quintessence parameter c, it follows that the maximum of temperature is shifted to lower values. Also, looking at subfigure (3.12)(c), we notice that the same behaviour appears when we decrease the other quintessence parameter ϵ.

At the end, we can also remark that the temperature decreases whatever the value of the rotating parameter and the quintessences parameters a, c and ϵ (See subfigures (3.12)(a), (b) and (c)). Therefore, we can say that when rotating, the black hole loses temperature, and quintessence behaves as a cooling energy decreasing the temperature.

In figure (3.13), we plotted the mass of the black hole, and we can see that it decreases, but starts increasing after reaching a minimum threshold. Moreover, this minimum is shifted to higher radius values r, as we increase the magnetic charge Q.

However, figure (3.14) shows that for high values of the entropy, the black hole reaches a second decrease in its mass (subfigure (3.14)(a)), but this does not appear without quintessence parameter c(subfigure (3.14)(b)). This means that quintessence energy could affect the behaviour of the black hole, causing the loss of mass for higher values of the event horizon radius. Thus, quintessence behaves as negative energy reducing the mass of the black hole.

Afterwards, finding the potential, through the Eq. (3.57), we obtain

$$\Phi = \frac{3Q^2}{2}\left(\frac{1}{\frac{S}{\pi} - a^2} + \frac{a^2}{\left(\frac{S}{\pi} - a^2\right)^2} - \frac{c}{\left(\frac{S}{\pi} - a^2\right)^{\frac{3\epsilon+2}{2}}}\right). \tag{3.59}$$

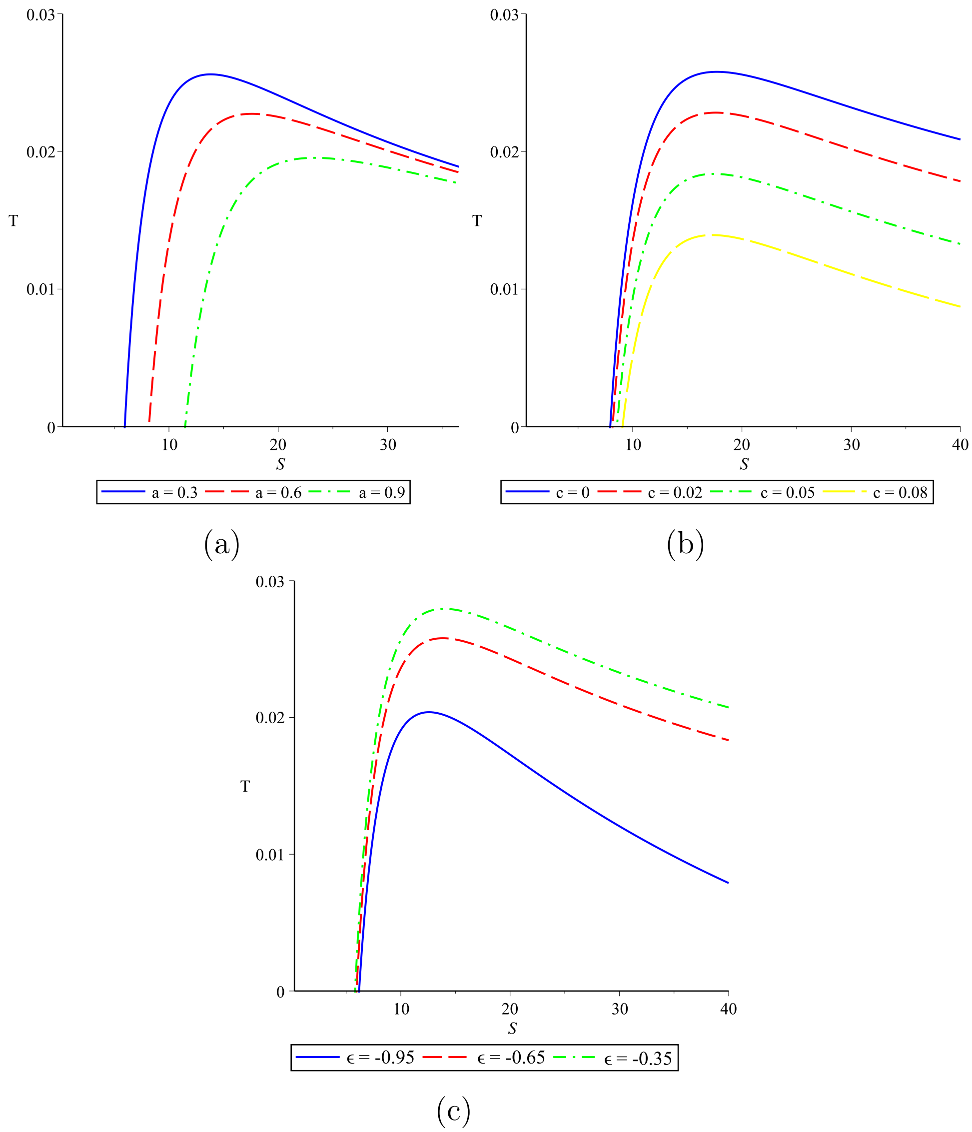

Figure 3.12: Change of the black hole temperature T in the presence of quintessence dark energy with $Q = 1$.

Its plot, which is depicted in figure (3.15) shows that the black hole potential decreases as the entropy increases. Also, the behaviour of the potential is not modified whatever the value of the quintessence parameter a. Moreover, for higher the quintessence parameter a, the behaviour of the potential seems to be closer to the exponential decay. Therefore, we can say that quintessence acts as negative energy allowing the lost of the black hole potential.

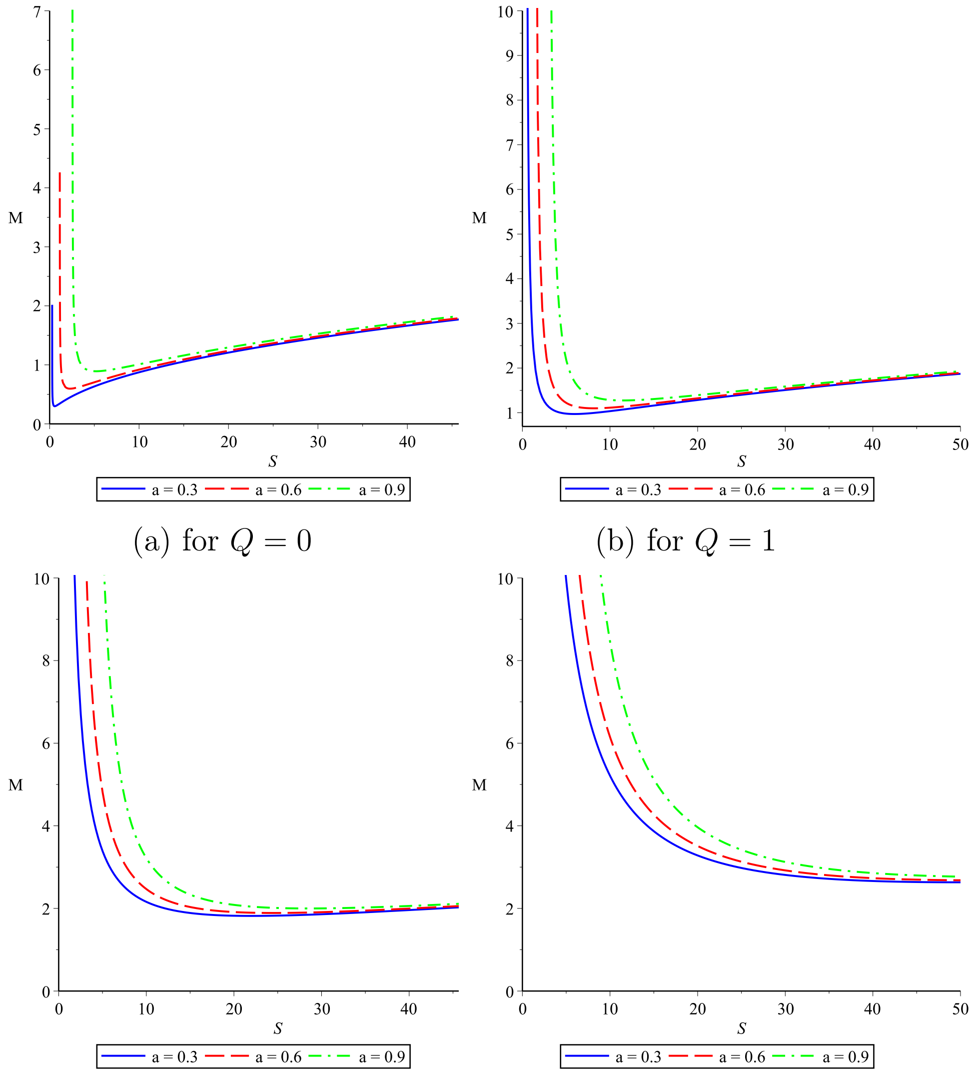

(a) for $Q = 0$ (b) for $Q = 1$

(c) for $Q = 2$ (d) for $Q = 3$

Figure 3.13: Change of the black hole mass M in the presence of quintessence dark energy with characteristics $(c, \epsilon) = (0.02, -\frac{2}{3})$. Here, $a = 0.3$ corresponds to blue continuous line, $a = 0.6$ to red dash and $a = 0.9$ to green dash-point.

3.5.3 Specific heat, Gibbs free energy

To analyse the stability of the black hole, we can start with finding the Gibbs free energy G, which is expressed as follows

$$G = H - TS, \tag{3.60}$$

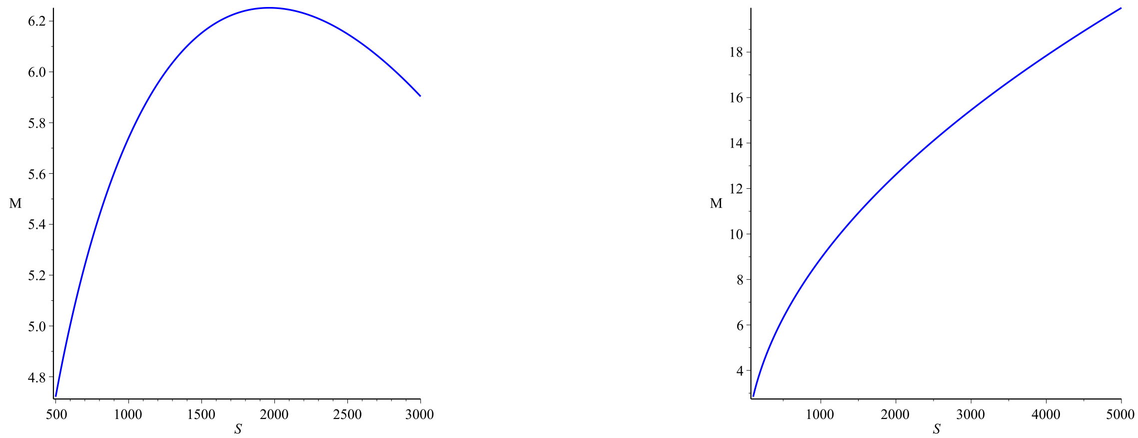

(a) for $c = 0.02$ (b) for $c = 0$

Figure 3.14: Change of the black hole mass M in the presence of quintessence dark energy with characteristics $(Q, a) = (1, 0.3)$.

where the enthalpy H is considered as the black hole mass M.

Furthermore, we depicted it in figure 3.16 with given values of Q, c_q and a. Its analysis shows that the black hole may have one entropy, then one horizon radius(see (3.50)), whatever the value of the Gibbs free energy G. However, this behaviour only appears for $\epsilon \leq -0.93$. Indeed, for higher values of ϵ, as for example $\epsilon = -0.65$ or $\epsilon = -0.40$, we notice that the black hole has two values of entropy, thus two horizon radii. Therefore, the plot of the Gibbs free energy shows that if the quintessence parameter ϵ increases, the black hole could undergo a small-large black hole phase transition.

Now, we can go further and we explore the expression of the heat capacity, to determine at which conditions the black hole could be stable.

The formula necessary to compute the heat capacity is [213]

$$C_{ax} = T\left(\frac{\partial S}{\partial T}\right)_x, \tag{3.61}$$

with some set of parameters, denoted by x, held constant. Furthermore, the system is stable if the heat capacity is positive, and it is unstable when the heat capacity is negative.

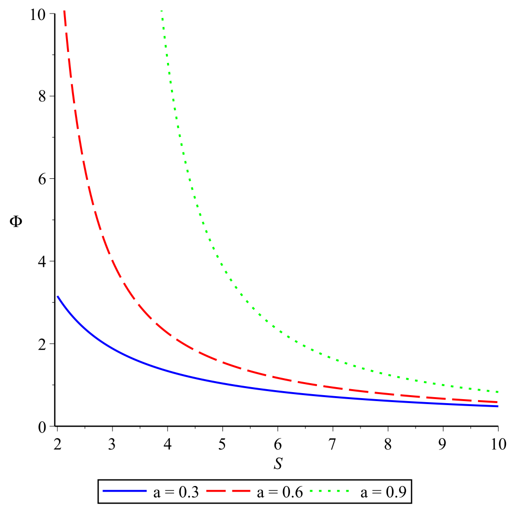

Figure 3.15: Variation of potential Φ for different values of the rotation parameter a.

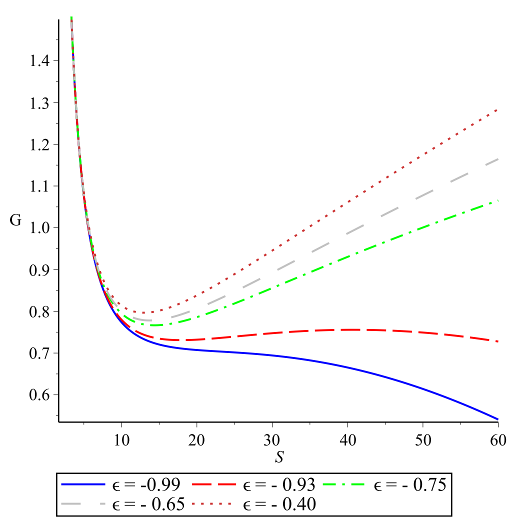

Figure 3.16: Variation of the Gibbs free energy G for different values of ϵ, with $(Q, c_q, a) = (1, 0.02, 0.3)$.

To find out if a second-order phase transition occurs, we first recall the relation between the heat capacity and the free enthalpy, and then plot it. For that, the best thermodynamic function adapted to the study of these transformations is then the free enthalpy G defined by

$$dG = -SdT + Vdp, \qquad S = -\left.\frac{\partial G}{\partial T}\right|_p. \tag{3.62}$$

Therefore, we have

$$C_a = -T\frac{\partial^2 G}{\partial T^2}. \tag{3.63}$$

Since C_a is the second derivative of the free enthalpy, we will study the curve of heat capacity to detect any presence of second-order phase transition. These phenomena appear when heat capacity changes its sign [49].

On the other hands, without losing generality, if we have a null magnetic charge Q and $\epsilon = -\frac{2}{3}$, we get easily the result obtained by Toshmatov et *al.* [46], expressed as follow

$$C_a = 2(S - \pi a^2)\frac{2c(S - \pi a^2)^{\frac{3}{2}} - \sqrt{\pi}(S - 2\pi a^2)}{\sqrt{\pi}(S - 4\pi a^2)}. \tag{3.64}$$

In figure (3.17), we plotted the heat capacity of rotating and nonlinear magnetic-charged black hole in the presence of quintessence dark energy with characteristic $(c, \epsilon) = (0.02, -\frac{2}{3})$.

Here $a = 0.3$, corresponds to blue continuous line, $a = 0.6$ to red dash and $a = 0.9$ to green dash-point. (e) corresponds to lower values of the entropy for $Q = 1$, and (f) corresponds to the change of heat capacity for different values of the quintessence parameter c.

Analysing these figures we can make a good appreciation of the black hole behaviour. Precisely, we notice that a second-order phase transition occurs, localized by the presence of a discontinuity onto the plot of the heat capacity. Precisely, analysing subfigure (3.17)(a), (b), (c) and (d), we notice that the black hole, being

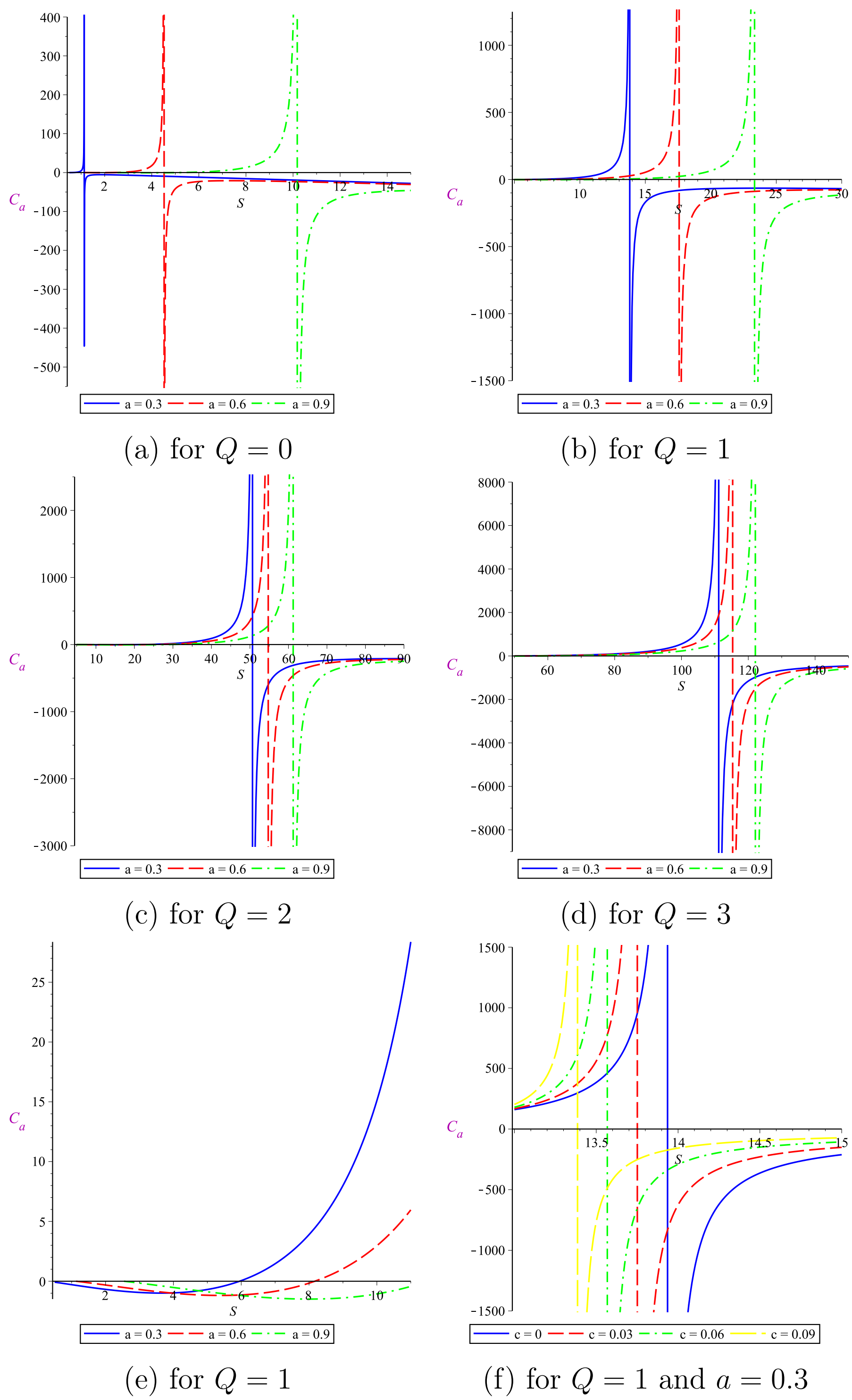

(a) for $Q = 0$ (b) for $Q = 1$

(c) for $Q = 2$ (d) for $Q = 3$

(e) for $Q = 1$ (f) for $Q = 1$ and $a = 0.3$

Figure 3.17: Change of the black hole heat capacity C_a.

stable($C_a > 0$), becomes unstable($C_a < 0$) after this second-order phase transition. Moreover, we notice that the phase transition is shifted towards higher values of the entropy as we increase the rotating parameter a or the magnetic parameter Q.

Another result we can get on the heat capacity is that if we choose $Q = 1$, and then make a comparison between subfigure (3.17)(b) and (e) both corresponding to $Q = 1$, we notice that for lower values of the entropy (subfigure (3.17)(e)), we have first a negative heat capacity, meaning that the black hole is firstly unstable, and then becomes stable without any second-order phase transition. This result tells that quintessence energy leads the black hole to change its phase twice, with the second change made through a second-order phase transition.

3.6 Conclusion

In this chapter, we aimed at studying the effects of dark energy, dark matter and rotation onto the thermodynamics of the nonlinear magnetic-charged black hole. Through the metrics found in chapter (2), we were able to put out four thermodynamic studies, for which we computed and plotted several thermodynamic quantities, in order to appreciate the impact of these given parameters.

Starting with the effects of quintessence dark energy, which is responsible for the accelerated expansion of the Universe, we showed that the entropy of the black hole is higher for a larger and more magnetic-charged black hole, then is not influenced by quintessence. However, this is not the case for the temperature, for which quintessence affects its behaviour, by reducing the maximum of temperature when increasing the quintessence parameter. For the thermodynamic potential, we showed that quintessence allows it to decrease and have lower values as the quintessence parameter increases. Regarding the heat capacity, the second-order phase transition appears. Afterwards, we studied the effects of perfect fluid dark matter, which is responsible for the irregular rotation speed curve of stars in galaxies, and we saw that the entropy of our black hole is also not affected by its presence, and for the temperature, the increase of dark matter parameter allows the maximum of temperature to be higher. About the heat capacity, we studied the influence of dark matter and we saw that the black hole also undergoes a second order phase transition. Now, considering at the same time quintessence dark energy and perfect fluid dark matter, we did the same analysis and we find for example that the second-order phase transition occurs on the black hole, but it is shifted towards higher values of horizon radius as we decrease the perfect fluid dark matter density, but increase the quintessence density. Also, since we considered here that the black hole is under an AdS spacetime, we found the first-order small/large phase transition, and the swallow tail on the plot of the Gibbs free energy. At the end, the analysis of the rotation coupled to quintessence revealed to that the entropy is a function of the angular momentum, and increases the entropy. Also, we showed that quintessence and rotation allow the black hole to loose its mass, and then to undergo a second-order phase transition.

CONCLUSION AND OUTLOOKS

In short, our goal was to study the impact of dark energy, dark matter and rotation onto the thermodynamics of the nonlinear magnetic-charged black hole. So, in chapter (1), starting from the generalities on black holes, we presented how they are classified according to their mass and according to their electrical charge and angular momentum. We also presented some types of dark energy(responsible for the accelerated expansion of the Universe), namely the cosmological constant, the quintessence and the phantom dark energy. After that we talked about dark matter, responsible for irregular rotation of stars in galaxies. Hence, it comes out that black holes are one of the most mysterious and fascinating space object, and there are many proofs of theirs existence, as for example the first ever observed image made in 2019 by the EHT collaboration, or gravitational waves detected. We have also shown that there exists an analogy between classical thermodynamics and black hole mechanics.

In chapter (2) of our dissertation, we presented the way to get solutions corresponding to the static case and the rotating case of the nonlinear magnetic-charged black hole. Especially, we derived the metric of the static and nonlinear magnetic-charged AdS black hole surrounded by quintessence, in the background of perfect fluid dark matter, by solving the Einstein-Maxwell equations. Then, we derived the rotating nonlinear magnetic-charged black hole surrounded by quintessence, through the modified Newman-Janis algorithm. Finally, we presented some tools for studying the thermodynamics of black holes, especially, we showed how to move from the laws of black hole mechanic to the thermodynamic laws of black hole, then we presented some thermodynamic quantities and also phase transitions. About phase transitions, we talked about the Ehrenfest classification, and also the van der Waals phase transition in fluids.

The chapter (3) was dedicated to the study of the influence of quintessence dark energy, perfect fluid dark matter and rotation onto the thermodynamics of the nonlinear magnetic-charged black hole. To achieve our goal, we worked with four metrics related to the nonlinear magnetic-charged black hole. Therefore, we computed and plotted several thermodynamic quantities in order to appreciate the impact of these parameters. About quintessence dark energy, we showed that it does not affect the entropy of the black hole, but reduces the maximum of temperature when increasing quintessence. Also, it allows the black hole to undergo a second-order phase transition. For perfect fluid dark matter, we did the same study and we noticed that when increasing it, it allows the maximum of temperature to be higher, and also leads the black hole to undergo a second-order phase transition. Afterwards, by combining both quintessence and perfect fluid dark matter, we showed for example that the second-order phase transition occurs, and it is shifted towards higher values of horizon radius as we decrease the perfect fluid dark matter density, but increase the quintessence density. Now, combining rotation with quintessence showed many phenomena such as the loss of black hole mass and also second-order phase transition, which appears as later as the rotation increases

This work and its results have allowed to think on how we can go further into our study. Indeed, one of the striking effects which could be able to appear on black holes is Hawking radiation, which is one of the ways from combination of quantum mechanics and general relativity. Hence, in the immediate future, we will continue investigating thoroughly the thermodynamics of the considered black hole in our work by studying the Hawking radiation which could be produced, and more other thermodynamic quantities such as Joules-Thompson expansion, which indicates that the heating and cooling zone emerge through the throttling process (adiabatic process with conservation of enthalpy). Furthermore, considering the quantum nature of gravity, we plane to study how quantum corrections could affect the entropy and the black hole thermodynamics. Moreover, we will study the thermal chaos under spatially/temporally periodic perturbations in the extended phase space of AdS black hole which could lead to have a link in establishing a connection among thermodynamics, gravitation and quantum statistical mechanics. Also, we will focus on gravitational solitons, considered as regular stationary spacetimes with finite energy. As we know, solitons are defined as having finite and localized energy, characteristic velocity of propagation and structural persistence. Another idea we shall develop is to study what could we have if we consider the dark matter as a real fluid, and also the hydrodynamics of black holes. Concerning the experimental study of black holes, we plan to put in place an observatory with telescopes in Cameroon, in order to study black holes and the universe experimentally.

List of projects and publications

As results of this thesis, we have obtained two articles published in a peer reviewed journal cited as follows

Ragil NDONGMO, Saleh MAHAMAT, Thomas Bouetou, and Timoleon Kofane, "Thermodynamics of a rotating and nonlinear magnetic-charged black hole in the quintessence field", *Physica Scripta*, 2021, vol. **96**, no 9, p. 095001.(IF: 2.928)

2. Ragil NDONGMO, Saleh MAHAMAT, Thomas Bouetou, Conrad Bertrand Tabi and Timoleon Kofane, "Thermodynamics of Non-linear magnetic-charged AdS black hole surrounded by quintessence, in the background of perfect fluid dark matter", *Physics of the Dark Universe Journal*, 2023, vol **42**, p. 101299.(IF: 5.119)

List of distinctions and nominations

During this thesis, I have received some distinctions and nominations, namely

1. Winner of the Best oral presentation award on Astrophysics and Cosmology, during "The second African Conference of Fundamental and Applied Physics", ACP2021, https://indico.cern.ch/event/1060503/contributions/4740759/,

2. Nominated for the "2022 International Young Leaders Forum in Physics", by the American Physical Society.

List of abbreviations

NASA: National Aeronautics and Space Administration,

LIGO: Laser Interferometer Gravitational Wave Observatory,

VIRGO: Like LIGO, is used for the detection of gravitational waves,

AdS anti-de Sitter,

dS de Sitter,

PFDM: Perfect fluid dark matter,

CDM: Cold Dark Matter,

CP: Charge-Parity,

EHT: Event Horizon Telescope,

GUT: Grand Unified Theory.

Bibliography

[1] S. W. Hawking. Particle creation by black holes. In *Euclidean quantum gravity*, pages 167–188. World Scientific, 1975.

[2] S. W. Hawking. Black hole explosions? *Nature*, 248(5443):30–31, 1974.

[3] J. D. Bekenstein. Black holes and entropy. *Physical Review D*, 7(8):2333, 1973.

[4] A. G. Riess, A. V. Filippenko, P. Challis, A. Clocchiatti, A. Diercks, P. M. Garnavich, R. L. Gilliland, C. J. Hogan, S. Jha, R. P. Kirshner, et al. Observational evidence from supernovae for an accelerating universe and a cosmological constant. *The Astronomical Journal*, 116(3):1009, 1998.

[5] A. G. Riess, R. P. Kirshner, B. P. Schmidt, S. Jha, P. Challis, P. M. Garnavich, A. A. Esin, C. Carpenter, R. Grashius, R. E. Schild, et al. Bvri light curves for 22 type ia supernovae. *The Astronomical Journal*, 117(2):707, 1999.

[6] S. Perlmutter, G. Aldering, G. Goldhaber, R. Knop, P. Nugent, P. Castro, S. Deustua, S. Fabbro, A. Goobar, D. Groom, et al. Measurements of ω and λ from 42 high-redshift supernovae. *The Astrophysical Journal*, 517(2):565, 1999.

[7] R. Tharanath and V. C. Kuriakose. Thermodynamics and spectroscopy of schwarzschild black hole surrounded by quintessence. *Modern Physics Letters A*, 28(04):1350003, 2013.

[8] L. M. Krauss and M. S. Turner. The cosmological constant is back. *General Relativity and Gravitation*, 27(11):1137–1144, 1995.

[9] S. Weinberg. The cosmological constant problem. *Reviews of modern physics*, 61(1):1, 1989.

[10] P. J. Peebles and B. Ratra. The cosmological constant and dark energy. *Reviews of modern physics*, 75(2):559, 2003.

[11] T. Padmanabhan. Cosmological constant—the weight of the vacuum. *Physics reports*, 380(5-6):235–320, 2003.

[12] M. Shahjalal. Thermodynamics of quantum-corrected schwarzschild black hole surrounded by quintessence. *Nuclear Physics B*, 940:63–77, 2019.

[13] W. Javed and R. Babar. Fermions tunneling and quantum corrections for quintessential kerr-newman-ads black hole. *Advances in High Energy Physics*, 2019:2759641, 2019.

[14] V. V. Kiselev. Quintessence and black holes. *Classical and Quantum Gravity*, 20(6):1187, 2003.

[15] S. Chen, B. Wang, and R. Su. Hawking radiation in a d-dimensional static spherically symmetric black hole surrounded by quintessence. *Physical Review D*, 77(12):124011, 2008.

[16] W. Yi-Huan and C. Zhong-Hui. Thermodynamic properties of a reissner—nordström quintessence black hole. *Chinese Physics Letters*, 28(10):100403, 2011.

[17] Bouetou B. T., M. Saleh, and C. T. Kofane. Thermodynamics and phase transition of the reissner–nordström black hole surrounded by quintessence. *General Relativity and Gravitation*, 44(9):2181–2189, 2012.

[18] Sharmanthie Fernando. Nariai black holes with quintessence. *Modern Physics Letters A*, 28(40):1350189, 2013.

[19] K. Ghaderi and B. Malakolkalami. Thermodynamics of the schwarzschild and the reissner–nordström black holes with quintessence. *Nuclear physics B*, 903:10–18, 2016.

[20] G-Q Li. Effects of dark energy on p–v criticality of charged ads black holes. *Physics Letters B*, 735:256–260, 2014.

[21] Z. Xu and J. Wang. Kerr-newman-ads black hole in quintessential dark energy. *Physical Review D*, 95(6):064015, 2017.

[22] A. Younas, M. Jamil, S. Bahamonde, and S. Hussain. Strong gravitational lensing by kiselev black hole. *Physical Review D*, 92(8):084042, 2015.

[23] J. de Oliveira and R. Fontana. Three-dimensional black holes with quintessence. *Physical Review D*, 98(4):044005, 2018.

[24] A. Abdujabbarov, B. Toshmatov, Z. Stuchlík, and B. Ahmedov. Shadow of the rotating black hole with quintessential energy in the presence of plasma. *International Journal of Modern Physics D*, 26(06):1750051, 2017.

[25] Z. Xu, X. Hou, and J. Wang. Kerr-anti-de sitter/de sitter black hole in perfect fluid dark matter background. *Classical and Quantum Gravity*, 35(11):115003, 2018.

[26] J. F. Navarro, C. S. Frenk, and S. D. White. A universal density profile from hierarchical clustering. *The Astrophysical Journal*, 490(2):493, 1997.

[27] K. Dutta, A. Ghosh, A. Kar, and B. Mukhopadhyaya. Decaying fermionic warm dark matter and xenon1t electronic recoil excess. *Physics of the Dark Universe*, 33:100855, 2021.

[28] J. A. Ruiz. Scalar field theory for warm dark matter. *The European Physical Journal Plus*, 136(1):33, 2021.

[29] M. Paranjape, R. MacKenzie, Z. Thomova, P. Winternitz, and W. Witczak-Krempa. *Quantum Theory and Symmetries: Proceedings of the 11th International Symposium, Montreal, Canada*. Springer Nature, 2021.

[30] L. E. Padilla, J. Solís-López, T. Matos, and A. A. Avilez-López. Consequences for the scalar field dark matter model from the mcgaugh observed-baryon acceleration correlation. *The Astrophysical Journal*, 909(2):162, 2021.

[31] G. F. Siddhartha, T. Matos, D. Nunez, and E. Ramirez. Quintessence-like dark matter in spiral galaxies. *Revista mexicana de física*, 49(3):203–206, 2003.

[32] K. Saurabh and K. Jusufi. Imprints of dark matter on black hole shadows using spherical accretions. *The European Physical Journal C*, 81(6):490, 2021.

[33] S. Shaymatov, B. Ahmedov, and M. Jamil. Testing the weak cosmic censorship conjecture for a reissner–nordström–de sitter black hole surrounded by perfect fluid dark matter. *The European Physical Journal C*, 81(7):588, 2021.

[34] M. Ghosh. Charged perfect fluid dark matter model: Known mass density function approach. *Modern Physics Letters A*, 36(07):2150043, 2021.

[35] T-C Ma, H-X Zhang, P-Z He, H-R Zhang, Y. Chen, and J-B Deng. Shadow cast by a rotating and nonlinear magnetic-charged black hole in perfect fluid dark matter. *Modern Physics Letters A*, page 2150112, 2021.

[36] Event Horizon Telescope Collaborat. First m87 event horizon telescope results. i. the shadow of the supermassive black hole. *Astrophysical Journal Letters*, 875(1):L1, 2019.

[37] K. Akiyama, A. Alberdi, W. Alef, K. Asada, R. Azulay, A-K Baczko, D. Ball, M. Baloković, J. Barrett, D. Bintley, et al. First m87 event horizon telescope results. ii. array and instrumentation. *The Astrophysical Journal Letters*, 875(1):L2, 2019.

[38] K. Akiyama, A. Alberdi, W. Alef, K. Asada, R. Azulay, A-K Baczko, D. Ball, M. Baloković, J. Barrett, D. Bintley, et al. First m87 event horizon telescope results. iii. data processing and calibration. *The Astrophysical Journal Letters*, 875(1):L3, 2019.

[39] Event Horizon Telescope Collaborat. First m87 event horizon telescope results. iv. imaging the central supermassive black hole. *Astrophysical Journal Letters*, 875(1):L4, 2019.

[40] K. Akiyama, W. Alberdi, A.and Alef, K. Asada, R. Azulay, A-K Baczko, D. Ball, M. Baloković, J. Barrett, D. Bintley, et al. First m87 event horizon telescope results. v. physical origin of the asymmetric ring. *The Astrophysical Journal Letters*, 875(1):L5, 2019.

[41] C. Bambi, K. Freese, S. Vagnozzi, and L. Visinelli. Testing the rotational nature of the supermassive object m87* from the circularity and size of its first image. *Physical Review D*, 100(4):044057, 2019.

[42] T. Kawashima, M. Kino, and K. Akiyama. Black hole spin signature in the black hole shadow of m87 in the flaring state. *The Astrophysical Journal*, 878(1):27, 2019.

[43] E. M. Murchikova, E. S. Phinney, A. Pancoast, and R. D. Blandford. A cool accretion disk around the galactic centre black hole. *Nature*, 570(7759):83, 2019.

[44] S. G. Ghosh. Rotating black hole and quintessence. *The European Physical Journal C*, 76(4):222, 2016.

[45] Y. Heydarzade and F. Darabi. Black hole solutions surrounded by perfect fluid in rastall theory. *Physics Letters B*, 771:365–373, 2017.

[46] B. Toshmatov, Z. Stuchlík, and B. Ahmedov. Rotating black hole solutions with quintessential energy. *The European Physical Journal Plus*, 132(2):98, 2017.

[47] M. Azreg-Aïnou. Generating rotating regular black hole solutions without complexification. *Physical Review D*, 90(6):064041, 2014.

[48] S. Hawking and R. Penrose. *The nature of space and time*. Princeton University Press, 2010.

[49] M. Saleh, Bouetou B. T., and C. T. Kofane. Thermodynamics and phase transition from regular bardeen black hole surrounded by quintessence. *International Journal of Theoretical Physics*, 57(9):2640–2647, 2018.

[50] E. Ayón-Beato and A. Garcıa. The bardeen model as a nonlinear magnetic monopole. *Physics Letters B*, 493(1-2):149–152, 2000.

[51] N. Bretón. Stability of nonlinear magnetic black holes. *Physical Review D*, 72(4):044015, 2005.

[52] A. Abdujabbarov, B. J. Ahmedov, and N. B. Jurayeva. Charged-particle motion around a rotating non-kerr black hole immersed in a uniform magnetic field. *Physical Review D*, 87(6):064042, 2013.

[53] R. Ruffini, Y-B Wu, and S-S Xue. Einstein-euler-heisenberg theory and charged black holes. *Physical Review D*, 88(8):085004, 2013.

[54] Y-K Lim. Motion of charged particles around a magnetized/electrified black hole. *Physical Review D*, 91(2):024048, 2015.

[55] A. Allahyari, M. Khodadi, S. Vagnozzi, and D. F. Mota. Magnetically charged black holes from non-linear electrodynamics and the event horizon telescope. *Journal of Cosmology and Astroparticle Physics*, 2020(02):003, 2020.

[56] C. H. Nam. Non-linear charged ds black hole and its thermodynamics and phase transitions. *The European Physical Journal C*, 78(5):418, 2018.

[57] C. A. Benavides-Gallego, A. Abdujabbarov, and C. Bambi. Rotating and nonlinear magnetic-charged black hole surrounded by quintessence. *Physical Review D*, 101(4):044038, 2020.

[58] S. W. Hawking and D. N. Page. Thermodynamics of black holes in anti-de sitter space. *unications in Mathematical Physics*, 87(4):577–588, 1983.

[59] N. Farhangkhah and Z. Dayyani. Extended phase space thermodynamics for third-order lovelock black holes with nonmaximally symmetric horizons. *Physical Review D*, 104(2):024068, 2021.

[60] B. Wu, C. Wang, Z-M Xu, and W-L Yang. Ruppeiner geometry and thermodynamic phase transition of the black hole in massive gravity. *The European Physical Journal C*, 81(7):626, 2021.

[61] S. H. Hendi and K. Jafarzade. Critical behavior of charged ads black holes surrounded by quintessence via an alternative phase space. *Physical Review D*, 103(10):104011, 2021.

[62] D. Kastor, S. Ray, and J. Traschen. Enthalpy and the mechanics of ads black holes. *Classical and Quantum Gravity*, 26(19):195011, 2009.

[63] D. Kastor, S. Ray, and J. Traschen. Mass and free energy of lovelock black holes. *Classical and Quantum Gravity*, 28(19):195022, 2011.

[64] D. Kastor, S. Ray, and J. Traschen. Black hole enthalpy and scalar fields. *Classical and Quantum Gravity*, 36(2):024002, 2018.

[65] B. P. Dolan. Pressure and volume in the first law of black hole thermodynamics. *Classical and Quantum Gravity*, 28(23):235017, 2011.

[66] B. P. Dolan. The cosmological constant and black-hole thermodynamic potentials. *Classical and Quantum Gravity*, 28(12):125020, 2011.

[67] S. Hendi, A. Nemati, K. Lin, and M. Jamil. Instability and phase transitions of a rotating black hole in the presence of perfect fluid dark matter. *European Physical Journal C*, 80(2001.01591):296, 2020.

[68] W. Hong, B. Mu, and J. Tao. Thermodynamics and weak cosmic censorship conjecture in the charged rn-ads black hole surrounded by quintessence under the scalar field. *Nuclear Physics B*, 949:114826, 2019.

[69] K-J He, X-Y Hu, and X-X Zeng. Weak cosmic censorship conjecture and thermodynamics in quintessence ads black hole under charged particle absorption. *Chinese Physics C*, 43(12):125101, 2019.

[70] J. M. Toledo and V. B. Bezerra. Kerr–newman–ads black hole with quintessence and cloud of strings. *General Relativity and Gravitation*, 52(4):34, 2020.

[71] X-Y Guo, H-F Li, L-C Zhang, and R Zhao. Continuous phase transition and microstructure of charged ads black hole with quintessence. *The European Physical Journal C*, 80(2):168, 2020.

[72] M. Chabab and S. Iraoui. Thermodynamic criticality of d-dimensional charged ads black holes surrounded by quintessence with a cloud of strings background. *General Relativity and Gravitation*, 52(8):75, 2020.

[73] J. Liang, B. Mu, and J. Tao. Thermodynamics and overcharging problem in extended phase space of charged ads black holes with cloud of strings and quintessence under charged particle absorption. *Chinese Physics C*, 45(2):023121, 2021.

[74] V. Husain and R. B. Mann. Thermodynamics and phases in quantum gravity. *Classical and Quantum Gravity*, 26(7):075010, 2009.

[75] J. R. Kamiko, M. Saleh, B. T. Bouetou, and C. T. Kofane. Thermodynamic phase transition and global stability of the regular hayward black hole surrounded by quintessence. *Modern Physics Letters A*, 35(16):2050129, 2020.

[76] R-G Cai, L-M Cao, and N. Ohta. Thermodynamics of black holes in hořava–lifshitz gravity. *Physics Letters B*, 679(5):504–509, 2009.

[77] K. R. Kamiko, M. Saleh, Bouetou B. T., and C. T. Kofane. Thermodynamics phase transition and hawking radiation of the schwarzschild black hole with quintessence-like matter and a deficit solid angle. *General Relativity and Gravitation*, 50(5):52, 2018.

[78] R. Tharanath, N. Varghese, and V. C. Kuriakose. Phase transition, quasinormal modes and hawking radiation of schwarzschild black hole in quintessence field. *Modern Physics Letters A*, 29(11):1450057, 2014.

[79] H-L Li and W. Li. Thermodynamic phase transition of black hole. *International Journal of Theoretical Physics*, 59(10):3032–3042, 2020.

[80] N. Don. *Black holes*. The Lucient library of science and technology, 2004.

[81] R. M. Wald. Gravitational collapse and cosmic censorship. In *Black Holes, Gravitational Radiation and the Universe*. Springer, 1999.

[82] D. Overbye. Black hole hunters. *NASA*, 8 June 2015.

[83] John Michell. Vii. on the means of discovering the distance, magnitude, &c. of the fixed stars, in consequence of the diminution of the velocity of their light, in case such a diminution should be found to take place in any of them, and such other data should be procured from observations, as would be farther necessary for that purpose. by the rev. john michell, bdfrs

in a letter to henry cavendish, esq. frs and as. *Philosophical transactions of the Royal Society of London*, (74):35–57, 1784.

[84] C. Montgomery, W. Orchiston, and I. Whittingham. (2009) michell, laplace and the origin of the black hole concept. *Journal of Astronomical History and Heritage*, **12**(2):90–96, 08-07-2016.

[85] A. Einstein. "the foundation of the general theory of relativity". *Annalen der Physik*, **354**(7):769, 1916.

[86] T. R. Nola. Black holes: Facts, theory and definition. *Science and Astronomy, Space.com Contributor*, 9 April 2015.

[87] Astronomy. The beginning to the end of the universe: How black holes die. *https://astronomy.com/magazine/news/2021/02/*, Consultation: 09/10/2022, 16h27.

[88] eso2007. Eso instrument finds closest black hole to earth. *https://www.eso.org/public/news/eso2007/*, Consultation: 07/10/2022, 12h50.

[89] P. T. Chruściel, J. L. Costa, and M. Heusler. Stationary black holes: Uniqueness and beyond. *Living Reviews in Relativity*, **15**(1):7, 2012.

[90] Wikipedia. Electric charge. *https://en.wikipedia.org/wiki/Electriccharge*, Consultation: 05-07-2022, 11h14.

[91] wikipedia. No hair theorem. *https://en.wikipedia.org/wiki/*, Consultation: 07/10/2022, 13h39.

[92] S. Bhattacharya and A. Lahiri. Black-hole no-hair theorems for a positive cosmological constant. *Physical review letters*, 99(20):201101, 2007.

[93] Photo by Roy Gendler. The orion nebula, a going cloud of gaz and dust, where we see stars forming. *w.w.w.pbs.org/seeingthedark/astronomy-topics/orionnebula.html*, Consultation:01-10-2021, 15h30.

[94] academy. Protostar: Definition, formation and facts. *w.w.w.com/academy/lesson/protostardefinition-facts.html*, Consultation:01-10-2021, 15h40.

[95] Astrolab. Astrolab. les etoiles. *w.w.w.globaia.org>pdf>etoiles*, Consultation:01-10-2021, 17h00.

[96] W-H Maya. Black holes, explained. *https://www.nationalgeographic.com/science/article/black-holes*, Consultation:01-10-2021, 15h30.

[97] Cosmos. Stellar black hole. *https://astronomy.swin.edu.au/cosmos/s/Stellar+Black+Hole*, Consultation: 03-10-2021, 15h01.

[98] wikipedia. Stellar black hole. *https://en.wikipedia.org/wiki/Stellar+black+hole*, Consultation: 08/10/2022, 09h20.

[99] Cosmos. Supermassive black hole. *https://astronomy.swin.edu.au/cosmos/S*, Consultation: 03-10-2021, 15h07.

[100] Imgur. Imgur gallery. *https://imgur.com/gallery/IYC9e*, Consultation: 03-20-2021, 15h19.

[101] J. L. Greenstein and M. Schmidt. The quasi-stellar radio sources 3c 48 and 3c 273. *The Astrophysical Journal*, 140:1, 1964.

[102] W. A. Fowler and F. Hoyle. Star formation. *Royal Greenwich Observatory Bulletins*, 67:301–320, 1963.

[103] R. P. Feynman, F. B. Morinigo, W. G. Wagner, B. Hatfield, J. Preskill, and K. S. Thorne. *Feynman lectures on gravitation*. CRC Press, 2018.

[104] wikipedia. Supermassive black hole. *https://en.wikipedia.org/wiki/*, Consultation: 08/10/2022, 10h10.

[105] E. E. Salpeter. Accretion of interstellar matter by massive objects. 1965.

[106] M. C. Begelman, M. Volonteri, and M. J. Rees. Formation of supermassive black holes by direct collapse in pre-galactic haloes. *Monthly Notices of the Royal Astronomical Society*, 370(1):289–298, 2006.

[107] D. Elbaz, K. Jahnke, E. Pantin, D. Le Borgne, and G. Letawe. Quasar induced galaxy formation: a new paradigm? *Astronomy & Astrophysics*, 507(3):1359–1374, 2009.

[108] wikipedia. Intermediate-mass black hole. *https://en.wikipedia.org/wiki/*, Consultation: 08/10/2022, 14h02.

[109] European Southern Observatory (ESO). S2 and central black hole. *http://www.solstation.com/xobjects/s2.htm*, Consultation: 08/10/2022, 14h17.

[110] D. Lin, J. Strader, A. J. Romanowsky, J. A. Irwin, O. Godet, D. Barret, N. A. Webb, J. Homan, and R. A. Remillard. Multiwavelength follow-up of the hyperluminous intermediate-mass black hole candidate 3xmm j215022. 4- 055108. *The Astrophysical Journal Letters*, 892(2):L25, 2020.

[111] B. J. Carr. Primordial black holes: Do they exist and are they useful? *arXiv preprint astro-ph/0511743*, 26 Nov 2005.

[112] J. R. Oppenheimer and H. Snyder. On continued gravitational contraction. *Physical Review*, 56(5):455, 1939.

[113] Y. B. Zeldovich and I. D. Novikov. Relativistic astrophysics. vol. 1: Stars and relativity. *Chicago: University of Chicago Press*, 1971.

[114] S. W. Hawking. Gravitationally collapsed objects of very low mass. *Monthly Notices of the Royal Astronomical Society*, 152(1):75–78, 1971.

[115] B. J. Carr and S. W. Hawking. Black holes in the early universe. *Monthly Notices of the Royal Astronomical Society*, 168(2):399–415, 1974.

[116] J. S. Bullock and J. R. Primack. Non-gaussian fluctuations and primordial black holes from inflation. *Physical Review D*, 55(12):7423, 1997.

[117] P. Ivanov. Nonlinear metric perturbations and production of primordial black holes. *Physical Review D*, 57(12):7145, 1998.

[118] J. S. Bullock and J. R. Primack. Comments on non-gaussian density perturbations and the production of primordial black holes. *arXiv preprint astro-ph/9806301*, 1998.

[119] M. A. Markov, V. A. Berezin, and V. P. Frolov. Proceedings of the third seminar on quantum gravity. 1985.

[120] A. G. Polnarev and M. Y. Khlopov. Cosmology, primordial black holes, and supermassive particles. *Soviet Physics Uspekhi*, 28(3):213, 1985.

[121] J. E. Lidsey, B. J. Carr, and J. H. Gilbert. Primordial black holes and the spectral index. *Nuclear Physics B-Proceedings Supplements*, 43(1-3):75–77, 1995.

[122] K. Schwarzschild. über das gravitationsfeld einer kugel aus inkopressibler flüssigkeit nach der einsteinschen theorie. *Sitzungsberichte der Deutschen Akademie der Wissenschaften zu Berlin, Klasse fur Mathematik, Phys.-Math. Klasse*, pages 424–434, 1916.

[123] wikipedia. Schwarzschild metric. *https://en.wikipedia.org/wiki/Schwarzschildmetric*, Consultation: 08/10/2022, 14h17.

[124] H. Reissner. über die eigengravitation des elektrischen feldes nach der einsteinschen theorie. *Annalen der Physik*, **50**(9):106–120, 1916.

[125] G. Nordström. On the energy of gravitational field in einstein's theory. *Verhandl. Koninkl. Ned. Akad. Wetenschap., Afdel. Natuurk., Amsterdam.*, **26**:1201–1208, 1918.

[126] JILA. Charged black holes: The reissner-nordström geometry. *https://jila.colorado.edu/ ajsh/bh/rn.html*, 2001.

[127] wikipedia. Reissner-nordström. *https://en.wikipedia.org/wiki/*, Consultation: 09/10/2022, 09h37.

[128] A. Qadir. Reissner-nordstrom repulsion. *Physics Letters A*, 99(9):419–420, 1983.

[129] R. P. Kerr. Gravitational field of a spinning mass as an example of algebraically special metrics. *Physical review letters*, 11(5):237, 1963.

[130] wikipedia. Kerr metric. *https://en.wikipedia.org/wiki/*, Consultation: 09/10/2022, 09h37.

[131] J. M. Bardeen. The four laws of black hole mechanics. *in: Conference Proceedings of GR5*, pages Tbilisi, USSR, p. 174, 1968.

[132] S. A. Hayward. Formation and evaporation of nonsingular black holes. *Physical review letters*, 96(3):031103, 2006.

[133] wikipedia. Magnetic monopole. *https://en.wikipedia.org/wiki/Magneticmonopole*, Consultation: 08/11/2022, 02h05.

[134] T. Richard, V. Loïc, and F. Pascal. Dictionnaire de physique. *edition de Boeck Université*, 02/2013.

[135] R. K. Walia, S. D. Maharaj, and S. G. Ghosh. Gravitational deflection of light by rotating black holes in horndeski gravity. *arXiv preprint arXiv:2109.08055*, 2021.

[136] F. Bacchini, B. Ripperda, A. Y. Chen, and L. Sironi. Generalized, energy-conserving numerical simulations of particles in general relativity. i. time-like and null geodesics. *The Astrophysical Journal Supplement Series*, 237(1):6, 2018.

[137] V. Nicolat. *Quelques aspects des horizons de trous noirs en relativité numérique*. PhD thesis, Université Denis Diderot-Paris VII, 2009.

[138] *La machine-univers. Voyage à travers l'Univers : Les Étoiles.* Amsterdam, Les Éditions Time-Life, mai 1989.

[139] LIGO. Gravitational waves detected 100 years after einstein's prediction. *LIGO Caltech, https://www.ligo.caltech.edu/news/ligo20160211*, 11 february 2016. Consultation: 03-08-2017, 11h 12.

[140] The Event Horizon Telescope Collaboration et *al.* First sagittarius a* event horizon telescope results. i. the shadow of the supermassive black hole in the center of the milky way. *The Astrophysical Journal Letters*, 930(2:L12).

[141] The Event Horizon Telescope Collaboration et *al.* First sagittarius a* event horizon telescope results. ii. eht and multiwavelength observations, data processing, and calibration. *The Astrophysical Journal Letters*, 930(2:L13).

[142] The Event Horizon Telescope Collaboration et *al.* First sagittarius a* event horizon telescope results. iii. imaging of the galactic center supermassive black hole. *The Astrophysical Journal Letters*, 930(2:L14).

[143] The Event Horizon Telescope Collaboration et *al.* First sagittarius a* event horizon telescope results. iv. variability, morphology, and black hole mass. *The Astrophysical Journal Letters*, 930(2:L15).

[144] The Event Horizon Telescope Collaboration et *al.* First sagittarius a* event horizon telescope results. v. testing astrophysical models of the galactic center black hole. *The Astrophysical Journal Letters*, 930(2:L16).

[145] The Event Horizon Telescope Collaboration et *al.* First sagittarius a* event horizon telescope results. vi. testing the black hole metric. *The Astrophysical Journal Letters*, 930(2:L17).

[146] R. R. Caldwell. Dark energy. *Physics World*, **17**(5):37, 2004.

[147] journaliste à *Pour la Science* Sean Bailly. L'énergie sombre est-elle une illusion? *Pour La Science, http://www.pourlascience.fr*, Consultation: 18-09-2017, 18h58.

[148] J. T. Florian and T. Mariette. Localisation de l'énergie dans un trou noir, **Ecole Normale Superieure Maroua, DIPES II**, physique, 2014-2015.

[149] P. J. Steinhardt. A quintessential introduction to dark energy. *Philosophical Transactions of the Royal Society of London. Series A: Mathematical, Physical and Engineering Sciences*, 361(1812):2497–2513, 2003.

[150] J. R. Kamiko. Effets of global monopole and dark energy on hawking radiation and thermodynamics of black holes.

[151] R. R. Caldwell, R. Dave, and P. J. Steinhardt. Cosmological imprint of an energy component with general equation of state. *Phys. Rev. Lett*, **80**:1582–1585, 1998.

[152] B. Philippe. La mystérieuse énergie noire. *consulté en 2021, disponible sur : https://www.futura-sciences.com/sciences/dossiers/univers-mysterieuse-energie-noire-1033/*, 2010.

[153] K. J. Ludwick. The viability of phantom dark energy: A review. *Modern Physics Letters A*, 32(28):1730025, 2017.

[154] R-G Cai and A. Wang. Cosmology with interaction between phantom dark energy and dark matter and the coincidence problem. *Journal of Cosmology and Astroparticle Physics*, 2005(03):002, 2005.

[155] G. Leon, A. Paliathanasis, and J. L. Morales-Martínez. The past and future dynamics of quintom dark energy models. *The European Physical Journal C*, 78(9):1–22, 2018.

[156] H. Wei and R-G Cai. Cosmological evolution of "hessence" dark energy and avoidance of the big rip. *Physical Review D*, 72(12):123507, 2005.

[157] J. Einasto. Dark matter. *Brazilian Journal of Physics*, 43(5):369–374, 2013.

[158] G. Bertone and T. M. Tait. A new era in the search for dark matter. *Nature*, 562(7725):51–56, 2018.

[159] G. Bertone, D. Hooper, and J. Silk. Particle dark matter: Evidence, candidates and constraints. *Physics reports*, 405(5-6):279–390, 2005.

[160] M. S. Turner. Windows on the axion. *Physics Reports*, 197(2):67–97, 1990.

[161] S. Tulin and H-B Yu. Dark matter self-interactions and small scale structure. *Physics Reports*, 730:1–57, 2018.

[162] V. V. Kiselev. Quintessential solution of dark matter rotation curves and its simulation by extra dimensions. *arXiv preprint gr-qc/0303031*, 2003.

[163] M-H Li and K-C Yang. Galactic dark matter in the phantom field. *Physical Review D*, 86(12):123015, 2012.

[164] G. Drake. thermodynamics. *https://www.britannica.com/science/thermodynamics*, Consultation: 17-08-2022, 17h21.

[165] B. Thompson. An inquiry concerning the source of heat which is excited by friction. *Philosophical transactions of the Royal Society of London*, **XVII**:286, 1798.

[166] Sadi C. Reflexions on the motive power of fire, and on machines fitted to develop that power. *Paris: Bachelier*, 1824.

[167] R. Clausius. *The mechanical theory of heat: with its Applications to the Steam Engine and to Physical Propreties of Bodies.* John van Voorst, 1865.

[168] J. Leland, W. Thomas, and G. A. Mansoori. Basic principles of classical and statistical thermodynamics. *University of Illinois, Chicago*, 2001.

[169] Wikipedia. Temperature. *https://en.wikipedia.org/wiki/Temperature*, Consultation: 05-07-2022, 11h14.

[170] Wikipedia. Entropy. *https://en.wikipedia.org/wiki/Entropy*, Consultation: 05-07-2022, 10h42.

[171] J. Ted. Introductory lectures on black hole thermodynamics. *Institute for Theoretical Physics University of Utrecht*, 26, 1996.

[172] J. M. Bardeen, B. Carter, and S. Hawking. The four laws of black hole mechanics. *Commun. Math. Phys.*, **31**(2):161–170, 1973.

[173] C. H. Nam. On non-linear magnetic-charged black hole surrounded by quintessence. *General Relativity and Gravitation*, 50(6):57, 2018.

[174] Y. Chen, H-X Zhang, T-C Ma, and J-B Deng. Optical properties of a nonlinear magnetic charged rotating black hole surrounded by quintessence with a cosmological constant. *arXiv preprint arXiv:2009.03778*, 2020.

[175] Z. Xu, X. Hou, J. Wang, and Y. Liao. Perfect fluid dark matter influence on thermodynamics and phase transition for a reissner-nordstrom-anti-de sitter black hole. *Advances in High Energy Physics*, 2019, 2019.

[176] J. Sadeghi, E. Mezerji, and S. Gashti. Universal relations and weak gravity conjecture of ads black holes surrounded by perfect fluid dark matter with small correction. *arXiv preprint arXiv:2011.14366*, 2020.

[177] H. Salazar, García D. A., and J. Plebański. Duality rotations and type d solutions to einstein equations with nonlinear electromagnetic sources. *Journal of mathematical physics*, 28(9):2171–2181, 1987.

[178] M. Novello, S. Bergliaffa, and J. Salim. Singularities in general relativity coupled to nonlinear electrodynamics. *Classical and Quantum Gravity*, 17(18):3821, 2000.

[179] C. H. Nam. Higher dimensional charged black hole surrounded by quintessence in massive gravity. *General Relativity and Gravitation*, 52(1):1, 2020.

[180] M. Sadeghi. Ads black brane solution surrounded by quintessence in massive gravity and kss bound. *arXiv preprint arXiv:2007.09688*, 2020.

[181] S. G. Ghosh, S. D. Maharaj, D. Baboolal, and T-H Lee. Lovelock black holes surrounded by quintessence. *The European Physical Journal C*, 78(2):90, 2018.

[182] C. G. Böhmer, N. Tamanini, and M. Wright. Interacting quintessence from a variational approach. i. algebraic couplings. *Physical Review D*, 91(12):123002, 2015.

[183] P. Wongjun. Einstein field equation. *https://indico.cern.ch/event/803128/contributions/3414994/attachments/1864993/3066228/lecturenote-EFE-SHEAP2019.pdf*, Consultation: 12/10/2022, 14h27.

[184] Einstein Relatively Easy. Variation of the metric determinant. *http://einsteinrelativelyeasy.com/index.php/general-relativity/118-variation-of-the-metric-determinant*, Consultation: 12/10/2022, 14h00.

[185] T. Gonzalez and I. Quiros. Exact models with non-minimal interaction between dark matter and (either phantom or quintessence) dark energy. *Classical and Quantum Gravity*, 25(17):175019, 2008.

[186] C. A. Rizwan, A. N. Kumara, K. Hegde, and D. Vaid. Coexistent physics and microstructure of the regular bardeen black hole in anti-de sitter spacetime. *Annals of Physics*, 422:168320, 2020.

[187] C. H. Nam. Non-linear charged ads black hole in massive gravity. *The European Physical Journal C*, 78(12):1016, 2018.

[188] H-X Zhang, Y. Chen, T-C Ma, P-Zh He, and J-B Deng. Regular (bardeen) black hole surrounded by perfect fluid dark matter. *Chinese Physics C*, 2021.

[189] E. T. Newman and A. I. Janis. Note on the kerr spinning-particle metric. *Journal of Mathematical Physics*, 6(6):915–917, 1965.

[190] B. Toshmatov, Z. Stuchlík, and B. Ahmedov. Generic rotating regular black holes in general relativity coupled to nonlinear electrodynamics. *Physical Review D*, 95(8):084037, 2017.

[191] R. Kumar and S. G. Ghosh. Rotating black hole in rastall theory. *The European Physical Journal C*, 78(9):750, 2018.

[192] Z. Xu, X. Gong, and S-N Zhang. Black hole immersed dark matter halo. *Physical Review D*, 101(2):024029, 2020.

[193] R. Shaikh. Black hole shadow in a general rotating spacetime obtained through newman-janis algorithm. *Physical Review D*, 100(2):024028, 2019.

[194] M. Broccoli and A. Vigano. Electromagnetic self-force in curved spacetime: New insights from the janis-newman algorithm. *Physical Review D*, 98(8):084007, 2018.

[195] H. Erbin. Janis–newman algorithm: Generating rotating and nut charged black holes. *Universe*, 3(1):19, 2017.

[196] E. J. de Urreta and M. Socolovsky. Extended newman-janis algorithm for rotating and kerr-newman de sitter and anti de sitter metrics. *arXiv preprint arXiv:1504.01728*, 2015.

[197] H. Erbin and L. Heurtier. Five-dimensional janis–newman algorithm. *Classical and Quantum Gravity*, 32(16):165004, 2015.

[198] A. J. Keane. An extension of the newman–janis algorithm. *Classical and Quantum Gravity*, 31(15):155003, 2014.

[199] C. Bambi and L. Modesto. Rotating regular black holes. *Physics Letters B*, 721(4-5):329–334, 2013.

[200] D. J. Lombardo. The newman–janis algorithm, rotating solutions and einstein–born–infeld black holes. *Classical and Quantum Gravity*, 21(6):1407, 2004.

[201] M. Azreg-Aïnou. From static to rotating to conformal static solutions: rotating imperfect fluid wormholes with (out) electric or magnetic field. *The European Physical Journal C*, 74(5):2865, 2014.

[202] B. Toshmatov, B. Ahmedov, A. Abdujabbarov, and Z. Stuchlík. Rotating regular black hole solution. *Physical Review D*, 89(10):104017, 2014.

[203] D. Van der Waals. *over de Continuiteit van der gas-en vloeistoftoestand.* PhD thesis, University of Illinois, 1873.

[204] R. A. Cowely. Structural phase transition 1. landau theory. *Advances in Physics*, **29**(1):1–110, 1980.

[205] J. A. Wilson and G. D. Pitt. Metal-insulation transition in nis_2. *philosophical Magazine*, **23**(186):1297–1310, 1971.

[206] P. Puzo. *THERMODYNAMQUE CLASSIQUE:Transition de Phase d'un corps pur*. ch7 thermo.pdf.

[207] Wikipedia. Heat capacity. *https://en.wikipedia.org/wiki/Heatcapacity*, Consultation: 05-07-2022, 15h53.

[208] F. Guillaume. *LP350 Etats de la matiȓe Transitions de phases 2*. Université Pierre et Marie Curie, 25 Novembre 2015.

[209] Stemed. ehrenfest classification. *http://stemed.site/NCSU/CH454/lab2/ehrenfest.pdf*.

[210] University of Olso. Lecture 12: Phase transitions and van der waals model. *https://www.uio.no*, Consultation: 06-04-2022, 19h30.

[211] Richard Fitzpatrick. Phase transformations in van der waals fluid. *https://farside.ph.utexas.edu/teaching/sm1/Thermalhtml/node123.html*, Consultation: 06-04-2022, 19h26.

[212] Wikipedia. Equation d'état de van der waals. *https://fr.wikipedia.org/wiki*, Consultation: 04-06-2022, 21h47.

[213] P. C. Davies. The thermodynamic theory of black holes. *Proceedings of the Royal Society of London. A. Mathematical and Physical Sciences*, 353(1675):499–521, 1977.